Dynamical Systems Methods for Waves in Fluids: Stability, Breaking and Mixing

De Melo Virissimo, Francisco

Award date:
2018

Awarding institution:
University of Bath

Dynamical Systems Methods for Waves in Fluids: Stability, Breaking and Mixing

submitted by

Francisco de Melo Viríssimo

for the degree of *Doctor of Philosophy*

of the

University of Bath

Department of Mathematical Sciences

November 2018

Declaration of any previous Submission of the Work

The material presented here for examination for the award of a higher degree by research has not been incorporated into a submission for another degree.

. . . . . .

Francisco de Melo Viríssimo

Declaration of Authorship

I am the author of this thesis, and the work described therein was carried out by myself personally, with the exception of Chapters 2 to 4, which contain research articles that originated from collaboration with my supervisor Paul Antoine Milewski.

. . . . . .

Francisco de Melo Viríssimo

Summary

In this thesis, we investigate the problem of density stratified interfacial flows of immiscible fluids in the shallow water limit. We focus our attention on the two-and-a-half- and three-layer flows, with and without the so-called Boussinesq approximation which requires small density differences. The governing equations are carefully derived and the dynamics of their solutions are studied from both analytical and numerical points of view, particularly the issues of modal decomposition and whether a solution maintains hyperbolicity (*i.e.* wave-like behaviour) or not. New explicit criteria for transition to the elliptic regime are provided using dynamical systems techniques. The existence of invariant hyperbolic regions is proven and examples are constructed using the so-called simple waves. In addition, the mixing and entrainment phenomena are discussed and modelled for the case of a two-layer shallow water flow. Extensions and future work are suggested at the end.

'Creio que a verdade é como uma sinfonia. Não estamos aqui a conversar, mas se amanhã nos pedirem para relatar o que se passou, cada um terá uma versão diferente. Só se unirmos as várias versões, as várias vozes, conseguiremos construir a História, que é uma soma dessas experiências individuais. A História colectiva é uma grande mentira. Quando ouvimos as pessoas, elas dizem coisas inesperadas, coisas que não sabíamos."

SVETLANA ALEXIEVICH[1]

[1]Extracted from an interview given by Svetlana to the Portuguese website Publico.pt and published online on the 26th April 2016. https://www.publico.pt/2016/04/27/culturaipsilon/noticia/svetlana-alexievich-a-historia-colectiva-e-uma-grande-mentira-1730225

Acknowledgements

First and foremost, I would like to thank my family, to whom I dedicate this thesis: my parents Maronice and Oswaldo; my siblings Gabriela, Heliana and Elivaldo; my nephews Matheus and Rafael; and my grandparents Francisco, Ilda, Eureste and Anna. I am grateful for all the support my family and I had from my uncle Ronaldo to whom I owe special thanks.

Secondly, it was only possible to produce this thesis due to the support I had from (quite) a few people. I would especially like to thank to my supervisor, Professor Paul Milewski: you helped me in so many ways that it would take at least a dozen pages to thank you properly. Your friendship and attitude towards life, particularly science, has sparked my curiosity and exponentially increased my passion for living. Now I am on the verge of becoming a professional scientist but without your support I would have never made it. Thank you again.

Although I am Brazilian, I can say I have a British family now. Very warm thanks to (my British parents) beloved friends Richard and Catharine Hunt, as well as to (my British siblings) Giles, Hugo and Lucas Hunt for all the love, support and incredible friendship. I love you so much!

I am eternally grateful for the support I had from some very special people I met during this process. Thank you so much Sofya Zaytseva, Yana Marchuk, Andrea Chavez Cornejo and Yasmin Daibs for your friendship and for being with me in my toughest times: without you there is no way I would be here! Many thanks to my housemate Tsimhei Wan and to my dear *"Pernambucana"* Alice Maciel Tabosa for listening to all my complaints about life, especially PhD life, Brazilian politics and (of course) girls.

I would like to thank my old friends, David Kohan Marzagão, Marcelo Matheus Gauy and to Bartira Maués (we made it!), three very special people (also PhDs in Mathematics) that have been with me over the last decade.

I will never forget the time I spent in the department. It was a great experience, mostly because of the amazing people I met there. I would like to thank my officemates Amy Middleton, James Roberts, James Green, Leonard Hardiman, Xavier Pellet, Anna Senkevich, Pablo Vinuesa, Matthew Griffiths, Amine Chakhchoukh and Matthias Klar for the support, laughs, patience, fun, help with the moths and for voting for me in the SU Elections (we almost made the uni great again...). I will miss you guys!

Many thanks to the Department Officers, especially to Myla Watts, Elaine Ritchie, Susie Douglas and Tess Thomas, for being so friendly and for the incredible work they have done during my time at Bath uni. Thanks to Dr Adrian Hill, our DoS, for being very supportive to me and to my fellow students. Thanks also to my colleagues and friends at the SIAM-IMA Committee: Ben Robinson, Amy Middleton, Dan Green, Owen Pembery, Malena Sabate Landman and Adwaye Rambojun.

Unfortunately, I do not have space to thank everyone, but here I would like to mention a few other very important people: Yue Wu (my first friend in the UK and one of the smartest people I have ever met), Alge Wallis (my second friend in Britain), Britta Katharina Matthes and Andreia Martins (my third and fourth friends in this country, respectively). Thanks also to Lucy Hellier, Débora Waltenberg and especially to Anna Li for being with me and for share your love and support during part of this journey.

A big thank you goes to Professor Esteban Tabak and Dr Jonathan Evans, the examiners of this thesis, for reading and making very valuable suggestions for the final version.

To everyone else that has not been mentioned here, my sincere apologies, but a big

thank you too!

Finally, I would like to thank all the COCEX team at CNPq, especially Standard Silva, for all the support during my PhD. This research was supported by a scholarship from CNPq - Conselho Nacional de Desenvolvimento Científico e Tecnológico (Brasil), under the grant number 249770/2013-0, to whom I am very grateful.

Contents

List of Figures

Chapter 1

Introduction

This thesis concerns the study of internal waves in fluids, particularly on the issues of dynamics, stability and breaking.

One can start therefore by the simple definition of wave, such as T. G. Zieliński's [Zie] (after D. J. Acheson's in his Fluid Mechanics monograph [Ach90]), who defines waves as "*the transport of a disturbance (or energy, or piece of information) in space not associated with motion of the medium occupying this space as a whole*". While this is a useful concept, it cannot be considered a general definition, as tidal waves (for example) could be interpreted as being associated with appreciable mean motion of the medium (in this case the ocean). Although the lack of a rigorous definition for the concept of waves does not obstruct mathematical studies in the area, it is always important to consider the physical context of the problem when working with waves [BK00], [Mun50].

Waves in fluids, when compared to mechanical (*e.g.* sound waves) or electromagnetic waves, do present an additional and substantial difference: while (for instance) both sound and light waves *do not* interact with each other, waves in fluids *do interact* with each other, usually in a very complex way. This behaviour is reflected by the mathematics of the problem: sound and light waves are linear phenomena, modelled by linear equations, which satisfies the principle of superposition; on the other hand, waves in fluids are usually a highly nonlinear phenomena, whose fundamental model is the Navier-Stokes equations [CRB11]. All these complications motivated the famous quote of Richard Feymann, made in 1963 on the occasion of one of his lectures at Caltech [FLS89]:

> *"[water waves] that are easily seen by everyone and which are usually used as an example of waves in elementary courses [...] are the worst possible example [...]; they have all the complications that waves can have."*

The first studies on waves in fluids date from Lagrange and his hydrodynamic theory [Sto48]. Most early studies of waves in fluids can be seen as the study of small disturbances in a fluid medium, with one of the principal examples being ocean surface waves [Sto48]. For such an ocean wave model, the main hypothesis are [Lan13], [Sto48] that the flow is irrotational, incompressible and inviscid. This leads from the Navier-Stokes to the incompressible Euler equations

$$\rho \frac{D\mathbf{u}}{Dt} = -\nabla p - \mathbf{F}, \tag{1.1}$$

$$\nabla \cdot \mathbf{u} = 0, \tag{1.2}$$

where $\mathbf{u}$ denotes the velocity field, p the pressure field, $\mathbf{F}$ the external forces field and ρ denotes the density of the fluid, which can be constant or not. These equations are usually the starting point for any mathematical study of waves in incompressible flows. Boundary conditions are of crucial importance as the waves usually present themselves as the motion of the boundary. Hence, the fundamental problem is one of the incompressible Euler equations with a 'free' boundary. Further details of the boundary conditions in our particular settings will be given in Chapters 2 and 3.

1.1. The Shallow Water Limit

A class of waves that it is of great interest is the one of waves propagating in a shallow region of fluid, also called *shallow water waves*. Most of large scale geophysical waves lie in this category [HM05], as the wave cloud shown in Figure 1-1. Physically, these are the waves whose horizontal characteristic dimensions L are much larger than the vertical ones H. This can be mathematically translated into the dimensionless parameter μ given by

$$\mu = \frac{H}{L}.$$

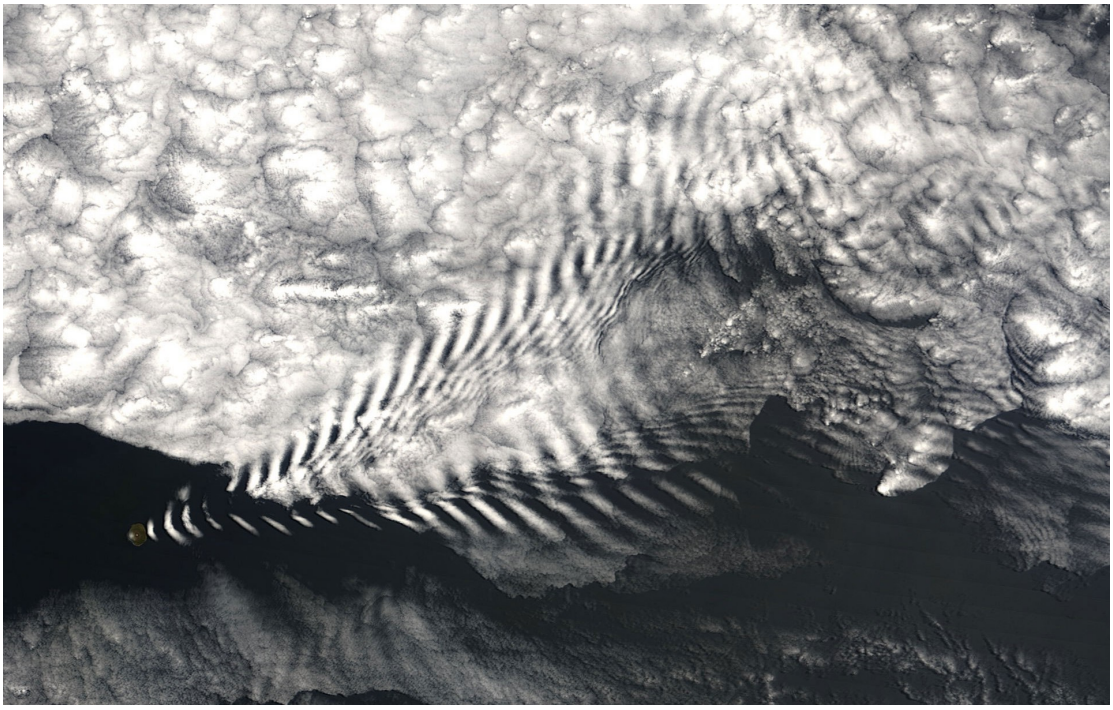

Figure 1-1: *NASA satellite image (MODIS imager on board the Terra satellite) of a wave cloud forming off of Amsterdam Island in the far southern Indian Ocean. Image taken on December 19, 2005. Credit: NASA. Reproduced from Wikipedia (open source).*

Hence, the shallow water case occurs when $\mu \ll 1$ and, for this reason, we refer to the asymptotic case $\mu \longrightarrow 0$ as the shallow water limit. Some authors [Con11] consider, for physical purposes, the shallow water range as being $\mu < 0.07$. Therefore, a classical example of a shallow water wave is a tsunami: it usually satisfies $\mu < 0.07$ as the deepest point in the ocean is attained in the Marianas Trench of the Western Pacific Ocean at 11021m [Con11], while a tsunami wavelength can be 200km long. This is also the case for the cloud waves in Figure 1-1: the wavelength is about two to three times bigger than the diameter of the Amsterdam Island (which is about 6km), while the distance measured from the sea level is of a few hundred meters. Other very appealing examples of shallow water waves are given by solitons and undular bores (see Figure 1-5) that are observed in the ocean and in the atmosphere [LWV15], [YFC$^+$09], [SO98]. These occur when μ is small but not zero.

The first model for shallow water waves was proposed by Adhémar Jean Claude Barré de Saint Venant in the context of river hydraulics [Cra04]. These equations,

known as the *St. Venant* or *shallow water equations*, read in the dimensionless form as

$$h_t = (hu)_x = 0,$$
$$(hu)_t + \left(hu^2 + \frac{h^2}{2}\right)_x = 0,$$

where h represents the layer thickness and u the horizontal component of the velocity field. These equations consists in a particular case of what is called *the water waves problem*, which is a very active topic of research in Mathematics, which a lot of attention devoted to the rigorous study of analytical properties of these [Lan13].

Although waves in shallow water are so common and striking, the works of St. Venant and others (such as Joseph Valentin Boussinesq [Sto48]) were for many years neglected by the hydrodynamicists and mathematicians, and did not receive much attention until the late 1940's [Sto48], when interest in the problem was rekindled due to the study of shock waves for applications in war. As the gas dynamics equations are very similar to the shallow water equations, further interest in the topic started again [Sto48], [SS53], [Ovs79]. The latter were also interested in this as a model for waves that arises in the interface between two fluids, starting therefore a new field in Applied Mathematics of the so-called internal waves, discussed in the next section.

1.2. Internal Waves

The existence of internal waves in geophysical stratified flows is an ubiquitous phenomena, with the ocean and the atmosphere as prime examples [CRB11]. One of the first scientific investigations of internal waves was in 1893, when the Norwegian oceanographer Fridtjof Nansen experienced a phenomenon he would later call 'dead water', in which a boat or ship might experience a very strong resistance in its forward motion in apparently calm wind and sea conditions [Wikb]. As reported by Nansen [Wal91]:

> *"When caught in dead water Fram appeared to be held back, as if by some mysterious force, and she did not always answer the helm. In calm weather, with a light cargo, Fram was capable of 6 to 7 knots. When in dead water she was unable to make 1.5 knots. We made loops in our course, turned sometimes right around, tried all sorts of antics to get clear of it, but to very little purpose."*

After bringing this back to his colleagues in Norway, they concluded that the reason was due to the generation of internal waves by the ship's motion: if a ship is moving through the sea on a layer of fresh water whose depth is comparable to the boat's draft, it would produce a wake of internal waves that dissipates a considerable amount of energy, preventing the ship from using its thrust to move. An example of internal waves in the ocean is presented in Figure 1-2.

The existence of internal waves is due to stratification. Even though modelled by incompressible equations, most geophysical flows are density-stratified, meaning that the density can change due to the concentration of sediments, substances or differences in the temperature in various parts of the flow.

The different models for internal waves depend on the particularities of the flow. The stratification, which opens the possibility of internal waves, can be continuous or not, and both scenarios can be used to model the same context. For instance, the ocean can be better modelled by a continuous stratification, but on the other hand, a discrete stratification is simpler in certain cases in nature as in Nansen's example above. In

Figure 1-2: *Ocean Internal waves in Rosario Strait, Washington State, USA. Source: TAF Lab at University of California (https://taflab.berkeley.edu/)*

this thesis, we will focus on discrete layered stratified models, particularly in the cases of two and three layer flows. This particular setting is illustrated in M. Grant Gross' classical monograph on Oceanography [Gro76], reproduced in Figure 1-3.

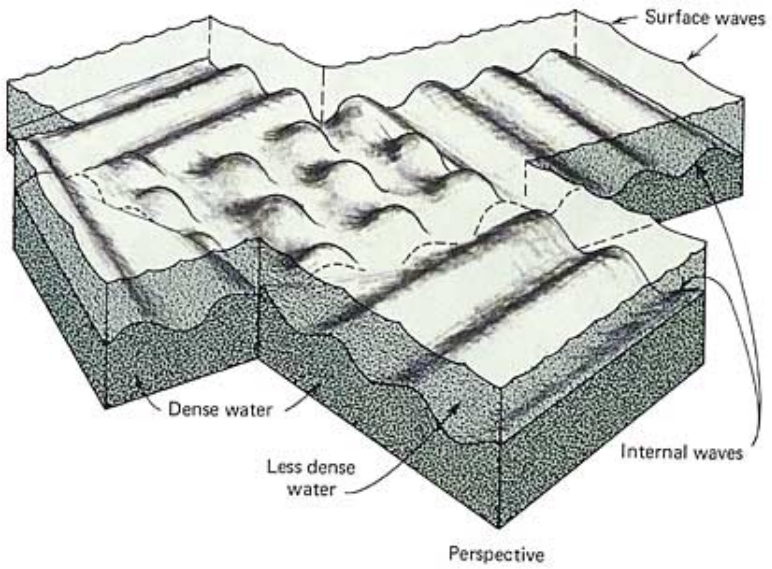

Figure 1-3: *Schematic representation of internal and surface waves in the ocean. Reproduced from [Gro76], p. 2014.*

Another very important point related to the stratification is the time scale. In the real world, even if you start with a discontinuous stratification at rest, the diffusion will mix the fluids, leading to a continuous and more homogeneous stratification after a long period of time. In this study, we assume that the timescales of waves are shorter than the diffusive timescales, which make the interfaces ticker and with well defined. Finally, we note that only the fundamental wave-modes are captured by a discrete

stratification, and therefore higher wave-modes arising from continuous stratification are neglected in this approximation.

1.3. The Boussinesq Approximation

In most geophysical flows, the fluid density does not vary substantially around a mean value, for example the ocean and the departure from adiabatic in the atmosphere [CRB11], [Bai95], [Maj03]. This can be translated into the following ad-hoc approximation: recall the Euler equations (1.1), which state

$$\rho_j \left(u_{j,t} + u_j u_{j,x} + v_j u_{j,y}\right) = -p_{j,x},$$
$$\rho_j \left(v_{j,t} + u_j v_{j,x} + v_j v_{j,y}\right) = -p_{j,y} - \rho_j g.$$

where j is the index of each layer and where we considered a gravitational force field $\mathbf{F}_j = (0, \rho_j g)$ for simplicity. The left hand side contains all the convective terms due to the velocity field, while the right hand side contains the pressure and external forces (in this case the gravity) terms.

The so-called *Boussinesq approximation* consists in neglecting the different densities that multiply the convective terms by making

$$\rho_j = \overline{\rho},$$

where $\overline{\rho}$ usually represents the mean density ($\overline{\rho} = (\sum_{j=1}^{n} \rho_j)/n$), and replacing this new value in the equations above. In other words, under this approximation, the difference of densities in the layers is not important in the convective terms in the left-hand side, only in the buoyancy ones.

Under this hypothesis, the equations above become

$$u_{j,t} + u_j u_{j,x} + v_j u_{j,y} = -\frac{p_{j,x}}{\overline{\rho}},$$
$$v_{j,t} + u_j v_{j,x} + v_j v_{j,y} = -\frac{p_{j,y}}{\overline{\rho}} - \frac{\rho_j}{\overline{\rho}} g.$$

In essence, the Boussinesq approximation states that while difference in inertia is negligible, gravity is sufficiently strong to make the specific weight appreciably different between the two fluids (for instance, sound waves are neglected when the Boussinesq approximation is used since sound waves move via density variations) [Wika]. Usually, in physical applications, this approximation is done without appreciable loss of accuracy in the model [CRB11] and makes the mathematics much simpler. As we shall see in Chapters 2 and 3, this is a major mathematical hypothesis, which can change the nature of the equations in question.

1.4. Dynamics and Stability

Layered-stratified models can either be weakly or fully nonlinear, and dispersive or non-dispersive. Physically, nonlinearity is controlled by the wave amplitude relative to the height of the fluid domain, whereas dispersion is controlled by the relative size of horizontal length scales compared to this domain height. Strongly nonlinear, non-dispersive approximations take the form of hyperbolic or mixed type first order PDEs, first derived in this context by Long [Lon56]. Weakly nonlinear dispersive approximations result in Korteweg-de Vries type models [Ben66], [GPT97] and fully

nonlinear dispersive approximations lead to the so-called Miyata-Camassa-Choi system [Miy88], [CC99].

In this thesis, we focus on the strongly nonlinear non-dispersive setting in the case of three layers (and thus two interfaces) on two settings: three-layer flows in a channel bounded by horizontal rigid walls; and two-later flows bounded below by an horizontal rigid bottom and above by a third unbounded and dynamically passive layer of fluid. These are important cases as they capture mode 2 (baroclinic) internal waves, which is a slower family of waves with out-of-phase pycnocline displacements (where the density gradient is the greatest), in addition to the faster mode 1 (barotropic) waves. These waves, although less common than mode 1 waves have now been observed in the ocean [YFC$^+$09]. In addition, since the equations are of mixed type, a initially hyperbolic solution may become elliptic before it breaks, meaning that Kelvin-Helmholtz instability appears due to large shear along the interface (see Figure 1-4). The case of two-layer flows between rigid lids, in the non-dispersive setting has been studied extensively (*e.g.* [Lon56], [Ovs79], [BM11]) and since the resulting equations are a system of 2 first order PDEs, certain results can be obtained analytically. For example, one can find precise conditions that ensure that the solutions remain in the hyperbolic domain up to breaking [BM11] or construct shock solutions in the internal dam-break (lock exchange) problem [RKBM11], [MT15]. The cases two-and-a-half- and three layer flows are much more complicated as the resulting equations are a system of 4 PDEs and many of the methods successfully used in the two-layer problem no longer apply, requiring new ideas and methods to be developed.

Figure 1-4: *Kelvin Helmholtz instability clouds in San Francisco. These clouds, sometimes called "billow clouds", are produced by instability, when horizontal layers of air brush by one another at different velocities. Reproduced from Wikipedia (open source).*

Figure 1-5: *Photo of a Morning Glory cloud formation taken from a plane near Burketown (plane heading to Normanton) in QLD, Australia. Credit: Mick Petroff. Reproduced from Wikipedia (open source).*

1.5. Breaking and Mixing

Layered-stratified shallow water flows, although driven primarily by the density differences between the layers, have the capacity to alter the underlying stratification. Most studies assume that the flow remains with the original density stratification over time and although this can be the case in many applications, shallow water waves tend to break and can change the stratification. At this point, the movement of particles in the flow can become quite turbulent, leading to mixing and entrainment processes [WTM12], [CZ10], [CZ11]. These are usually guided by small scale motions that are difficult to model in detail [RSG10]. In this thesis, we approach breaking waves using conservation laws which avoid small scale dynamics.

Mathematically, as a solution breaks, it loses smoothness and no longer satisfies the differential equations that govern its motion. One could continue it as a solution of the integral, or 'weak', formulation, but there are usually several choices as the integral formulation is not unique [LeV02], [Smo94]. Hence, the question of how to continue the solution after a wave breaks arises. This is an important question and its resolution must include some additional information usually in the form of physical constraints. There is an accepted solution to this in shallow water hydraulics (hydraulic jumps), but this is not the case for internal waves [MJT08], [RKBM11], [Fri17].

A possible answer to this problem was given in [MT15], based on the choice of conservation laws that allow for entrainment. In that case, the layerwise conservation of mass was replaced by conservation of energy, and the conservation of total momentum was replaced by conservation of circulation, giving uniqueness to the shock solution. This is an approach that we will explore further in the Chapter 4 of this thesis.

1.6. Outline of the Thesis

The thesis contains original research carried by the author over the last 4 years, presented in the form of 3 papers through Chapters 2 to 4. It focuses on the nonlinear and complex aspects of waves in fluids, according to Figure 1-6, and is divided as follows.

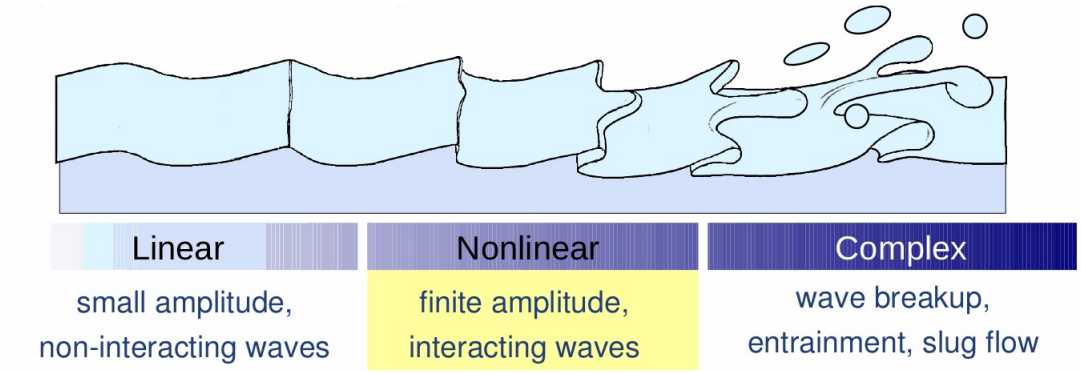

Figure 1-6: *The evolution of a shallow water wave eventually falls in one of the three categories in the picture: linear, nonlinear and complex. Credit: Lawrence C. Cheung [CZ10], [CZ11]. Reproduced with permission.*

In Chapter 2, we formulate and discuss the problem of a three-layer shallow water flow, bounded above and below by rigid walls. This is done in the more general non-Boussinesq case, where small density differences are not required. We focus on the evolutionary properties of the mathematically simpler Boussinesq case and use simple waves to propose and study reduced two-dimensional models for waves in this flow. In Chapter 3, we move our attention to the so called two-and-a-half-layer shallow water flow, in which the upper rigid wall is removed and the upper layer is replaced by an unbounded and dynamically passive layer of fluid. This is a realistic model for ocean waves for example, as pointed out earlier, with the unbounded layer representing the atmosphere. Again, the problem is formulated and its governing equations are derived. Both the dynamics and stability properties of the flow are then studied through simple waves. In Chapter 4, shock solutions for density-stratified flows are then studied. This is done through a novel methodology based on the adequate choice of conservation laws to model the system in this non-smooth context. We model and study the mixing and entrainment in a two-layer shallow water flow in the non-Boussinesq case. Finally, we conclude with Chapter 5, where our findings are summarised and further directions for the work in this thesis are presented.

All numerical simulations in the present thesis were performed in MATLAB®, except for the ones in Figure 5 of Chapter 3, which were run in Mathematica®. All the illustrations in the thesis were done with the aid of the software GeoGebra®.

1.6.1 Notation

The standard notation to be used in this thesis is introduced below.

• **Vectors and scalars.** Vectorial functions will be written in bold, while scalar functions will appear in standard characters. For example, consider

$$\mathbf{u} = (u, v, w).$$

Here, $\mathbf{u}$ means a vector in a three-dimensional space, while u is one of its components

and therefore is a scalar whose image lies in an one-dimensional space.

The scalar (or 'dot') product is denoted by $\cdot$, which means that, if $\mathbf{u}$ and $\mathbf{v}$ are n-dimensional vectors, then

$$\mathbf{u} \cdot \mathbf{v} = u_1 v_1 + ... + u_n v_n.$$

• **Derivatives.** We shall use subscripts for the derivatives of a function. For example, if $u(x, y, t)$ is a scalar function, then

$$u_t(x, y, t) = \frac{\partial u}{\partial t}(x, y, t)$$

and similarly for u_x and u_y. Also, for a function $u_j(x, y, t)$, its partial derivatives will be denoted by $u_{j,t}$, $u_{j,x}$ and $u_{j,y}$, *i.e.*,

$$u_{j,t}(x, y, t) = \frac{\partial u_j}{\partial t}(x, y, t)$$

and similarly for $u_{j,x}$ and $u_{j,y}$.

The gradient operator will be denoted by ∇, which means that for a scalar function of n variables, say $u(x_1, ..., x_n)$, we have

$$\nabla u(x_1, ..., x_n) = \left(u_{x_1}(x_1, ..., x_n), ..., u_{x_n}(x_1, ..., x_n)\right).$$

Finally, the material derivative is defined by

$$\frac{D}{Dt} = \frac{\partial}{\partial t} + \mathbf{u} \cdot \nabla$$

where, for $\mathbf{u}(x_1, ..., x_n) = (u_1(x_1, ..., x_n), ..., u_n(x_1, ..., x_n))$,

$$\mathbf{u} \cdot \nabla = u_1 \frac{\partial}{\partial x_1} + ... + u_n \frac{\partial}{\partial x_n}.$$

• **A short note on functions.** All functions in these notes are assumed analytic or as smooth as needed in the context they appear, unless further assumptions. Also, in order to simplify the notation, we shall ommit the independent variables when they are not strictly necessary. For example, we could write the product $u(x, y, t)v(x, y, t)$ and the sum $h_1(x, t) + h_2(x, t)$ simply as $uv(x, y, t)$ and $(h_1 + h_2)(x, t)$ or uv and $h_1 + h_2$ only.

Chapter 2

Three-layer Flows in the Shallow Water Limit

In this chapter, the problem of three-layer flows (bounded by two horizontal rigid walls) under the shallow water limit is considered. This is a one-dimensional model in the horizontal direction, which extends to infinity in both directions. After a careful formulation of the general non-Boussinesq case, the evolutionary properties of the realistic, but mathematically simpler, Boussinesq case are studied. The work presented is joint with Paul A. Milewski, which was submitted to the scientific journal *Studies in Applied Mathematics* and is currently in process of revision [dMVM17].

2.1. Outline of the Article

The paper starts by highlighting the importance of the study of density-stratified flows, as most geophysical flows share this property [CRB11]. A concise literature review of some relevant advances in the area is also presented.

In Section 2, the problem is stated and the governing equations for the non-Boussinesq problem are derived in a systematic and careful way, leading to a system of 5 quasi-linear, mixed-type and nonlocal PDEs, which are one-dimensional in space and can be reduced to a system of 4 PDEs for certain boundary conditions in the horizontal direction. In addition, the Boussinesq equations are obtained from the latter through a simple limit, which is for this reason called the 'Boussinesq limit' [BM11].

Section 3 starts with a discussion on the the nonlocal nature of the problem, which leads to an 'inertia Paradox' [CCF$^+$12] in which the total horizontal momentum is not conserved even without the presence of external forces. After this, our attention turns to the evolutionary properties of the Boussinesq system, in the physically simpler case where the jumps in density are the same on both layers. In Section 3.2, it is shown that the system captures the two fundamental modes of waves in geophysical flows, the so-called mode 1, which corresponds to fast waves, and the slower mode 2, which is physically associated to slower waves with more internal structure [Bai95]. This structure is explored in Section 3.3, where a modal change of variables is proposed, enabling us to find symmetric solutions and a 'pure' mode 2 invariant subspace of dimension 2. In this subspace, the three-layer shallow water equations reduce to the two-layer shallow water equation, a fact that is remarked in the paper and proved later in this thesis (see Section 2.2 of the present chapter). We also prove that 'pure' mode 1 solutions do not form an invariant subspace in the phase space. However, one can construct such 'pure' mode 1 solutions using simple waves, which is done in Section 3.4. We also use simple waves to propose two-dimensional reduced models, done in Section 3.5, which captures much of the features of the (full model) solutions.

Finally, Section 4 summarises our findings and discusses further directions for this work.

Appendix B: Statement of Authorship

This declaration concerns the article entitled:									
Thee-layer Flows in the Shallow Water Limit									
Publication status (tick one)									
draft manuscript		**Submitted**	X	**In review**		**Accepted**		**Published**	
Publication details (reference)	Studies in Applied Mathematics Authors: Francisco de Melo Viríssimo, Paul Antoine Milewski								
Candidate's contribution to the paper (detailed, and also given as a percentage).	The bulk of the calculations have been performed by the author of the thesis (100%). All authors contributed equally to the presentation of the content (50%). The numerical computations have been performed by the author of the thesis (100%).								
Statement from Candidate	This paper reports on original research I conducted during the period of my Higher Degree by Research candidature.								
Signed					**Date**	7.11.2018			

Three-layer Flows in the Shallow Water Limit

By Francisco de Melo Viríssimo and Paul A. Milewski

Dedicated to Roger Grimshaw

In this work, we formulate and discuss the shallow water limit dynamics of the layered flow with three layers of immiscible fluids of different densities bounded above and below by horizontal walls. We obtain a resulting system of four equations, which may be non-local in the non-Boussinesq case. We provide a systematic way to pass to the Boussinesq limit, and then study those equations, which are first order PDEs of mixed type, more carefully. We show that in a symmetric case the solutions remain on an invariant surface and using simple waves we illustrate that this is not the case for non-symmetric cases. Reduced models consisting of systems of 2 equations are also proposed and compared to the full system.

1. Introduction

The study of internal waves in stratified fluids continues to attract much attention, as these waves are ubiquitous in the atmosphere and the ocean (see e.g. [1], [2]). They play an important role in transporting energy over long distances, and, when they break, contribute to mixing [3]. Horizontally propagating waves are usually long: their horizontal scales are much longer than the vertical ones [4]. The simplest fluid configuration for internal waves are layered interfacial flows, where the fluid is assumed to be stratified in layers of constant density. The study of these flows in the long wave limit approximates physical settings where there are sharp density variations, and yield a variety of mathematical models, depending on the relative strength of different effects. The resulting models

Address for correspondence: Prof. P. A. Milewski, Department of Mathematical Sciences, University of Bath, Bath, BA2 7AY, United Kingdom; email: P.A.Milewski@bath.ac.uk

DOI: 10.1111/((please add article doi))
STUDIES IN APPLIED MATHEMATICS AA:1–32

can either be weakly or fully nonlinear, and dispersive or non-dispersive. Physically, nonlinearity is controlled by the wave amplitude relative to the height of the fluid domain, whereas dispersion is controlled by the relative size of horizontal length scales compared to this domain height. Strongly nonlinear, non-dispersive approximations take the form of hyperbolic or mixed type first order PDEs, first derived in this context by Long [5]. Weakly nonlinear dispersive approximations result in Korteweg-de Vries type models [6], [7] and fully nonlinear dispersive approximations lead to the so-called Miyata-Camassa-Choi system [8], [9].

In this paper we consider a strongly nonlinear non-dispersive setting in the case of three layers (and thus two interfaces) bounded above and below by horizontal walls. This case is important as it captures mode 2 internal waves - which is a slower family of waves with out-of-phase pycnocline displacements - in addition to the faster mode 1 waves. These waves, although less common than mode 1 waves have now been observed in the ocean [10]. The case of two-layer flows in the non-dispersive setting has been studied extensively (see e.g. [5], [11], [12]) and since the resulting equations are a system of 2 first order PDEs, certain results can be obtained analytically. For example, one can find precise conditions that ensure that the solutions remain in the hyperbolic domain up to breaking [12] or construct shock solutions in the internal dam-break (lock exchange) problem [13], [14]. The case of three layer flows is much more complicated as the resulting equations are a system of 4 PDEs and many of the methods used before no longer apply.

We first derive the equations governing the flow in the non-Boussinesq case and show that the nature of the resulting system is dependent on the boundary conditions. For many cases the system is non-local, a result linked to the paradox of non-conservation of horizontal momentum [15]. We then turn to the dynamics in the Boussinesq limit, where we show that certain symmetric mode 2 solutions are confined to an invariant 2 dimensional subspace of the 4 dimensional phase plane and propose new variables that better capture mode 1 and mode 2 solutions and use simple waves to show that this invariant manifold construction is not possible for non-symmetric solutions. Finally we propose some reduced models in terms of systems of 2 PDEs that can be used to approximate the individual modes.

2. Formulation

Consider a two-dimensional, irrotational flow of ideal, incompressible and immiscible fluids in three layers of different densities, under the action of

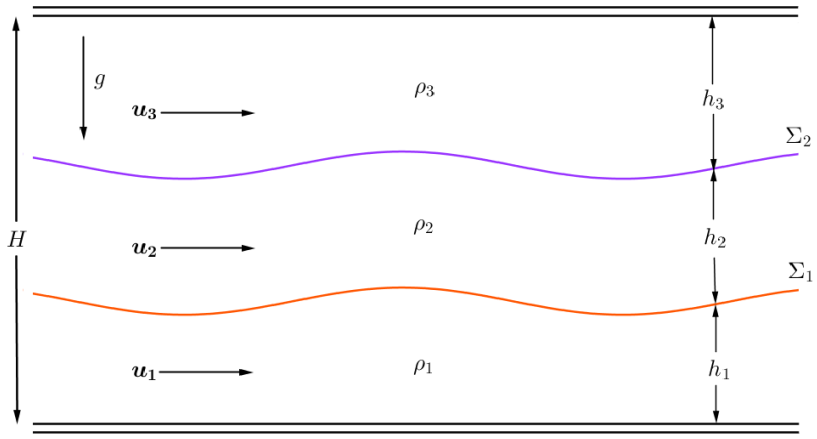

Figure 1: Schematic illustration for the three-layer problem.

gravity and bounded by horizontal rigid lids at the bottom and at the top, as shown in Figure 1.

The fluid pressure and velocity fields in each layer are given by $p_j(x,y,t)$ and $\mathbf{u}_j(x,y,t) = (u_j(x,y,t), v_j(x,y,t))$ respectively, with $j = 1$ representing the lower layer, $j = 2$ representing the middle layer and $j = 3$ representing the upper layer. The fluid density is given by ρ_j, $j = 1,2,3$, where the fluid in a layer is denser than the one above it, *i.e.*, $\rho_1 \geq \rho_2 \geq \rho_3$. The height of each of the active layers is given by $h_j(x,t)$ and the interface between the layers, assumed to be a graph, are given by $\Sigma_1 = \{(x,y)\colon y = h_1(x,t)\}$ and $\Sigma_2 = \{(x,y)\colon y = (h_1+h_2)(x,t)\}$, as schematically indicated in the Figure 1.

The mathematical model [4], [16] for the dynamics in each layer is given by the incompressible Euler equations

$$\rho_j \frac{D\mathbf{u}_j}{Dt} = -\nabla p_j - \mathbf{F}_j \tag{1}$$

$$\nabla \cdot \mathbf{u}_j = 0, \text{ for } j = 1,2,3. \tag{2}$$

for $j = 1,2,3$, with $\mathbf{F}_j$ being the external force field. In this model, only gravitational forces act, with $\mathbf{F}_j = (0, \rho_j g)$.

The boundary conditions are the impermeability condition at the bottom and top walls respectively:

$$v_1 = 0 \quad \text{on} \quad y = 0, \tag{3}$$

$$v_3 = 0 \quad \text{on} \quad y = H, \tag{4}$$

the *kinematic conditions* (KBC) and the *dynamic condition* (DBC) on Σ_1 respectively given by

$$h_{1,t} + u_1 h_{1,x} = v_1, \tag{5}$$
$$h_{1,t} + u_2 h_{1,x} = v_2, \tag{6}$$
$$p_1 = p_2, \tag{7}$$

while on Σ_2 these conditions are

$$(h_1 + h_2)_t + u_2 (h_1 + h_2)_x = v_2, \tag{8}$$
$$(h_1 + h_2)_t + u_3 (h_1 + h_2)_x = v_3, \tag{9}$$
$$p_2 = p_3. \tag{10}$$

The KBCs above imply, for $j = 1, 2$, and $\mathbf{n}_j$ being the normal to Σ_j

$$\mathbf{n}_j \cdot \mathbf{u}_j = \mathbf{n}_j \cdot \mathbf{u}_{j+1}$$

on the interface Σ_j. This states the continuity of normal velocity across interfaces. The model can also be shown to satisfy

$$h_1 + h_2 + h_3 = H, \tag{11}$$

where H is the constant total height of the channel, as shown in Figure 1.

This gives us a free boundary problem for 9 first order partial differential equations with 9 boundary conditions for the 9 unknowns u_j, v_j, p_j, $j = 1, 2, 3$. The unknown domain appears through the heights h_j in the boundary conditions.

2.1. Governing equations

Our aim here is to rewrite equations (1) to (11) as a 4×4 system of first order PDEs [12], in the *long wave limit* [4], [16], [17] where the vertical variation in the horizontal velocity is small, and its vertical average represents this velocity well.

In order to proceed, we shall compute the vertical average of the quantities u_j, v_j and p_j on each layer. The vertical mean of u_j, for $j = 1, 2, 3$, is defined as

$$\overline{u_j}(x,t) \doteq \frac{1}{h_j(x,t)} \int_{y_j(x,t)}^{y_j(x,t)+h_j(x,t)} u_j(x,y,t)dy,$$

where $y_j(x,t)$ is the coordinate of the lower interface of the j-th layer, and with similar definitions for $\overline{v_j}$ and $\overline{p_j}$. Using the Leibniz rule we write expressions for the integrals of quantities such as $u_{j,x}$, $u_{j,t}$ and $p_{j,x}$, for

$j = 1, 2, 3$, in terms of the averages above. For instance,

$$(h_j\overline{u_j})_x = \int_{y_j}^{y_j+h_j} u_{j,x}dy + \left((y_j + h_j)_x u_j|_{y=y_j+h_j} - y_{j,x}u_j|_{y=y_j}\right). \quad (12)$$

2.1.1. Conservation of volume equations. Consider the incompressibility condition (2)

$$\nabla \cdot \mathbf{u}_j = u_{j,x} + v_{j,y} = 0.$$

Taking the vertical integral and using (12) leads to

$$(h_j\overline{u_j})_x - \left((y_j + h_j)_x u_j|_{y_j+h_j} - y_{j,x}u_j|_{y_j}\right) + \left(v_j|_{y_j+h_j} - v_j|_{y_j}\right) = 0. \quad (13)$$

From the KBCs on each interface, and taking $j = 1, 2, 3$ we have

$$h_{j,t} + (h_j\overline{u_j})_x = 0, \quad (14)$$

which states the *conservation of volume* for the flow in each layer. Note that, since the density is constant in each layer, conservation of volume is equivalent to *conservation of mass*.

2.1.2. Momentum equations. We now recall the Euler equations (1), written for each layer in horizontal and vertical components respectively

$$\begin{aligned} \rho_j\left(u_{j,t} + u_j u_{j,x} + v_j u_{j,y}\right) &= -p_{j,x}, & (15)\\ \rho_j\left(v_{j,t} + u_j v_{j,x} + v_j v_{j,y}\right) &= -p_{j,y} - \rho_j g. & (16)\end{aligned}$$

Our aim here is to carry out an averaging as in the previous section. Consider the lowest layer. From equation (15) for $j = 1$, after integrating and using (12) for x and time derivatives and using bottom impermeability, we obtain

$$\begin{aligned} \rho_1\left((h_1\overline{u_1})_t + \left(h_1\overline{u_1^2}\right)_x\right) &- \rho_1 u_1|_{h_1}(h_{1,t} + u_1|_{h_1}h_{1,x} - v_1|_{h_1})\\ &= -(h_1\overline{p_1})_x + p_1|_{h_1}h_{1,x}. \quad (17)\end{aligned}$$

This equation can be simplified by using that the KBC on Σ_1 and becomes

$$\rho_1\left((h_1\overline{u_1})_t + \left(h_1\overline{u_1^2}\right)_x\right) = -(h_1\overline{p_1})_x + P_1 h_{1,x}, \quad (18)$$

where here and in what follows we have denoted p on Σ_j by P_j, and P_0, P the bottom and top pressures respectively. A similar vertical integration of the vertical momentum equation (16) for $j = 1$ leads to

$$\rho_1((h_1\overline{v_1})_t + (h_1\overline{u_1 v_1})_x - v_1|_{h_1}(h_{1,t} + u_1|_{h_1}h_{1,x} - v_1|_{h_1})) = P_0 - P_1 - g\rho_1 h_1,$$

which using the KBC on Σ_1 simplifies to

$$\rho_1\left((h_1\overline{v_1})_t + (h_1\overline{u_1 v_1})_x\right) = P_0 - P_1 - g\rho_1 h_1. \quad (19)$$

This same routine can be applied to the middle layer to get equations

$$\rho_2\left((h_2\overline{u_2})_t + \left(h_2\overline{u_2^2}\right)_x\right) = -(h_2\overline{p_2})_x + P_1 h_{1,x} - P_2(h_1+h_2)_x, \quad (20)$$

$$\rho_2\left((h_2\overline{v_2})_t + (h_2\overline{u_2 v_2})_x\right) = P_1 - P_2 - g\rho_2 h_2, \quad (21)$$

and also to the upper layer, resulting in

$$\rho_3\left((h_3\overline{u_3})_t + \left(h_3\overline{u_3^2}\right)_x\right) = -(h_3\overline{p_3})_x - P_2(h_1+h_2)_x, \quad (22)$$

$$\rho_3\left((h_3\overline{v}_3)_t + (h_3\overline{u_3 v_3})_x\right) = P_2 - P - g\rho_3 h_3. \quad (23)$$

Equations (19)-(23) are exact but are not closed, as they relate the evolutions of mean quantities to higher order moments. The shallow water approximation allows us to close the system.

2.1.3. The shallow water limit. The continuation of the derivation involves the shallow water (or long wave) approximation, that is, that horizontal variations are slowly-varying compared to vertical ones. This is done by scaling horizontal derivatives with a small parameter μ relative to vertical derivatives. As we must satisfy incompressibility in each layer, we obtain that v must scale with μ also. We then turn to the vorticity equation in each layer

$$\omega_{j,t} + u_j\omega_{j,x} + v_j\omega_{j,y} = 0, \quad (24)$$

where

$$\omega_j = \mu^2 v_{j,x} - u_{j,y}. \quad (25)$$

The vorticity equation describes simple advection and therefore the vorticity is preserved along particle paths. If we therefore assume that the initial data satisfies $u_{j,y} = \mathcal{O}(\mu^2)$ and $v_{j,x} = \mathcal{O}(1)$, we have that $\omega_j = \mathcal{O}(\mu^2)$ for all time, and can conclude that $u_{j,y} = \mathcal{O}(\mu^2)$ for all time. This implies that the horizontal velocities are uniform in y to leading order and can be written

$$u_j(x,y,t) = \overline{u_j}(x,t) + \mu^2\tilde{u}_j(x,y,t), \quad (26)$$

From this one immediately concludes that

$$\overline{u_j^2} = \overline{u_j}^2 + \mu^4\,\overline{\tilde{u}_j^2}, \quad (27)$$

$$\overline{u_j v_j} = \overline{u_j}\;\overline{v_j} + \mu^2\,\overline{\tilde{u}_j v_j}. \quad (28)$$

A similar rescaling of the vertical component of the Euler equations (equation (16)) is given by [12]

$$\mu^2\left(v_{j,t} + u_j v_{j,x} + v_j v_{j,y}\right) = -\frac{p_{j,y}}{\rho_j} - g, \quad (29)$$

from which one concludes that the leading order pressure satisfies the hydrostatic balance

$$p_{j,y} = -g\rho_j + \mathcal{O}(\mu^2), \tag{30}$$

which can be integrated, and, together with the continuity of pressure at each interface yields

$$\begin{aligned} p_1(x,y,t) &= \rho_1 g(h_1 - y) + \rho_2 g h_2 + \rho_3 g h_3 + P, & (31)\\ p_2(x,y,t) &= \rho_2 g(h_1 + h_2 - y) + \rho_3 g h_3 + P, & (32)\\ p_3(x,y,t) &= \rho_3 g(H - y) + P. & (33) \end{aligned}$$

From equations (27) and (31)-(33), we are able to simplify the averaged horizontal momentum equations. After some calculations, we get

$$\begin{aligned} \rho_1 \left(u_{1,t} + u_1 u_{1,x}\right) + (\rho_1 - \rho_3) h_{1,x} + (\rho_2 - \rho_3) h_{2,x} &= -P_x, & (34)\\ \rho_2 \left(u_{2,t} + u_2 u_{2,x}\right) + (\rho_2 - \rho_3)(h_{1,x} + h_{2,x}) &= -P_x, & (35)\\ \rho_3 \left(u_{3,t} + u_3 u_{3,x}\right) &= -P_x. & (36) \end{aligned}$$

Note that we have dropped the bars over in u_j and set $g = 1$. Conservation of mass reads

$$h_{j,t} + (h_j u_j)_x = 0, \tag{37}$$

for $j = 1, 2, 3$. The height H and average density can be normalised:

$$h_1 + h_2 + h_3 = 1, \tag{38}$$

$$\frac{\rho_1 + \rho_2 + \rho_3}{3} = 1. \tag{39}$$

The set (34)-(38) consists of a closed system of seven equations for seven unknowns $(h_1, h_2, h_3, u_1, u_2, u_3, P)$. In solving for the pressure below we will see that in most cases the equation for P has an elliptic nature with various consequences.

2.1.4. The volume flux. An important quantity is the *volume flux*, defined as

$$Q(x,t) \doteq h_1 u_1 + h_2 u_2 + h_3 u_3. \tag{40}$$

From the conservation of mass equations,

$$Q_x(x,t) = (h_1 u_1 + h_2 u_2 + h_3 u_3)_x = -(h_1 + h_2 + h_3)_t = 0.$$

and hence Q is a function of t only. The time evolution of the flux will provide the equation for P:

$$\begin{aligned} Q'(t) &= h_{1,t}u_1 + h_1u_{1,t} + h_{2,t}u_2 + h_2u_{2,t} + h_{3,t}u_3 + h_3u_{3,t}. \\ &= -\left(h_1u_1^2 + h_2u_2^2 + h_3u_3^2 + \frac{h_1^2+h_2^2}{2}\right)_x \\ &\quad -h_2h_{1,x} - h_1\left(\frac{\rho_2}{\rho_1}h_{2,x} + \frac{\rho_3}{\rho_1}h_{3,x}\right) - \frac{\rho_3}{\rho_2}h_2h_{3,x} \\ &\quad -\left(\frac{h_1}{\rho_1} + \frac{h_2}{\rho_2} + \frac{h_3}{\rho_3}\right)P_x. \end{aligned} \tag{41}$$

For certain cases, Q is set by the boundary conditions on u_j, and is therefore constant in time. Two scenarios in which this occurs are in the presence of vertical sidewalls, implying $Q = 0$, and when far field inlet conditions fix Q to a constant value (which could be set as zero by choosing an appropriate reference frame) [12]. The equation above then becomes immediately an equation for P. On the other hand if boundary conditions are known in P (e.g. for a periodic domain) then the equation can be solved for P_x, integrated and the boundary conditions applied, yielding an expression for Q'. which can be substituted back into (41) again yielding again an equation for P. We shall postpone a detailed discussion of these to the next chapter.

2.1.5. Reduction to smaller systems. We shall recast the system in new variables. Introduce the *differences of layer thickness*

$$\begin{aligned} d_1 &= h_2 - h_1, \\ d_2 &= h_3 - h_2, \end{aligned}$$

which track the displacement of interfaces, and the *shear* variables

$$\begin{aligned} w_1 &= u_2 - u_1, \\ w_2 &= u_3 - u_2. \end{aligned}$$

These together with the identities (38) and (40) give a transformation between the variables $(h_1, h_2, h_3, u_1, u_2, u_3)$ and the variables (d_1, d_2, w_1, w_2, Q). The evolution depends only on these 5 variables, and we write these equations below. In what follows, consider the parameters

$$r_1 = \frac{\rho_2}{\rho_1} = 1 - r \quad \text{and} \quad r_2 = \frac{\rho_3}{\rho_2} = 1 - rR,$$

where $r \geq 0,\ R > 0$ are positive constants (*Atwood numbers* [4]), and the rescaled variables:

$$\begin{aligned} \tilde{w}_j &= \frac{w_j}{\sqrt{r}}, \\ \tilde{t} &= t\sqrt{r}, \\ q &= \frac{Q}{\sqrt{r}}, \\ \frac{P}{(1+r_1+r_1r_2)} &= rp. \end{aligned}$$

Under these changes, our equations become

$$\begin{aligned} d_{1,t} + qd_{1,x} + \left(\frac{w_1}{3}(1-d_2) - \frac{d_1}{3}(w_1+w_2)\right)_x \\ - \left(\frac{d_1^2}{3}(2w_1+w_2) + \frac{d_1d_2}{3}(w_1+2w_2)\right)_x = 0, \end{aligned} \tag{42}$$

$$\begin{aligned} d_{2,t} + qd_{2,x} + \left(\frac{w_2}{3}(1+d_1) + \frac{d_2}{3}(w_1+w_2)\right)_x \\ - \left(\frac{d_2^2}{3}(w_1+2w_2) + \frac{d_1d_2}{3}(2w_1+w_2)\right)_x = 0, \end{aligned} \tag{43}$$

$$\begin{aligned} w_{1,t} + qw_{1,x} &+ \left(\left(\frac{2d_1+d_2}{3}\right)(1-w_1^2) - \frac{w_1w_2}{3}(1+d_1+2d_2) - \frac{w_1^2}{6}\right)_x \\ &- \frac{rR}{3}\left(\frac{1+d_1+d_2}{3}\right)_x = rp_x, \end{aligned} \tag{44}$$

$$\begin{aligned} w_{2,t} + qw_{2,x} &+ \left(\left(\frac{d_1+2d_2}{3}\right)(R-w_2^2) + \frac{w_1w_2}{3}(1-2d_1-d_2) + \frac{w_2^2}{6}\right)_x \\ &= rR(1-r)p_x, \end{aligned} \tag{45}$$

and

$$\begin{aligned} q'(t) + (F_D(d_1,d_2,w_1,w_2,q) + F_H(d_1,d_2,R))_x \\ -\frac{rR}{9}(1-2d_1-d_2)(1+d_1+2d_2)_x \\ = -F_p(d_1,d_2,r,R)p_x, \end{aligned} \tag{46}$$

where

$$F_D(d_1,d_2,w_1,w_2,q) = \left(q^2 - \left((1-2d_1-d_2)\,\frac{w_1}{3} + (2-d_1-2d_2)\,\frac{w_2}{3}\right)^2\right) + \left(\left(\frac{1-2d_1-d_2}{3}\right)(w_1+w_2)^2 + \left(\frac{1+d_1-d_2}{3}\right)w_2^2\right),$$

$$F_H(d_1,d_2,R) = \left(\frac{(1-2d_1-d_2)^2 + R((1+d_1-d_2)+(1-2d_1-d_2))^2}{18}\right)$$

and

$$\begin{aligned} F_p(d_1,d_2,r,R) &= 3D(r,R) + rD(r,R)\big[(R(r-1)-2) \\ &+ (2+R(1-2r))d_1 + (1+R(2-r))d_2\big], \end{aligned} \tag{47}$$

with

$$D(r,R) = \frac{[3+r(R(r-1)-2)]^2}{3\,[1+r(R(r-1)-1)]},$$

and where we have dropped the tildes for simplification. The set of equations (42) to (46) may now be rewritten as the *non-Boussinesq* system, given by equations (42), (43) and

$$\begin{aligned} w_{1,t} + qw_{1,x} &+ \left(\left(\frac{2d_1+d_2}{3}\right)(1-w_1^2) - \frac{w_1w_2}{3}\,(1+d_1+2d_2) - \frac{w_1^2}{6}\right)_x \\ &- \frac{rR}{3}\left(\frac{1+d_1+d_2}{3}\right)_x \\ &- \frac{r^2R}{9}\left(\frac{(1-2d_1-d_2)\,(1+d_1+2d_2)_x}{F_p(d_1,d_2,r,R)}\right) \\ &+ r\left(\frac{(F_D(d_1,d_2,w_1,w_2,q)+F_H(d_1,d_2,R))_x}{F_p(d_1,d_2,r,R)}\right) \\ &= -\frac{rq'}{F_p(d_1,d_2,r,R)}, \end{aligned} \tag{48}$$

$$\begin{aligned} w_{2,t} + qw_{2,x} &+ \left(\left(\frac{d_1+2d_2}{3}\right)(R-w_2^2) + \frac{w_1w_2}{3}\,(1-2d_1-d_2) + \frac{w_2^2}{6}\right)_x \\ &+ rR(1-r)\left(\frac{(F_D(d_1,d_2,w_1,w_2,q)+F_H(d_1,d_2,R))_x}{F_p(d_1,d_2,r,R)}\right) \\ &- \frac{r^2R^2(1-r)}{9}\left(\frac{(1-2d_1-d_2)\,(1+d_1+2d_2)_x}{F_p(d_1,d_2,r,R)}\right) \\ &= -\frac{rR(1-r)q'}{F_p(d_1,d_2,r,R)}. \end{aligned} \tag{49}$$

2.2. The Boussinesq equations

The Boussinesq limiting case, when the difference of densities are negligible, can be seen as a particular case of the equations above. First, note that in the limit $r \to 0$, equation (47) becomes

$$F_p(d_1, d_2, r, R) = 9.$$

It follows that (41) can be written in conservation form

$$q'(t) + (F_D(d_1, d_2, w_1, w_2, q) + F_H(d_1, d_2, R) + 9p)_x = 0,$$

and that the flux is a global conserved quantity depending on the boundary values of $F_D - F_H + p$. For example $q' = 0$ in a periodic domain, in which case we can set $q = 0$ by a Galilean transformation.

Thus, the three-layer shallow water Boussinesq equations in a periodic domain can be derived by setting $q = 0$ and by taking the limit $r \to 0$ in the non-Boussinesq equations (42), (43), (48) and (49). It follows that

$$\begin{aligned} &d_{1,t} + \left(\frac{w_1}{3}(1 - d_2) - \frac{d_1}{3}(w_1 + w_2)\right)_x \\ &\quad - \left(\frac{d_1^2}{3}(2w_1 + w_2) + \frac{d_1 d_2}{3}(w_1 + 2w_2)\right)_x = 0, \end{aligned} \tag{50}$$

$$\begin{aligned} &d_{2,t} + \left(\frac{w_2}{3}(1 + d_1) + \frac{d_2}{3}(w_1 + w_2)\right)_x \\ &\quad - \left(\frac{d_2^2}{3}(w_1 + 2w_2) + \frac{d_1 d_2}{3}(2w_1 + w_2)\right)_x = 0, \end{aligned} \tag{51}$$

$$w_{1,t} + \left(\left(\frac{2d_1 + d_2}{3}\right)(1 - w_1^2) - \frac{w_1^2}{6} - \left(\frac{1 + d_1 + 2d_2}{3}\right) w_1 w_2\right)_x = 0, \tag{52}$$

$$w_{2,t} + \left(\left(\frac{d_1 + 2d_2}{3}\right)(R - w_2^2) + \frac{w_2^2}{6} + \left(\frac{1 - 2d_1 - d_2}{3}\right) w_1 w_2\right)_x = 0. \tag{53}$$

We shall refer to this limit as the *Boussinesq limit*. The rescaling and limit above is a mathematically formal way of deriving the Boussinesq system, instead of the physically based approach of ignoring density variations in the inertial terms, commonly used in the literature [4].

3. Results on three-layer flows

3.1. Boundary conditions and the Benjamin-Camassa paradox

The flux q and the deviation pressure p are related by the equation (46), which may result in the non-locality of the pressure, depending on the boundary conditions. As shown before, in the Boussinesq case, the volume flux is constant (unless externally forced to be non-constant) and can be eliminated from the system.

Sidewalls or *no-flux* conditions force a behaviour similar to the non-Boussinesq case, as $q = 0$ and equation (46) becomes

$$p_x = -\frac{(F_D + F_H)_x}{F_p} + \frac{rR}{9}\frac{(1 - 2d_1 - d_2)\,(1 + d_1 + 2d_2)_x}{F_p}. \qquad (54)$$

One can then insert (54) into equations (48) and (49) and close the system, eliminating the pressure.

For the case of *periodic* boundary conditions (of period L), then we can remove the pressure from (46) and find a nonlocal evolution equation for the flux:

$$q' = -\left(\int_{-L/2}^{L/2}(F_p)^{-1}dx\right)^{-1}\int_{-L/2}^{L/2}(F_p)^{-1}(F_H + F_D)_x dx$$
$$+\frac{rR}{9}\left(\int_{-L/2}^{L/2}(F_p)^{-1}dx\right)^{-1}\int_{-L/2}^{L/2}(F_p)^{-1}\,(1 - 2d_1 - d_2)\,(1 + d_1 + 2d_2)_x\,dx.$$

One can then replace q' above in (46) to compute the pressure, which can then be substituted in (48) and (49) to close the system which itself becomes nonlocal.

A related issue is the *Benjamin-Camassa paradox* (*Camassa et al.* [15] and *Benjamin* [18]) which arises from the observation that stratified flows between two horizontal walls may not conserve horizontal momentum - a paradox as there is no apparent mechanism for a net horizontal force to be applied on the fluid.

Consider the case in which far-field conditions are imposed. There are two possibilities, either q is time-independent, and one can set $q = q' = 0$ and the sidewall case is recovered, or, one may have even stronger far-field conditions imposed on the physical variables, such as h_j achieving the same constant value and $u_j \to 0$ as $x \to \pm\infty$. Thus, $q = 0$ and one can compute the difference of the values attained by the pressure at the

far-field extremes, denoted by $[p]_{-\infty}^{+\infty}$, from equation (46), yielding

$$[p]_{-\infty}^{+\infty} = -\int_{-\infty}^{+\infty} (F_p)^{-1}(F_H + F_D)_x dx \\ - \frac{rR}{9}\int_{-\infty}^{+\infty} (F_p)^{-1}\,(1-2d_1-d_2)\,(1+d_1+2d_2)_x\,dx. \tag{55}$$

The total (horizontal) momentum is defined as the integral of the local horizontal momentum

$$M = \rho_1 h_1 u_1 + \rho_2 h_2 u_2 + \rho_3 h_3 u_3,$$

written above in the flow variables h_j, u_j. Note that the momentum equations (34) to (36) implies that

$$M_t + \left(\sum_{j=1}^{3} \rho_j h_j u_j^2 + (\rho_1-\rho_3)\frac{h_1^2}{2} + (\rho_2-\rho_3)\frac{h_2^2}{2}(\rho_1-\rho_3)h_1 h_2\right)_x = -P_x$$

and hence, rescaling the variables as in Section 2.1.5, integrating in x from $-\infty$ to $+\infty$ and using that $u_j \to 0$ at infinity and that h_j tend to a same constant value when $x \to \pm\infty$ lead to

$$\frac{d}{dt}\int_{-\infty}^{+\infty} M dx = -\,[p]_{-\infty}^{+\infty}\,.$$

Therefore, the total horizontal momentum is conserved if and only if the integrals on the right-hand side of (55) are zero, which is not the case for all choices of d_j, w_j, r and R.

This non-conservation arises from the fact that equation (46) can be thought of as an elliptic problem for the pressure, and hence allowing the propagation of information about the flow at infinite speed to $\pm\infty$. This is not the case, for example, if the rigid lid is removed and replaced with either a free-surface or a flexible lid. Note that, for $r \to 0$, which corresponds to the Boussinesq approximation, the second integral disappears and denominator of the integrand F_p tends to 1, making the right-hand side a total derivative in x and therefore the conservation of momentum is recovered.

3.2. Linear waves on quiescent flows

Consider the general situation shown in Figure 1 and described by Equations (1) to (11). By perturbing the uniform state of constant $h_j \equiv H_j$ and zero u_j, v_j, with travelling wave modes proportional to $e^{i(kx-\omega t)}$, one

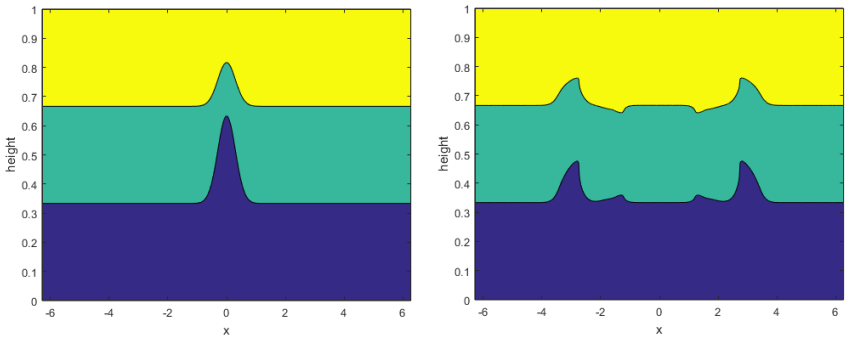

Figure 2: Evolution of a Gaussian pulse in a three-layer flow and its decomposition into mode 1 and mode 2 waves. The nonlinear equations (50) to (53) were solved to demonstrate both the splitting of pulses and the nonlinear steepening behind the mode 1 pulses.

obtains the following *dispersion relation* for ω:

$$
\begin{aligned}
&[\rho_2 \cosh(|k|H_2)(\rho_3 \coth(|k|H_3) + \rho_1 \coth(|k|H_1)) \\
&+ \sinh(|k|H_2)(\rho_2^2 + \rho_1 \coth(|k|H_1))\rho_3 \coth(|k|H_3)))]\omega^4 \\
&+ g|k|[\rho_2(\rho_3 - \rho_1)\cosh(|k|H_2) + \sinh(|k|H_2)((\rho_3 - \rho_2)\rho_1 \coth(|k|H_1) \\
&+ (\rho_2 - \rho_1)\rho_3 \coth(|k|H_3))]\omega^2 \\
&+ (g|k|)^2(\rho_3 - \rho_2)(\rho_1 - \rho_2)\sinh(|k|H_2)\omega = 0.
\end{aligned}
$$

Rescaling the variables as before and taking the shallow water limit, where $|k|H_1, |k|H_2, |k|H_3 \ll 1$, gives the equation for wave-speeds $\lambda = \omega/k$:

$$
\begin{aligned}
&(\rho_2\rho_3 R_1 + \rho_1\rho_3 R_2 + \rho_1\rho_2 R_3)\,\lambda^4 \\
&+ ((\rho_2 - \rho_1)\rho_3 R_1 R_2 + (\rho_3 - \rho_1)\rho_2 R_1 R_3 + (\rho_3 - \rho_2)\rho_1 R_2 R_3))\,\lambda^2 \\
&+ (\rho_2 - \rho_1)(\rho_3 - \rho_2)R_1 R_2 R_3 = 0.
\end{aligned}
$$

Here, $R_j = H_j/H$ with R_1/R_2, R_2/R_3 or order 1. This biquadratic equation corresponds to two modes in each direction, one being the fast mode, usually called *mode 1* and the other being the slow mode, commonly referred as *mode 2*. These are numerically illustrated in Figure 2, where the evolution of a gaussian pulse decomposes into 4 smaller pulses (righr panel), two of them travelling faster and with in-phase vertical displacements (mode 1 waves, seen at $x \approx \pm 3$) and two moving slower and out-of-phase vertical displacements (mode 2 waves, seen at $x \approx \pm 1.5$).

3.3. Symmetric solutions and evolutionary properties

In this section, we shall discuss the Boussinesq system, mainly in the special case where $R = 1$ (i.e. the jumps in density are the same on both interfaces). Denoting the vector of solutions $\mathbf{U} = (d_1, d_2, w_1, w_2)^T$, the system may be written as

$$\mathbf{U}_t + A(\mathbf{U})\mathbf{U}_x = 0, \tag{56}$$

where $A(\mathbf{U})$ is given from equations (50) to (53) by

$$-\frac{1}{3}\begin{pmatrix} w_1(1+4d_1+d_2) & w_1(1+d_1) & d_1(1+2d_1+d_2) & d_1(1+d_1+2d_2) \\ +w_2(1+2d_1+2d_2) & +w_2(2d_1) & +(d_2-1) & \\ w_1(2d_2) & w_1(2d_1+2d_2-1) & d_2(2d_1+d_2-1) & d_2(d_1+2d_2-1) \\ +w_2(d_2-1) & +w_2(d_1+4d_2-1) & & -(d_1+1) \\ 2(w_1^2-1) & (w_1^2-1) & w_1(1+4d_1+2d_2) & w_1(1+d_1+2d_2) \\ +w_1w_2 & +2w_1w_2 & +w_2(1+d_1+2d_2) & \\ (w_2^2-R) & 2(w_2^2-R) & w_2(2d_1+d_2-1) & w_1(2d_1+d_2-1) \\ +2w_1w_2 & +w_1w_2 & & +w_2(2d_1+4d_2-1) \end{pmatrix}$$

For $R = 1$, these equations are invariant under the symmetry transformation

$$\begin{aligned} d_1 &\longleftrightarrow -d_2, \\ w_1 &\longleftrightarrow -w_2. \end{aligned}$$

More formally, for $\mathbf{U} = (d_1, d_2, w_1, w_2)^T$, there is an isomorphism Φ

$$\Phi(\mathbf{U}) = (-d_2, -d_1, -w_2, -w_1)^T.$$

and the system

$$\mathbf{U}_t + A(\mathbf{U})\mathbf{U}_x = 0 \tag{57}$$

is equivalent to

$$\tilde{\mathbf{U}}_t + A(\tilde{\mathbf{U}})\tilde{\mathbf{U}}_x = 0,$$

where $\tilde{\mathbf{U}} \doteq \Phi(\mathbf{U})$. Physically, this invariance corresponds to reversing the direction of gravity and exchanging the layers accordingly. For this reason, we shall refer to this configuration when $R = 1$ as the *symmetric Boussinesq case*.

An immediate consequence is that the symmetric Boussinesq system allows pure mode 2 solutions. Suppose that

$$\begin{aligned} h_1(x,t) &= H(x,t) \\ h_2(x,t) &= h(x,t) \\ h_3(x,t) &= H(x,t), \end{aligned}$$

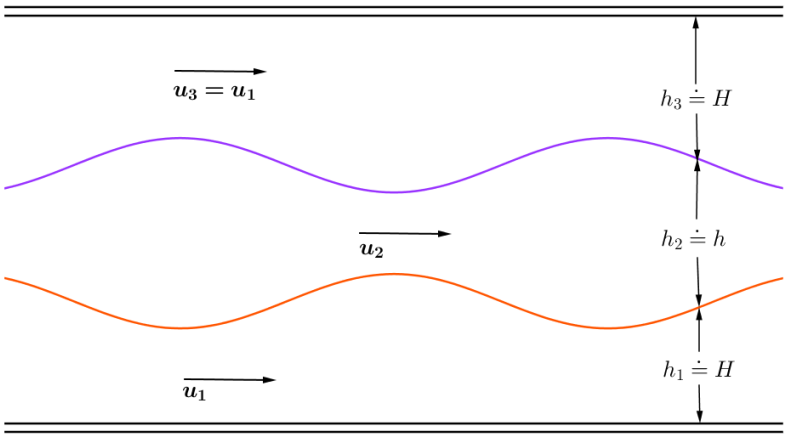

Figure 3: Illustration of a pure mode 2 solution in a three-layer flow.

as ilustrated in Figure 3. Then,

$$d_1 = h - H = -(H - h) = -d_2.$$

Define u_j in a similar fashion so that

$$w_1 = -w_2.$$

Writing

$$d \doteq d_1 \text{ and } w \doteq w_1,$$

the 4×4 system of symmetric Boussinesq equations reduces to a pair of equations given by

$$d_t + \left(\frac{w}{3}(1 + d - 2d^2)\right)_x = 0,$$
$$w_t + \left(\frac{d}{3}(1 - 2w^2) + \frac{w^2}{6}\right)_x = 0.$$

It is possible to show [19] that these pure mode 2 equations are equivalent to the two-layer shallow water ones [20]. This is physically evident in Figure 3 by imagining a boundary in the midline of the configuration. Consequently, this pure mode 2 dynamics is a two-dimensional invariant subspace of the four-dimensional system, and within that invariant subspace all prior results for the two-layer system applies. Most relevant is the result that the hyperbolic region in phase space $(d, w) \in (-1/2, 1) \times (-1/\sqrt{2}, 1/\sqrt{2})$ (with $w = w_1 = -w_2$, and $d = d_1 = -d_2$) is invariant under the evolution of the PDE. From a fluid dynamics perspective this means that for initial data satisfying this condition everywhere,

the evolution remains wavelike and does not exhibit Kelvin-Helmholtz like instabilities.

Motivated by these considerations, we propose describing the system using the variables

$$\begin{aligned} \overline{d} &= d_1 + d_2, \qquad & \tilde{d} &= d_2 - d_1, \\ \overline{w} &= w_1 + w_2, \qquad & \tilde{w} &= w_2 - w_1. \end{aligned}$$

Note that $\overline{d} = 0$ and $\overline{w} = 0$ are equivalent to the "pure" mode 2 case previously examined. Under this change of variables, the governing equations can be rewritten as

$$\overline{d}_t + \left(\frac{\overline{w}}{6} \left(2 - 3\overline{d}^2 \right) + \left(\frac{\overline{d}\tilde{w} + \tilde{d}\overline{w} - \overline{d}\tilde{d}\tilde{w}}{6} \right) \right)_x = 0, \tag{58}$$

$$\tilde{d}_t + \left(\frac{\tilde{w}}{6} \left(2 - \tilde{d}^2 \right) - \left(\frac{\overline{d}\overline{w} + \tilde{d}\tilde{w} + 3\overline{d}\tilde{d}\overline{w}}{6} \right) \right)_x = 0, \tag{59}$$

$$\overline{w}_t + \left(\frac{\overline{d}}{2} \left(2 - \overline{w}^2 \right) + \frac{\overline{w}\tilde{w}}{6} \left(1 - \tilde{d} \right) \right)_x = 0, \tag{60}$$

$$\tilde{w}_t + \left(\frac{\tilde{d}}{6} \left(2 - \tilde{w}^2 \right) + \left(\frac{\overline{w}^2}{4} - \frac{\tilde{w}^2}{12} - \frac{\overline{d}\overline{w}\tilde{w}}{2} \right) \right)_x = 0. \tag{61}$$

which, in the form (56) with $\mathbf{U} = (\overline{d}, \tilde{d}, \overline{w}, \tilde{w})^T$, has $A(\mathbf{U})$ given by

$$\frac{1}{6} \begin{pmatrix} \tilde{w} - \tilde{d}\tilde{w} - 6\overline{d}\overline{w} & \overline{w} - 6\overline{d}\tilde{w} & 2 + \tilde{d} - 3\overline{d}^2 & \overline{d}(1 - \tilde{d}) \\ -\overline{w}(1 + \tilde{d}) & -(\tilde{w} + 2\tilde{d}\tilde{w} + 3\overline{d}\overline{w}) & -\overline{d}(1 + \tilde{d}) & 2 - \tilde{d} - \tilde{d}^2 \\ 6 - 3\overline{w}^2 & -\overline{w}\tilde{w} & \tilde{w} - \tilde{d}\tilde{w} - 6\overline{d}\overline{w} & \overline{w}(1 - \tilde{d}) \\ -3\tilde{w}\overline{w} & 2 - \tilde{w}^2 & 3(\overline{w} - \overline{d}\tilde{w}) & -(\tilde{w} + 2\tilde{d}\tilde{w} + 3\overline{d}\overline{w}) \end{pmatrix}. \tag{62}$$

The phase space $\mathbb{R}^4$ can be decomposed as a direct sum of B_1 and B_2:

$$B_1 = \{\mathbf{U} = (\overline{d}, \tilde{d}, \overline{w}, \tilde{w})^T \text{ such that } \tilde{d} = \tilde{w} = 0\},$$

$$B_2 = \{\mathbf{U} = (\overline{d}, \tilde{d}, \overline{w}, \tilde{w})^T \text{ such that } \overline{d} = \overline{w} = 0\}.$$

We shall consider the evolution of periodic solutions in phase space, where they correspond to closed curves. This situation is schematically presented in Figure 4.

If the initial condition $\overline{d}|_{t=0} = \overline{w}|_{t=0} = 0$ holds for all points in the domain, then, from (58)-(61), $\overline{d} = \overline{w} = 0$ for all $t > 0$ and the system reduces to a pair of equations, which are the two-layer shallow water Boussinesq equations previously mentioned. The solution is the trapped in the invariant plane B_2 and shown in Figure 4(a).

Suppose now that the initial data is tangent to B_2 at a single point, say $x = x^*$, as shown in Figure 4(b). Thus $\mathbf{U}_x|_{t=0,x=x^*}$, which is the tangent vector to the solution curve is in B_2 and therefore it can be shown from (62) that $(A(\mathbf{U})\mathbf{U}_x)|_{t=0,x=x^*} = -\mathbf{U}_t|_{t=0,x=x^*}$ is also in this plane. Contrary to intuition, this is not enough to guarantee that the point of tangent contact will always remain in B_2. In fact the point of contact will lose tangency and then may escape from B_2 given that B_2 has co-dimension greater than one. (Such behaviour does not occur in 2×2 systems where invariant subspaces are simple waves, and periodic solutions never lose tangency to a simple wave [12].) A direct consequence of this is that periodic initial data that transverses B_2 can also leave B_2 as the wave evolves. This is shown schematically in Figure 4(c) and a numerical solution illustrating the loss of tangency is presented in Figure 5.

Now, suppose that $\tilde{d}|_{t=0} = \tilde{w}|_{t=0} = 0$, so that $\mathbf{U}|_{t=0}$ is in B_1. It follows from Equations (59) and (61) that

$$\tilde{d}_t|_{t=0} = \frac{1}{6}\left(\overline{d}\overline{w}\right)_x \neq 0, \tag{63}$$

$$\tilde{w}_t|_{t=0} = -\frac{1}{4}\left(\overline{w}^2\right)_x \neq 0, \tag{64}$$

which implies that, in general, $\tilde{d}_t \neq 0$ and $\tilde{w}_t \neq 0$ for $t > 0$. Equations (63) and (64) represent the mode 2 production of a mode 1 wave. Consequently, any solution that is initially in B_1 will immediately leave this region, as shown in Figure 4 (d). Physically, this means that no matter the initial "rest" configuration, if pycnoclines are initially displaced equally the evolution will generate mode 2 waves. Of course, "pure" mode 1 waves can be constructed using simple waves as shown below.

3.4. Simple waves

For a system of PDEs of the form (56), *simple waves* [21] (sometimes called *rarefaction waves* [22]) are special solutions that can be written as

$$\mathbf{U}(x,t) \doteq \mathbf{V}(\theta(x,t)). \tag{65}$$

These are important because they correspond to the individual waves of the system. Replacing the equation (65) in (56) yields

$$\mathbf{V}_\theta\, \theta_t + A(\mathbf{V})\mathbf{V}_\theta\, \theta_x = 0, \tag{66}$$

which has a solution only if $A(\mathbf{V})\mathbf{V}_\theta$ is proportional to $\mathbf{V}_\theta$, leading to the eigenvalue problem

$$\left[A(\mathbf{V}(\theta)) - \lambda(\theta) I\right] \mathbf{V}_\theta(\theta) = 0, \tag{67}$$

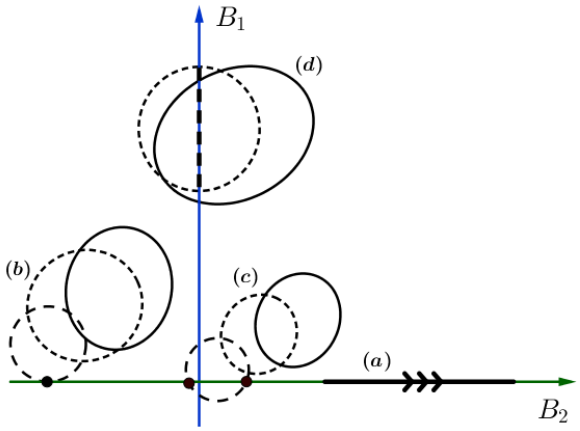

Figure 4: Decomposition of the four-dimensional phase space in the modal variables and schematic representation of a few solutions: in (c), it is shown that a given solution that initially touches the B_2 might not intersect it anymore in future times. This happens even if the initial condition is tangent to B_2 as in (b). On the other hand, if the initial condition is a pure mode 2, the solution will remain in mode 2 for all time (up to breaking) schematically shown in (a). The same does not happen for a initial condition lying in B_1. This set is not an invariant subspace and a general solution escapes as soon as it evolves on time, as seen in (d).

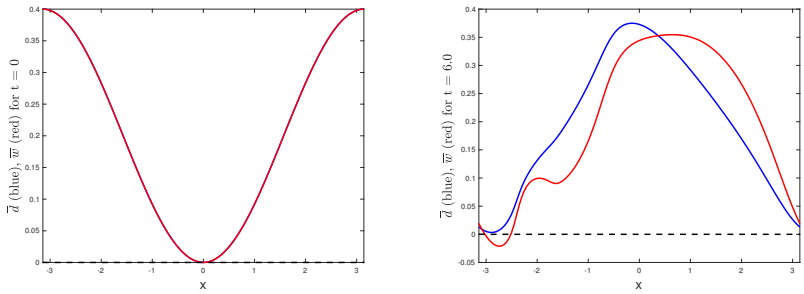

Figure 5: Numerical example of a solution which is initially tangent to the invariant plane B_1. Note that at $t = 0$, the solution satisfies $\overline{d}'(x_0) = \overline{w}'(x_0) = 0$ for $x_0 = 0$ and therefore this is a point of tangency. At $t = 6$, this condition is no longer satisfied for any x_0 in the domain.

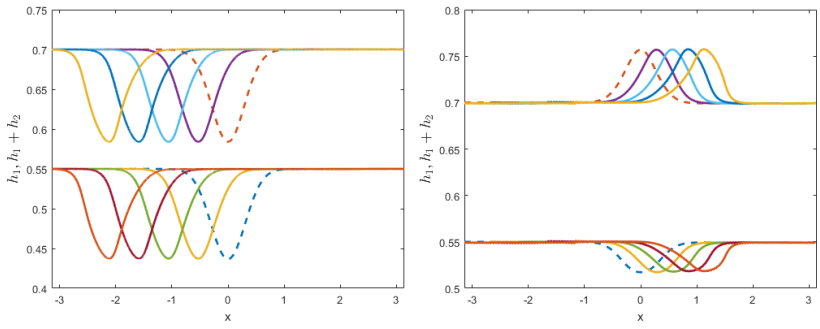

Figure 6: The evolution of the interfaces for a mode 1 (left) and mode 2 (right) simple wave solutions to the Boussinesq equations (50)-(53). The vertical extent of the channel is $[0, 1]$. The dashed line is the initial data and the solution is shown at various times. Note the nonlinear steepening of the wave.

and where $\theta(x, t)$ must obey the hyperbolic PDE (if the original system is hyperbolic)

$$\theta_t + \lambda(\theta)\theta_x = 0. \tag{68}$$

The eigenvectors $\mathbf{V}_\theta$ from equation (67) yield, for each eigenvalue family, a vector field in the phase space whose integral curves are the simple waves ($\mathbf{V}_\theta$ is tangent to these curves). For regions in phase space where our system is strictly hyperbolic, this implies the existence of 4 curves through each point. Each of these curves is a simple wave and is invariant under the evolution of the PDE: solutions starting on these curves remain on them, only the parametrisation $\theta(x, t)$ changes with time. Thus the 4 eigenvectors at each point yield a local basis of the phase space providing a decomposition based on in terms of the wave speeds λ, or, physically speaking, in terms of the two (fast) mode 1 waves and the two (slow) mode 2 waves. Examples of numerically computed evolution of simple in the physical system are shown in Figures 6, 7 and 8. Figures 7 and 8 also highlight the effectiveness of the modal decomposition in approximating the different families.

We remark also that the Boussinesq systems have a "left-right" symmetry which can be seen in phase space. Given a simple wave through a point $\mathbf{U} = (d_1, d_2, w_1, w_2)^T$ at which the characteristic speed is λ, there is a corresponding "reflected" simple wave through the point $\tilde{\mathbf{U}} = (d_1, d_2, -w_1, -w_2)^T$ with characteristic speed $-\lambda$, i.e. propagating in the other direction. This is physically intuitive and can be seen explicitly by the structure of $A(\mathbf{U})$.

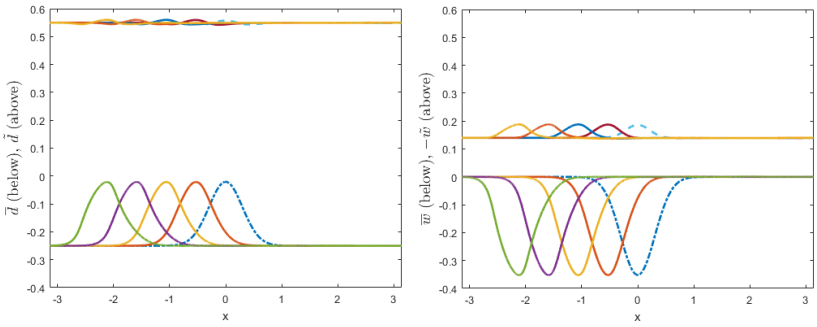

Figure 7: Evolution of the mode 1 simple wave solution shown in Figure 6, now in the modal variables of (58)-(61). Note the relatively small $\tilde{d}$ and $\tilde{w}$ components.

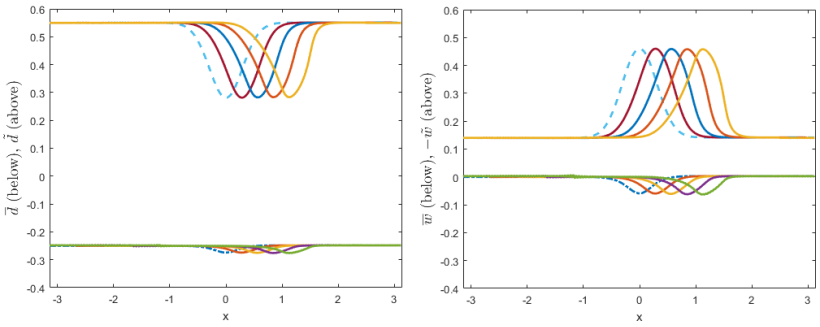

Figure 8: Evolution of the mode 2 simple wave solution shown in Figure 6, now in the modal variables of (58)-(61). Note the relatively small $\bar{d}$ and $\bar{w}$ components.

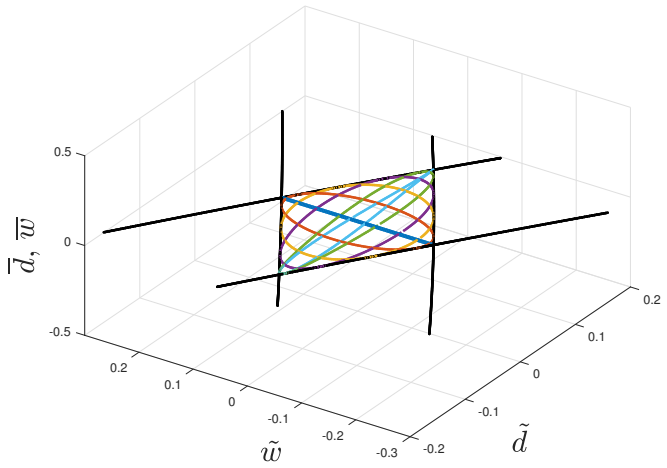

Figure 9: Evolution of a solution of (58)-(61) starting in the invariant mode 2 plane, trapped by four bounding simple waves (in black). The initial condition is given by the blue straight line joining two edges of the quadrilateral, and the coloured curves are the solutions at different times.

Simple waves are of crucial importance in the study of nonlinear first order hyperbolic PDEs. In two-dimensional systems, they define invariant regions [23], [12] due to the property that simple waves do not allow a general solution to cross it tangentially [24]. Furthermore, for mixed-type first order PDE systems, if an initial condition can be bounded by simple waves that do not themselves reach the boundary of the hyperbolic region, then the solution will remain hyperbolic until breaking. Therefore, using simple waves one can build the largest such region, which can be seen as a sharp bound to on hyperbolic initial data that prevents the solution straying into the elliptic region and therefore rendering the problem ill-posed [12]. Figure 9 illustrates the use of simple waves. It shows the evolution of a periodic initial condition in the invariant plane $\bar{d} = \bar{w} = 0$, and bounding simple waves.

In systems larger than two-dimensions, simple waves still provide a construction of "pure" wave solutions, but are less useful for bounding solutions, except in particular cases, for example when there is an invariant subspace as discussed above and showed in Figure 9.

Our first question is to explore whether there are other two-dimensional subspaces for mode 1 or mode 2 waves. These manifolds would contain families of both simple waves that exist for each mode

of motion and would allow one to construct initial data that has waves propagating in both directions in a single mode of the system.

Such manifolds do not exist for general systems. The reason is due to the non-existence of an integrating factor for general differential forms in dimensions greater than two and, which implies that Riemann invariants, which would allow us to construct such manifolds, do not exist generically [25].

In general, a n-dimensional system of PDEs of the form (56) can be associated with up to n Riemann invariants. The j^{th} Riemann invariant is a smooth function R_j associated to the j^{th} eigenvalue, and satisfying

$$\nabla R_j = \mu \mathbf{w}_j,$$

where μ is a function (the integrating factor) and $\mathbf{w}_j$ is the j^{th} left eigenvector of the system,

$$\mathbf{w}_j^T A(\mathbf{U}) = \mathbf{w}_j^T \lambda_j.$$

In our case, all of these are functions of $\mathbf{U} = (\overline{d}, \tilde{d}, \overline{w}, \tilde{w})^T$.

Since the gradient of the j^{th} Riemann invariant is parallel to the j^{th} left eigenvector, it follows that the k^{th} right eigenvector $\mathbf{v}_k$ is tangent to the surface defined by constant R_j if $j \neq k$, because $\mathbf{w}_j \cdot \mathbf{v}_k = \delta_{j,k}$. Furthermore, if $\mathbf{U}_k(\theta)$ is an integral curve of $\mathbf{v}_k$ (i.e. a simple wave), then the j^{th} Riemann hypersurface contains this curve since

$$\frac{d}{d\theta} R_j(\mathbf{U}_k(\theta)) = \nabla R_j \cdot \mathbf{v}_k = 0.$$

Thus, in general, the hypersurface defined by $R_j =$ constant contains $n-1$ linearly independent simple waves associated to the $n-1$ right eigenvalues of the system, λ_k for $k \neq j$.

Hence, if one wishes a family of, say, mode 2 simple waves to form a two-dimensional manifold in a four-dimensional phase space, it is necessary and sufficient that there be Riemann invariants associated to the other two eigenvalues. The intersection of the surfaces defined by these two Riemann invariants then defines the manifold.

We have numerically attempted to construct such surfaces. This involves choosing a point in phase space and computing the two simple wave curves from a particular family (mode 1 or mode 2) that go through that point. These are the "spines" of an attempt to construct a mesh of simple waves: along each of these spines at regular intervals we construct new simple waves transversal to the spine. If the resulting mesh lies on a surface - i.e. all the simple waves intersect - we have evidence of an invariant subspace for the problem. As shown in Figures 10 and 11, families of simple waves for either mode 1 or mode 2 in the symmetric Boussinesq system do not intersect each other and therefore do not form a surface.

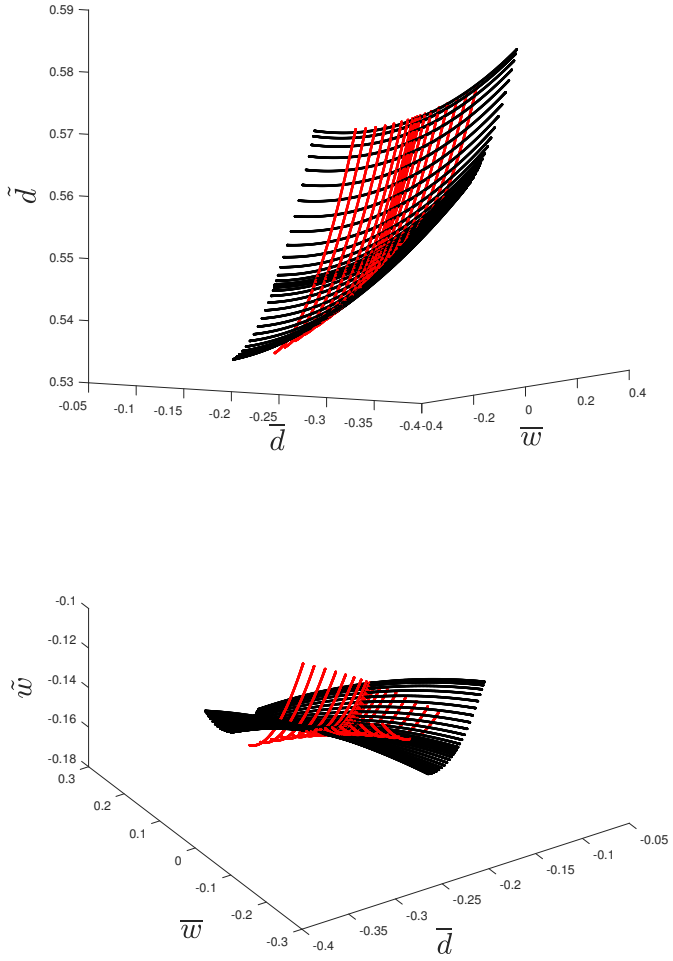

Figure 10: Families of mode 1 simple waves for the symmetric Boussinesq system (62). The two colours correspond to the two eigenvalues. Top: the projection onto $\tilde{w} = 0$ shows that the curves almost lie on a surface. Bottom: For the projection onto $\tilde{d} = 0$, there is clear non-intersection of simple waves.

Nevertheless the remarkable proximity to a surface can motivate different approximations that reduce the system.

3.5. Two-dimensional reduced models

Although the modal decomposition does not hold in general, Figures 7 and 8 suggest that an approximate decomposition might work well for the system. For mode 1 waves, notice that $\tilde{d} \approx$ constant and that $\tilde{w}$ varies slightly through the whole evolution of the wave. Therefore their dynamics could be simplified. We propose to set $\tilde{d} \doteq \tilde{d}_0 \equiv$ constant, and solve Equation (59) to obtain $\tilde{w} = f(\overline{d}, \overline{w}; \tilde{d}_0)$ and hence get a two-dimensional system by replacing the latter on the equations (58) and (60) for $\overline{d}$ and $\overline{w}$. The results of this approach are shown by Figures 12-15. In this particular example, we choose a Gaussian initial condition satisfying $\tilde{d}(x, 0) = 0$ and $\tilde{w}(x, t) = 0$ so that the solution lies in the hypothetical mode 1 plane defined by B_1. Note that there is a very good agreement between the full solution (plotted in solid blue) and the one given by the approximate 2 dimensional reduced model (plotted in dashed red lines). Figures 12 and 13 show the evolution of the mode 1 wave (as computed by the equations (58) and (60) whereas Figure 14 shows the error arising from assuming a constant $\tilde{d}$ and Figure 15 shows the post-computed $\tilde{w}$. Since $\tilde{w} = f(\overline{d}, \overline{w}; \tilde{d}_0)$, the approximation qualitatively captures the mode 1 (fast) component of $\tilde{w}$ but fails to capture its mode 2 (slower) component.

In Figures 16-19, a similar reduction is attempted for a mode 2 wave, and the agreement between both models is even better. For these, we choose an initial condition satisfying $\overline{d}(x, 0) = -0.15$ and $\overline{w}(x, 0) = 0$ so that it lies in a plane parallel to the invariant plane B_2. In this case, we reduced the system by considering $\overline{d} = \overline{d}_0 = -0.15$ and $\overline{w} = f(\tilde{d}, \tilde{w}; \overline{d}_0)$ as given by Equation (58). Figures 16 and 17 show the evolution of the mode 2 wave (as computed by the equations (59) and (61) whereas Figure 18 shows the error arising from assuming a constant $\bar{d}$ and Figure 19 shows the post-computed $\bar{w}$. Since $\bar{w} = f(\tilde{d}, \tilde{w}; \bar{d}_0)$, the approximation qualitatively captures the mode 2 (slow) component of $\bar{w}$ but, as expected, fails to capture its faster mode 1 component.

4. Conclusions

We have derived the equations for long waves in a three-layer channel and explored some of their properties, both in the Boussinesq and in the general case. In the Boussinesq case, when the density jumps between layers is equal, a simple change of variables aids in separating the mode 1 and mode 2 dynamics. We then make use of simple waves in the Boussi-

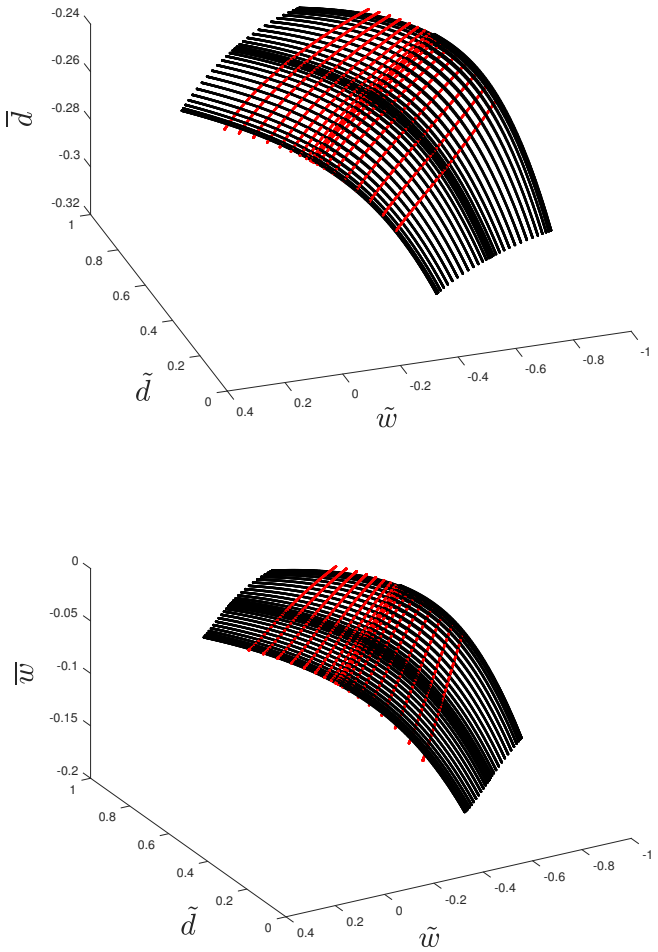

Figure 11: Families of mode 2 simple waves for the symmetric Boussinesq system (62). Both top and bottom figures show that, although the agreement is surprisingly good, these families do not form a surface.

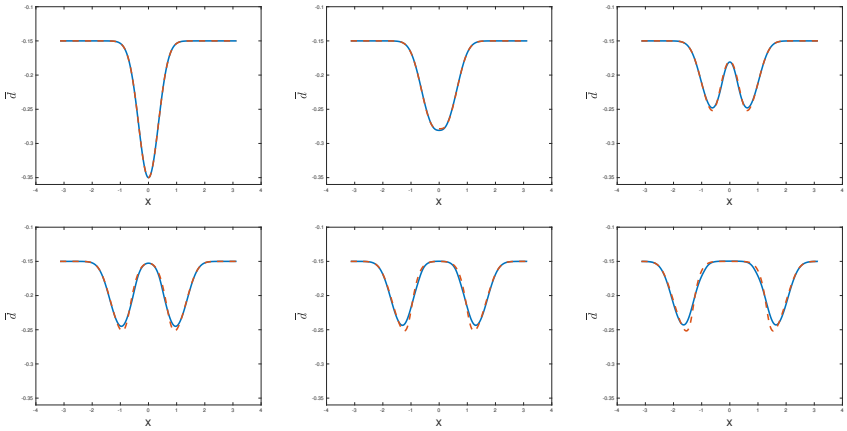

Figure 12: Solution of a reduced model for mode 1 waves (dashed line) compared to the solution of the full system (58) to (61) (solid line). From top left to bottom right, $\overline{d}$ is plotted for $t = 0, 0.6, 1.2, 1.8, 2.4$ and 3.0.

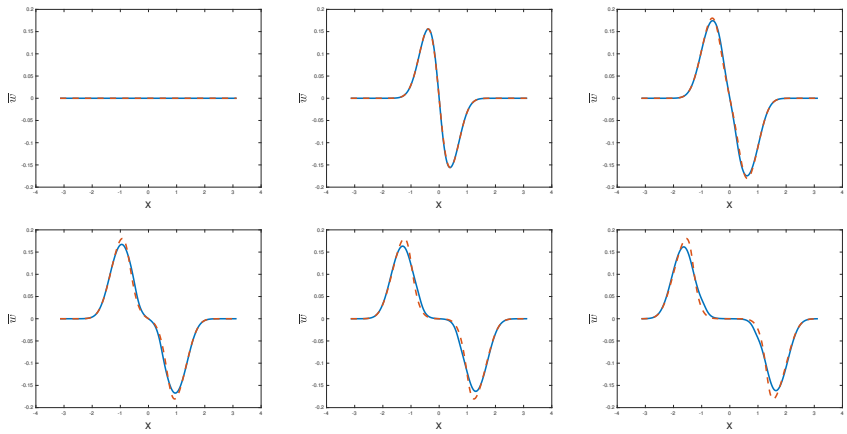

Figure 13: Solution of a reduced model for mode 1 waves (dashed line) compared to the solution of the full system (58) to (61) (solid line). From top left to bottom right, $\overline{w}$ is plotted for $t = 0, 0.6, 1.2, 1.8, 2.4$ and 3.0.

nesq case to test whether lower dimensional solution spaces can be constructed. We find that such invariant subspaces cannot be constructed, but that some ad-hoc reductions motivated by the computations are successful at capturing much of the features of the solution. These ideas provide a framework for creating reduced models which warrant further exploration.

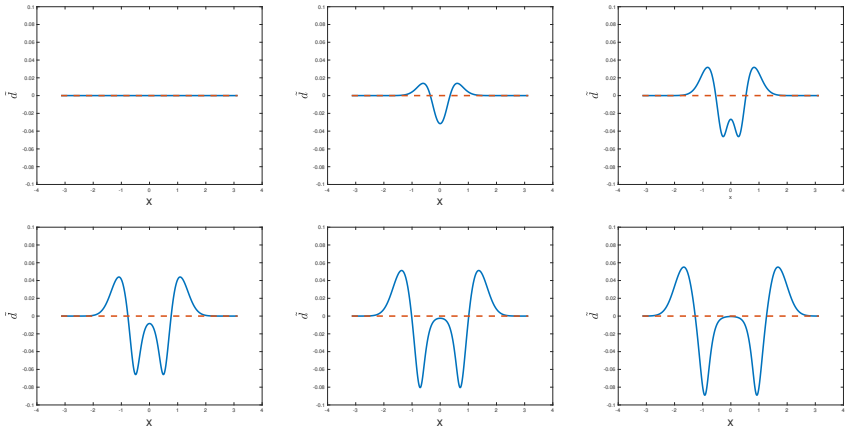

Figure 14: Solution of a reduced model for mode 1 waves (dashed line) compared to the solution of the full system (58) to (61) (solid line). From top left to bottom right, $\tilde{d}$ is plotted for $t = 0, 0.6, 1.2, 1.8, 2.4$ and 3.0.

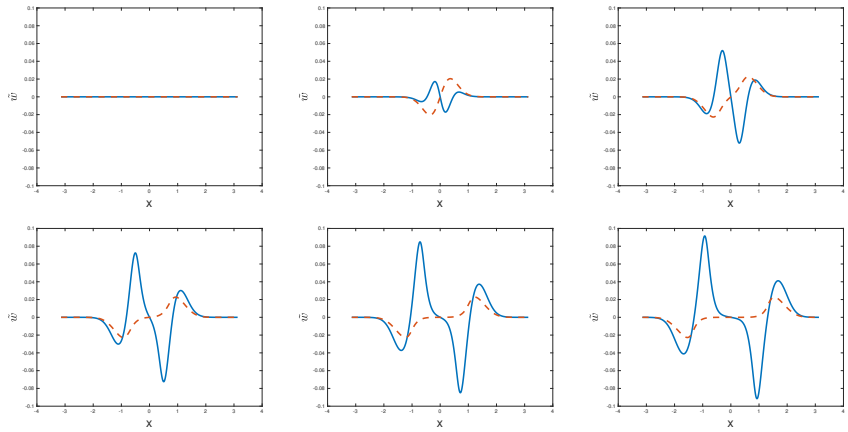

Figure 15: Solution of a reduced model for mode 1 waves (dashed line) compared to the solution of the full system (58) to (61) (solid line). From top left to bottom right, $\tilde{w}$ is plotted for $t = 0, 0.6, 1.2, 1.8, 2.4$ and 3.0.

All solutions that we compute break after some time, and an interesting question is the inclusion of shocks in the dynamics. In particular whether there is a choice of shock conditions which can allow for a realistic model of entrainment between the layers.

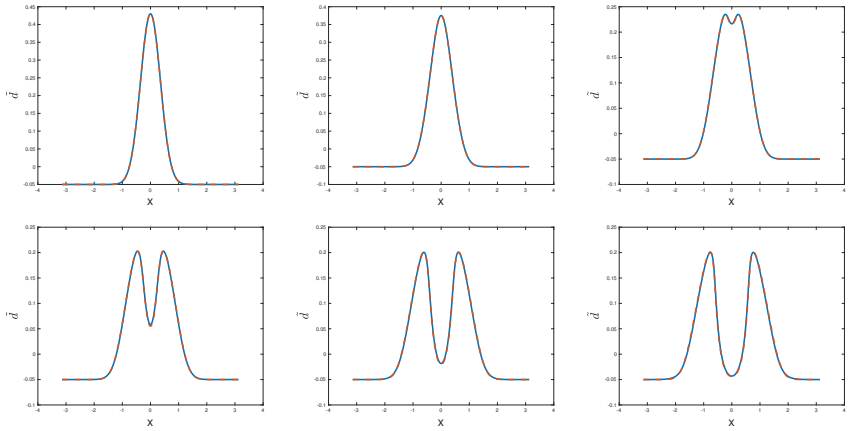

Figure 16: Solution of a reduced model for mode 2 waves (dashed line) compared to the solution of the full system (58) to (61) (solid line). From top left to bottom right, $\tilde{d}$ is plotted for $t = 0, 0.6, 1.2, 1.8, 2.4$ and 3.0.

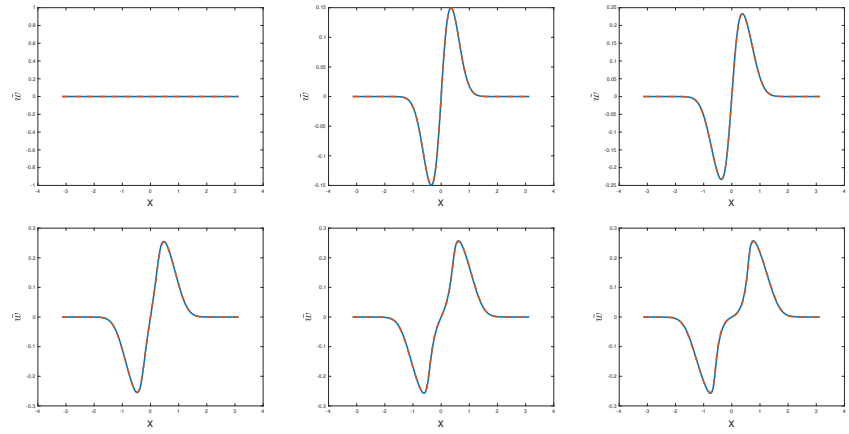

Figure 17: Solution of a reduced model for mode 2 waves (dashed line) compared to the solution of the full system (58) to (61) (solid line). From top left to bottom right, $\tilde{w}$ is plotted for $t = 0, 0.6, 1.2, 1.8, 2.4$ and 3.0.

Acknowledgments

The work of F.d.M.V. was supported by the CPNq - Conselho Nacional de Desenvolvimento Científico e Tecnológico (Brasil), under the grant number 249770/2013-0, to whom both researchers are grateful.

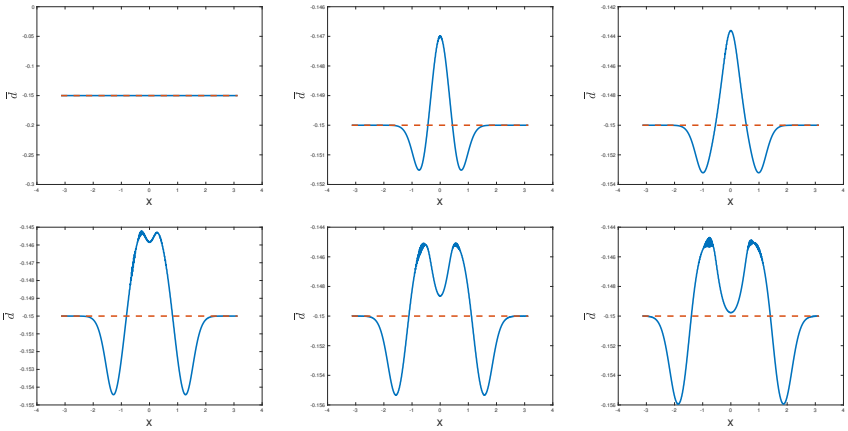

Figure 18: Solution of a reduced model for mode 2 waves (dashed line) compared to the solution of the full system (58) to (61) (solid line). From top left to bottom right, $\overline{d}$ is plotted for $t = 0, 0.6, 1.2, 1.8, 2.4$ and 3.0.

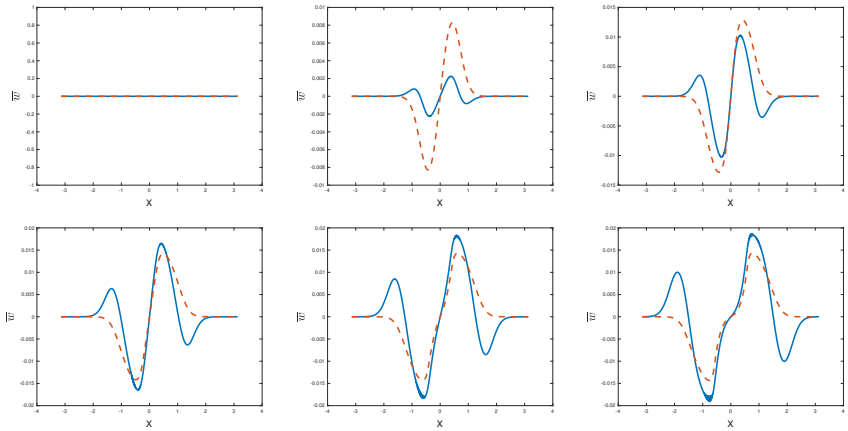

Figure 19: Solution of a reduced model for mode 2 waves (dashed line) compared to the solution of the full system (58) to (61) (solid line). From top left to bottom right, $\overline{w}$ is plotted for $t = 0, 0.6, 1.2, 1.8, 2.4$ and 3.0.

References

1. T. P. Stanton and L. Ostrovsky, Observations of highly nonlinear internal solitons over the continental shelf, *Geophys. Res. Lett.* 25:2695–2698 (1998).
2. D. Christie and R. White, The morning glory of the gulf of carpentaria, *Aust. Meteorol. Mag* 41:21–60 (1992).

3. K. R. Helfrich and W. K. Melville, Long nonlinear internal waves, *Annu. Rev. Fluid Mech.* 38:395–425 (2006).
4. B. Cushman-Roisin and J.-M. Beckers, *Introduction to Geophysical Fluid Dynamics - Physical and Numerical Aspects*, 2nd ed., Academic Press, Waltham, 2011.
5. R. Long, Long waves in a two-fluid system, *J. Meteorol.* 13:70–74 (1956).
6. D. J. Benney, Long non-linear waves in fluid flows, *Journal of Mathematics and Physics* 45:52–63 (1966).
7. R. Grimshaw, E. Pelinovsky, and T. Talipova, The modified korteweg-de vries equation in the theory of large-amplitude internal waves, *Nonlinear Processes in Geophysics* 4:237–250 (1997).
8. M. Miyata, Long internal waves of large amplitude, Nonlinear water waves, Springer, 1988, pp. 399–406.
9. W. Choi and R. Camassa, Fully nonlinear internal waves in a two-fluid system, *Journal of Fluid Mechanics* 396:1–36 (1999).
10. Y. J. Yang, Y. C. Fang, M.-H. Chang, S. R. Ramp, C.-C. Kao, and T. Y. Tang, Observations of second baroclinic mode internal solitary waves on the continental slope of the northern south china sea, *Journal of Geophysical Research: Oceans* 114 (2009), no. C10.
11. L. Ovsyannikov, Two-layer "shallow water" model, *Journal of Applied Mechanics and Technical Physics* 20:127–135 (1979).
12. A. Boonkasame and P. A. Milewski, The stability of large-amplitude shallow interfacial non-Boussinesq flows, *Stud. in Appl. Math.* 128:40–58 (2011).
13. R. Rotunno, J. B. Klemp, G. H. Bryan, and D. J. Muraki, Models of non-Boussinesq lock exchange flow, *J. Fluid Mech.* 675:1–26 (2011).
14. P. A. Milewski and E. G. Tabak, Conservation law modelling of entrainment in layered hydrostatic flows, *J. Fluid Mech.* 772:272–294 (2015).
15. R. Camassa, S. Chen, G. Falqui, G. Ortenzi, and M. Pedroni, An inertia 'paradox' for incompressible stratified Euler fluids, *J. Fluid Mech.* 695:330–340 (2012).
16. P. G. Baines, *Topographic Effects in Stratified Flows*, 1st ed., Cambridge University Press, Cambridge, 1995.
17. R. S. Johnson, *A Modern Introduction to the Mathematical Theory of Water Waves*, 1st ed., Cambridge University Press, Cambridge, 1997.
18. T. B. Benjamin, On the Boussinesq model for two-dimensional wave montions in heterogeneous fluids, *J. Fluid Mech.* 165:445–474 (1986).
19. F. de Melo Viríssimo, *Dynamical System Methods for Waves in Fluids: Stability, Breaking and Mixing*, Ph.D. thesis Department of Mathematical Sciences, University of Bath, United Kingdom (in preparation, 2018).
20. P. A. Milewski, E. G. Tabak, C. V. Turner, R. R. Rosales, and F. A. Menzaque, Nonlinear stability of two-layer flows, *Comm. Math. Sci.* 2:427–442 (2004).
21. P. Lax, *Hyperbolic Systems of Conservation Laws and the Mathematical Theory of Shock Waves*, 1st ed., CBMS-NSF Regional Conference Series in Applied Mathematics, 1973.
22. A. A. Mailybaev and D. Marchesin, Hyperbolicity singularities in Rarefaction Waves, *J. Dynam. Differ. Eq.* 20:1–29 (2008).
23. L. Chumakova, F. A. Menzaque, P. A. Milewski, R. R. Rosales, and E. G. Tabak, Shear instability for stratified hydrostatic flows, *Comm. on Pure and Applied Math* 62:183–197 (2009).

24. L. Chumakova and E. G. Tabak, Simple waves do not avoid eigenvalue crossings, *Comm. on Pure and Applied Math* 63:119–132 (2010).
25. G. B. Whitham, *Linear and Nonlinear Waves*, 1st ed., Wiley-Interscience, 1974.

Department of Mathematical Sciences, University of Bath, Bath, United Kingdom, BA2 7AY

2.2. Reduction to Two-layer Shallow Water Boussinesq Equations

As mentioned in the Section 3.3 in article [dMVM17], it turns out that the symmetric Boussinesq (mode 2) equations, given by

$$\begin{aligned} d_t + \left(\frac{w}{3}(1 + d - 2d^2)\right)_x &= 0, \\ w_t + \left(\frac{d}{3}(1 - 2w^2) + \frac{w^2}{6}\right)_x &= 0. \end{aligned}$$

are equivalent to the two-layer shallow water Boussinesq system [MTT+04]. The visual explanation for that is presented in the Figure 2-1 below.

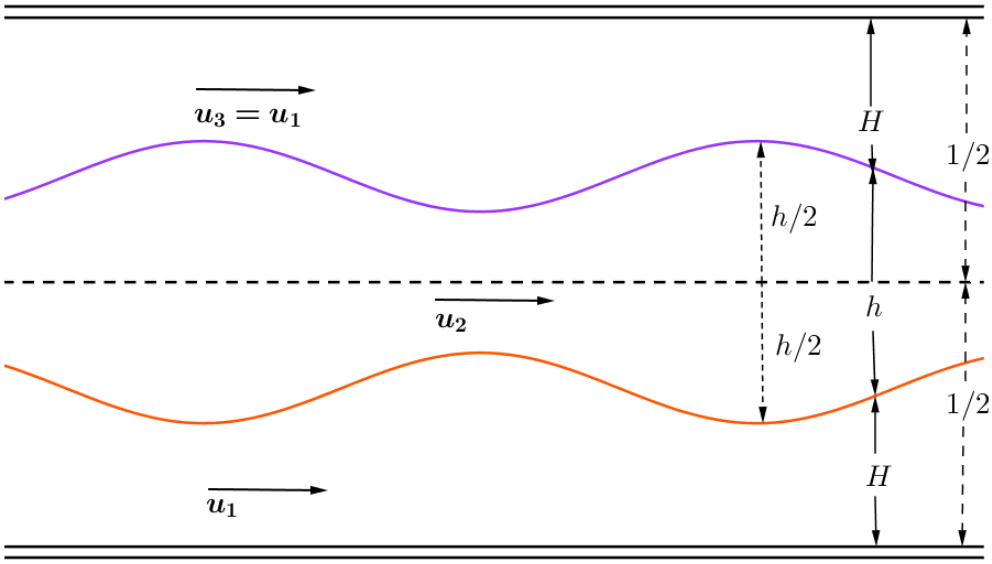

Figure 2-1: *Illustration of a 'pure' mode 2 solution and its reduction to a pair of 'two-layer solutions'.*

This fact can be mathematically proved as follows. First, introduce the variable

$$\tilde{d} = h_3 - \frac{h_2}{2}$$

as shown in Figure 2-2. This variable 'replaces' d_2 in this new configuration, keeping the same meaning.

Recall that

$$h_3 = \frac{1 + d_1 + 2d_2}{3}, \quad h_2 = \frac{1 + d_1 - d_2}{3},$$

so that, using that $d \doteq d_1 = -d_2$ one gets

$$h_3 = \frac{1 - d}{3}, \quad h_2 = \frac{1 + 2d}{3}.$$

Hence,

$$\tilde{d} = h_3 - \frac{h_2}{2} = \left(\frac{1 - d}{3}\right) - \frac{1}{2}\left(\frac{1 + 2d}{3}\right) = \frac{1 - 4d}{6}$$

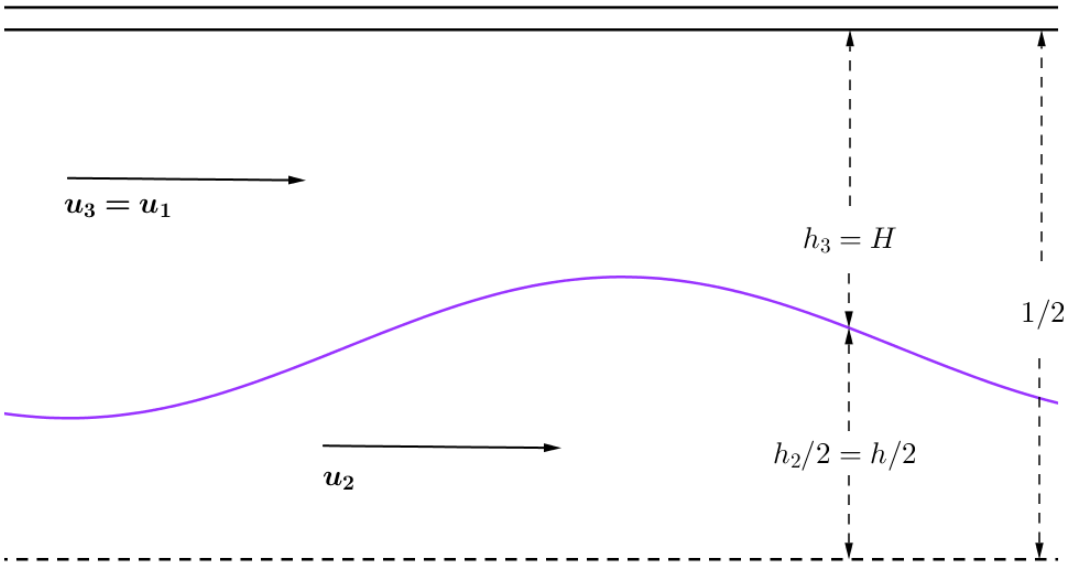

Figure 2-2: *Reduction from the three-layer shallow water Boussinesq problem to two-layer one.*

and so

$$d = \frac{1}{4} - \frac{3}{2}\tilde{d}.$$

Now, replacing these identities into the equations gives

$$(-2\tilde{d})_t + \left(\frac{w}{2}(1-(-2\tilde{d})^2)\right)_x = 0,$$
$$\sqrt{2}(\sqrt{2}w)_t + \left(\frac{-2\tilde{d}}{2}(1-(\sqrt{2}w)^2)\right)_x = 0.$$

Now, redefine

$$\tilde{d} = -2\tilde{d} \quad \text{and} \quad w = \sqrt{2}w.$$

Finally, by substituting these into the equations above and dropping the tildes one gets

$$d_t + \frac{1}{\sqrt{2}}\left(\frac{w}{2}(1-d^2)\right)_x = 0,$$
$$w_t + \frac{1}{\sqrt{2}}\left(\frac{d}{2}(1-w^2)\right)_x = 0,$$

which, rescaling x as $\sqrt{2}x$, gives the two-layer shallow water equations in the Boussinesq case, as shown in [MTT$^+$04].

We conclude by remarking that is not hard to verify that this reduction works for other situations. The idea is shown in Figure 2-3 for the case of a five-layer flow with a modal symmetry.

2.3. Conclusions

The formulation of the three-layer shallow water problem was considered and the governing equations were derived in the more general non-Boussinesq context, in which the equations are non-local as the pressure appears as an unknown. We show that this is not the case for the Boussinesq equations and we put a special emphasis on the latter. In addition, motivated by [BM11], we provide a simple and mathematically rigorous

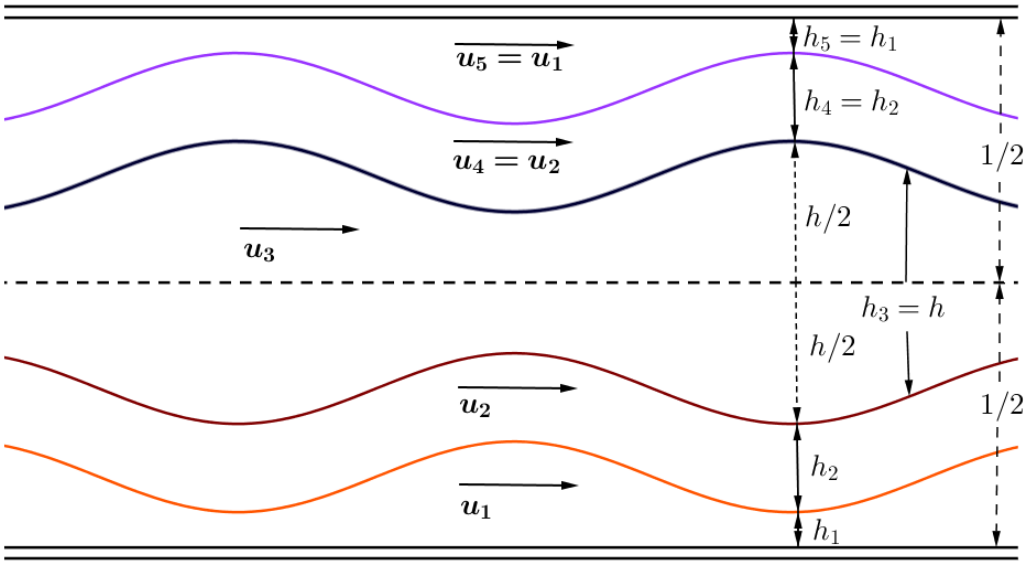

Figure 2-3: *Reduction from a five-layer symmetric flow to a three-layer one.*

way to derive the Boussinesq equations from the non-Boussinesq one, through the limit $r \longrightarrow 0$, which justifies this being called the 'Boussinesq limit'.

The first result proved in the paper is the existence of a special symmetry in the system in the physically relevant case $R = 1$, which allows the existence of 'pure' mode 2 solutions, with these constituting an invariant subspace of dimension 2 lying in the four-dimensional phase space. In other words, we proved that if a wave starts being a pure mode 2, it will remain mode 2 until it breaks or loses hyperbolicity.

Motivated by this result, a new 'modal' change of variables is proposed, which allows one to decompose the phase space in the direct sum of two sets: one of mode 1 waves, denoted by B_1 and another of mode 2 waves, denoted by B_2. While the B_2 is actually a two-dimensional invariant space, as mentioned above, we prove that this is not the case for B_1. In fact, any wave starting in B_1 is subjected to a dynamics given by Equations (63) and (64) which makes it to leave B_1 immediately.

As 'pure' mode 1 initial conditions do not preserve this feature in general, one use an alternative way to find these solutions. This was done through simple waves [CT10], which is a very important dynamical system tool for the study of mixed-type systems of hyperbolic PDEs [CMM$^+$09].

Finally, we find that, although a modal decomposition that preserves mode 1 solutions is not always possible, an approximate decomposition do preserve the main features of the solution and reduces the problem from 4 to 2 dimensions. These new reduced models are then explored numerically and their performance is compared to the full model.

Another example of a three-layered flow that is very important in applications is derived when (in a three-layer flow) we remove the upper rigid lid and replace the upper layer by an unbounded layer of lighter and dynamically passive fluid. Despite the flow being composed by three layers, only two of them are dynamically active and for this reason, this is called a 'two-and-a-half-layer' flow, being a good model for surface and internal ocean waves [SS53]. This model is studied in the next chapter.

Chapter 3

Nonlinear Stability of Two-layer Shallow Water Flows with a Free Surface

In this chapter, we turn our focus to two-and-a-half-layer flows under the shallow water limit. Again, we start by formulating the problem in the general non-Boussinesq case and then investigate both dynamics and stability properties of the flow in the case where the upper layer has zero density, also known as the 'free surface' case. The work presented in this chapter is joint with Paul A. Milewski, and will be submitted shortly to the scientific journal *European Journal of Mechanics B/Fluids* [dMVM18b].

3.1. Outline of the Article

Ocean waves are one of the most studied phenomena in geophysical fluid mechanics. The idea of modelling the ocean as a 'three-layer' flow has been explored by researchers at least since the late 40's [SS53]. In this configuration, we have two layers of 'heavy' fluid, which models the ocean water (*e.g.* salty and fresh layers of water), and an unbounded layer of passive and almost zero density fluid, which represents the atmosphere. For this reason, this is called 'two-and-a-half-layer' configuration [Bai95], as one of the layers is dynamically passive. The fact that the displacement of surface waves is very small if compared to the internal waves suggests that this could be approximated by a two-layer rigid lid problem [Ovs79]. Although the latter results in a system of 2 equations of much simpler mathematical treatment, it only captures the baroclinic internal wave (see Section 2.1 of the paper) modes and not the barotropic waves. This motivates further studies on the more complex two-and-a-half-layer problem.

Section 1 highlights the main prior mathematical and numerical advances in the field. In Section 2, the problem is stated and the governing equations are derived. It leads to a 4×4 system of PDEs, which are one-dimensional in space and local even in the non-Boussinesq case, contrasting to both two- and three-layer rigid lid problems, whose equations are nonlocal in general [BM11], [dMVM17]. We show the six conservation laws for the system [Bar06], which are essential in the study of shock solutions [MT15].

In Section 3, we turn our attention to the dynamics and stability analysis of the equations. These are of mixed-type, as discussed in Section 3.2, meaning that a hyperbolic (wave-like) solution might become elliptic in finite time, before it breaks, resulting in an ill-posedness (or nonlinear instability) of the system. In Section 3.3, we show that the actual stability properties of the system depends only on two 'baroclinic' quantities and use this result to project the phase space in the plane, allowing the transition to ellipticity to be clearly monitored. This result also suggests a new change of variables that allow us to rewrite the system in terms of these two quantities plus the other two 'barotropic' ones, which only affect the dynamics and not the stability. In Section 3.4, we explore this idea further through the use of simple waves [CT10] which correspond to the individual baroclinic and barotropic waves of the system. We then discuss the use of these as a tool to study the long time well-posedness [CMM$^+$09] of the system and raise questions that we aim to answer in the future.

We conclude with Section 4 by summarising our findings and pointing out directions for future investigations.

Appendix B: Statement of Authorship

This declaration concerns the article entitled:									
Nonlinear Stability of Two-layer Shallow Water Flows with a Free Surface									
Publication status (tick one)									
draft manuscript	X	**Submitted**		**In review**		**Accepted**		**Published**	
Publication details (reference)	To be submitted to: European Journal of Mechanics B/Fluids Authors: Francisco de Melo Viríssimo, Paul Antoine Milewski								
Candidate's contribution to the paper (detailed, and also given as a percentage).	The bulk of the calculations have been performed by the author of the thesis (100%). All authors contributed equally to the presentation of the content (50%). The numerical computations have been performed by the author of the thesis (100%).								
Statement from Candidate	This paper reports on original research I conducted during the period of my Higher Degree by Research candidature.								
Signed					**Date**	7.11.2018			

NONLINEAR STABILITY OF TWO-LAYER SHALLOW WATER FLOWS WITH A FREE SURFACE

F. DE MELO VIRÍSSIMO[1] AND P. A. MILEWSKI[2]

Abstract. The problem of two layers of immiscible fluid, bordered above by an unbounded layer of passive fluid and below by a flat bed, is formulated and discussed. The resulting equations are given by a first order, four-dimensional system of PDEs of mixed-type. The relevant physical parameters in the problem are presented and used to write the equations in a non-dimensional form. The conservation laws for the problem, which are known to be only six, are explicitly written and discussed in both non-Boussinesq and Boussinesq cases. Both dynamics and nonlinear stability of the Cauchy problem are discussed, with focus on the case where the upper unbounded passive layer has zero density, also called the free surface case. In this situation, we prove that the stability of a solution depends only on two parameters: the shear and the difference of layer thickness, the former being the most important one. We also discuss the use of simple waves as a tool to bound solutions and preventing a hyperbolic initial data to become elliptic. We conclude presenting further directions for this research.

1 Introduction

Internal waves are a major topic of scientific interest [HM05], playing a key role in climate and weather studies [SO98], [RSG10], and mathematical models and their analysis play an important part in their understanding [Maj03], [Ped82]. Internal waves can, in certain cases be modelled as interfacial waves, which are waves propagating due to the difference in density between layers of fluid. This approach simplifies the problem substantially and yet may be used to model well the horizontal propagation of disturbances.

The correspondence between interfacial (or layered) models and the more geophysically relevant continuous stratification case is clear when the stratification has

[1]Department of Mathematical Sciences, University of Bath, United Kingdom. e-mail: F.de.Melo.Virissimo@bath.ac.uk.

[2]Corresponding Author. Department of Mathematical Sciences, University of Bath, BA2 7AY, Bath, United Kingdom. e-mail: P.A.Milewski@bath.ac.uk.

sharp pycnoclines but is also used more broadly based on the idea of an "effective layer depth". This is when the layer depths are chosen to match the wave-speeds of the first few modes arising from the physical stratification. In general, layered flow models in the geophysical context are considered in the long wave (or 'shallow water') limit, where horizontal length scales are much larger than layer depths. The resulting models can be either weakly or strongly nonlinear, and dispersive or not. KdV equations arise in the balance of weak dispersion and weak nonlinearity [Ben66], [GPT97] whereas MCC type equations arise in the fully nonlinear, weakly dispersive case [Miy88],[CC99]. Strongly nonlinear non-dispersive models yield first order PDEs of mixed-type which allow for the study of breaking waves and instabilities arising from large shear. Such phenomena are difficult to study in MCC systems where it is not known whether waves can break, and where stability is difficult to study and instabilities tend to be "filtered" for numerical simulations.

In this paper we focus on this strongly nonlinear, non-dispersive case, and we study the dynamics of two layers of immiscible fluids, bounded below by a horizontal bottom and above by an unbounded layer of fluid, which is dynamically passive but has density, contributing hydrostatically to the pressure. This is sometimes called a 'two-and-a-half-layer' configuration in contrast with the two-layer free surface case which we also study and for which the upper fluid has zero density [Bai95]. The PDEs resulting from these equations are of mixed-type: hyperbolic or elliptic, depending on the local layer depths and shear. In such a mixed-type model, a crucial mathematical question is whether initially wave-like (hyperbolic) solutions remain inside the hyperbolic domain. It is known that this is always the case for two-layer flows with a rigid lid in the Boussinesq approximation [MTT$^+$04], but that it fails in the non-Boussinesq case [BM11], where more restricted initial data needs to be imposed to ensure hyperbolicity.

For two-layer flows with a free surface, the situation is similar: a wave-like initial condition might also leave the hyperbolic region before it breaks [Ovs79], meaning that the Cauchy problem is ill-posed (or nonlinearly unstable). This fact contrasts to one-layer flows with a free surface, as the latter is known to be always well posed and connected to the two-layer Boussinesq equations through a map [CMM$^+$09b]. The stability of these equations has been an active topic of research for decades [SS53], [Arm86], [Law90], but most progress has been made towards numerical studies [CMP01], [CDFNGVn11] rather than analytical ones [BC08], [GK14], [JC14]. In particular, no explicit criteria that prevents a solution to leave the hyperbolic region is known, although local stability was proven [Mon15]. In this paper, we shed some light into the problem by presenting a way of visualising the phase plane in two dimensions, and use simple waves [CT10], [MM08] to study the stability of the system.

The paper is organised as follows. In Section 2, we first state the problem and

derive the governing equations for the general (*i.e.* non-Boussinesq) case resulting in a semilinear system of first-order PDEs. The relevant physical parameters for the problem are introduced and used to write the system in a non-dimensional form. Some limit cases are discussed, in particular the Boussinesq case (in which the density differences contributes only in the buoyancy terms) and the free surface case (in which the density in the upper unbounded and passive layer of fluid is assumed to be zero), being the latter a very common model for internal ocean waves. Section 2 concludes with a discussion of the conservation laws for this problem in both non-Boussinesq and Boussinesq cases. In Section 3, we turn our attention to the dynamical and nonlinear stability properties of the model. It is shown that in the free surface case, the stability of the system depends only on two physical quantities: the shear and the difference of layer thickness. This result allows a characterisation of the phase space and its hyperbolic region in a plane, and to see the transition to ellipticity without the need to for a four-dimensional space (as the PDE system is 4×4). Finally, we discuss the use of simple waves as a way to look into individual waves of the system, as well as a dynamical system tool to investigate and prevent the transition from the hyperbolic to the elliptic region. In Section 4 we summarise our findings and discuss further extensions to the present work.

2 Two-and-a-half-layer shallow water flows

Consider a two-dimensional, irrotational flow of ideal, incompressible and immiscible fluids in two layers, under the action of gravity, bounded below by a horizontal rigid bottom and above by an unbounded layer of fluid, as shown in Figure 1. The dynamics in the upper layer of fluid is neglected and all its effects in the dynamics of the flow is due to the hydrostatic pressure exerted on the lower layers.

The fluid density, pressure and velocity fields in each layer are given by ρ_j, $p_j(x,y,t)$ and $\mathbf{u}_j(x,y,t) = (u_j(x,y,t), v_j(x,y,t))$ respectively, with $j = 1$ representing the lower layer and $j = 2$ representing the upper layer. The passive unbounded fluid above, represented by $j = 0$, has no velocity field and the pressure due to it is assumed to be hydrostatic below a reference level height H_{ref} at which it is constant (of course, the resulting equations are independent of H_{ref}). Usually this represents is a layer of much lower density such as the atmosphere above a stratified ocean. The height of each of the active layers is given by $h_j(x,t)$ and the interface between the layers are given by $\Sigma_1 = \{y = h_1\}$ and $\Sigma_2 = \{y = h_1 + h_2\}$, as schematically indicated in Figure 1. In this paper, we only consider the case where $\rho_1 \geq \rho_2 \geq \rho_0$. In the real world (*e.g.* the ocean), ρ_1 usually varies from $1010 - 1050\ kg/m^3$ (very salty water), ρ_2 ranges from $999 - 1010\ kg/m^3$ (fresh water) and ρ_0 (atmosphere) is considerably smaller, being around $1.2\ kg/m^3$ at

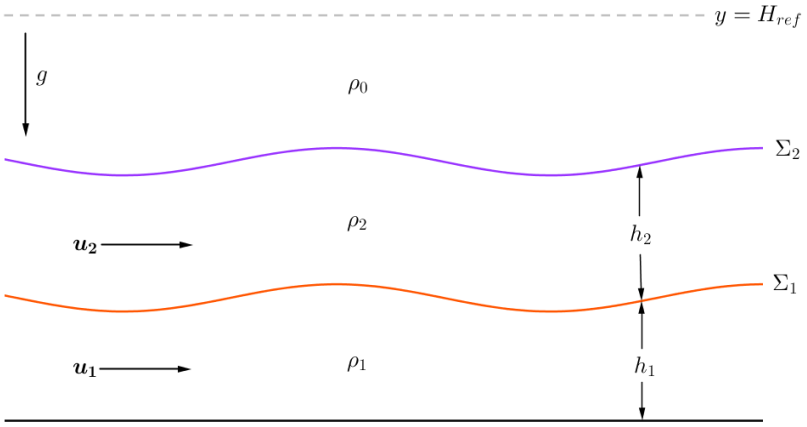

Figure 1: Schematic illustration for the two-and-a-half-layer problem.

the sea level.

The mathematical model [CRB11], [Bai95] for the dynamics in each layer is given by the incompressible Euler equations

$$\rho_j \frac{D\mathbf{u}_j}{Dt} = -\nabla p_j - \mathbf{F}_j, \tag{2.1a}$$

$$\nabla \cdot \mathbf{u}_j = 0, \tag{2.1b}$$

for $j = 1, 2$, with $\mathbf{F}_j$ being the force field due to external sources. In this model, only gravitational forces play a significant role and so we will consider $\mathbf{F}_j = (0, \rho_j g)$.

The boundary conditions are the impermeability condition at the bottom wall

$$v_1 = 0 \quad \text{on} \quad y = 0, \tag{2.2}$$

the kinematic conditions (KBC) and the dynamic condition (DBC) on Σ_1 respectively given by

$$h_{1,t} + u_1 h_{1,x} = v_1, \tag{2.3a}$$
$$h_{1,t} + u_2 h_{1,x} = v_2, \tag{2.3b}$$
$$p_1 = p_2, \tag{2.3c}$$

while on Σ_2 those conditions are

$$(h_1 + h_2)_t + u_2 (h_1 + h_2)_x = v_2, \tag{2.4a}$$
$$p_2 = p_0. \tag{2.4b}$$

Considering the normal vector on Σ_1, $\mathbf{n} = (-h_{1,x}, 1)$ and combining (2.3a) and (2.3b), gives

$$\mathbf{n} \cdot \mathbf{u}_1 = \mathbf{n} \cdot \mathbf{u}_2 \tag{2.5}$$

on the interface Σ_1, which implies the continuity of normal velocity condition between the active fluid. The tangential velocity, however, can be discontinuous at the interface.

This gives us a set of 6 first order equations with 6 boundary conditions for the 6 unknowns u_j, v_j, p_j, $j = 1, 2$. This is a *free boundary problem*, as the domain is also unknown and appears through h_1 and h_2 in the boundary conditions. This configuration is called the 'two-and-a-half-layer' model.

2.1 Nondimensionalisation and relevant parameters

We introduce the following non-dimensional parameters

$$\tilde{x} = x/L, \quad \tilde{y} = y/H, \quad \tilde{t} = t(\sqrt{gH}/L), \quad \tilde{\rho}_j = \rho_j/\overline{\rho},$$
$$\tilde{h}_j = h_j/H, \quad \tilde{u}_j = u_j/\sqrt{gH}, \quad \tilde{v}_j = v_j/\mu\sqrt{gH}, \quad \tilde{p}_j = p_j/\overline{\rho}gH.$$

Here $\overline{\rho} = (\rho_1 + \rho_2)/2$ is the average density in the layers, H and L are respectively the typical reference height and length and

$$\mu = \frac{H}{L} \tag{2.6}$$

is the *long wave (or shallow water) parameter*, which is small in the shallow water limit. Physically, $H = H_1 + H_2$, where H_j is the undisturbed height for the j-th layer of fluid. From now on, we will drop the tildes and work only with the rescaled non-dimensional variables. A direct consequence of the rescaling is that

$$\overline{\rho} \doteq \frac{\rho_1 + \rho_2}{2} = 1. \tag{2.7}$$

2.2 Shallow water limit and the governing equations

The *shallow water* (or *long wave*) limit corresponds to the case $\mu \ll 1$, which implies that the horizontal velocity is well represented by its average and that the pressure is hydrostatic. The vertical mean of u_j, for $j = 1, 2$ is defined by

$$\overline{u_j}(x,t) \doteq \frac{1}{h_j(x,t)} \int_{y_j(x,t)}^{y_j(x,t)+h_j(x,t)} u_j(x,y,t)dy,$$

where $y_j(x,t)$ is the coordinate of the lower interface of the j-th layer. The averaged quantities $\overline{v_j}$ and $\overline{p_j}$ can be defined in a similar fashion. Consequences of the shallow

water limit are that the pressure is hydrostatic, and that, if the flow is irrotational in each layer,

$$u_j(x,y,t) = \overline{u_j}(x,t) + \mathcal{O}(\mu^2). \tag{2.8}$$

This means the equations for the mean horizontal velocities can be decoupled from the vertical components [dMV18], resulting in a closed system for $\overline{u_j}$ and h_j. For simplicity we drop the bars and in the shallow water limit $\mu \longrightarrow 0$, the governing equations become

$$h_{1,t} + (h_1 u_1)_x = 0, \tag{2.9}$$

$$h_{2,t} + (h_2 u_2)_x = 0, \tag{2.10}$$

$$\rho_1 \left((h_1 u_1)_t + \left(h_1 u_1^2\right)_x\right) + (\rho_1 - \rho_0)\left(\frac{h_1^2}{2}\right)_x + (\rho_2 - \rho_0) h_1 h_{2,x} = 0, \tag{2.11}$$

$$\rho_2 \left((h_2 u_2)_t + \left(h_2 u_2^2\right)_x\right) + (\rho_2 - \rho_0)\left(\frac{h_2^2}{2}\right)_x + (\rho_2 - \rho_0) h_2 h_{1,x} = 0. \tag{2.12}$$

For more details, the reader is referred to [dMVM17], where a similar derivation for the three-layer rigid-lid shallow water equations is carried out.

Note that these constitute 4 equations for the 4 variables u_1, u_2, h_1 and h_2, which makes the system mathematically closed. The (hydrostatic) pressure do not appear as an additional unknown in these equations, meaning that they are local evolution equations even in the non-Boussinesq case and for any boundary conditions in the horizontal direction. This is a major difference from the layered problems with a rigid lid [BM11], [dMVM17], where the pressure appears in the momentum equations in the non-Boussinesq case as an additional unknown, generally requiring a nonlocal equation to close the problem. This difficulty appears because the pressure at the lid (or another reference level) is unknown whereas in the present case the pressure is known in a reference location.

We note that of the three density ratios appearing in the problem

$$\frac{\rho_1 - \rho_0}{\rho_1}, \quad \frac{\rho_2 - \rho_0}{\rho_1} \quad \text{and} \quad \frac{\rho_2 - \rho_0}{\rho_2},$$

result from only 2 independent parameters (say ρ_0/ρ_1 and ρ_2/ρ_1).

2.3 Limiting cases

There are generally several further approximations possible in this problem. One can make the *free surface approximation* where $\rho_0 = 0$. This is applicable, for example when modelling interfacial waves in the ocean, with the atmosphere represented in the model by the upper unbounded layer having much lower density. In this approximation, the number of independent parameters reduces from 2 to 1.

Both the dynamics and stability for this case will be discussed in detail in Section 3.

A second possible approximation is the *Boussinesq approximation* [dMV18]. This is usually an approximation imposed *ab initio* by considering that the density differences only affect the buoyancy terms and not the acceleration terms. Under this approximation, Equations (2.11) and (2.12) then become

$$(h_1u_1)_t + \left(h_1u_1^2\right)_x + (\rho_1 - \rho_0)\left(\frac{h_1^2}{2}\right)_x + (\rho_2 - \rho_0)h_1h_{2,x} = 0, \tag{2.13}$$

$$(h_2u_2)_t + \left(h_2u_2^2\right)_x + (\rho_2 - \rho_0)\left(\frac{h_2^2}{2}\right)_x + (\rho_2 - \rho_0)h_2h_{1,x} = 0, \tag{2.14}$$

were the densities multiplying the acceleration terms where replaced by the average density $\overline{\rho} = 1$. In contrast with the rigid lid case, the Boussinesq approximation in the free surface case does not change the nature of the equations. It only changes the numerical value of the coefficients of the buoyancy terms, and the physical interpretation of the resulting conservation laws. On the other hand, the Boussinesq approximation in the rigid lid case changes the nature of equations by making them local [BM11], [dMVM17].

From the two-and-a-half-layer Boussinesq equations, one can then derive the two-layer rigid-lid Boussinesq equations as a special limiting case. In the limit of when the ratio of the speed of the internal mode to the surface mode tends to zero in (2.9), (2.10), (2.13), (2.14), which occurs when $(\rho_1 - \rho_2)/\rho_0 \ll 1$ with ρ_0 fixed [MT15], the two-layer rigid-lid Boussinesq equations are recovered. Introducing the variables

$$d = h_1 - h_2, \quad w = u_1 - u_2, \quad D = h_1 + h_2, \quad P = h_1u_1 + h_2u_2, \tag{2.15}$$

under appropriate rescaling, taking the limit $(\rho_1 - \rho_2)/\rho_0 \longrightarrow 0$, one can obtain

$$d_t + \left(\frac{w}{2}(1 - d^2)\right)_x = 0, \tag{2.16}$$

$$w_t + \left(\frac{d}{2}(1 - w^2)\right)_x = 0, \tag{2.17}$$

$$\left(\frac{w^2}{2}(1 - d^2) + (\rho_2 - \rho_0)D + \frac{1}{8}(1 + d^2)\right)_x = 0, \tag{2.18}$$

$$D_t + P_x = 0. \tag{2.19}$$

where the first two equations are the two-layer rigid-lid equations and are independent of the last two. The physical interpretation of these is discussed in [MT15].

2.4 Conservation laws

A *conservation law* is an expression of the form

$$(q(x,t))_t + (F(q(x,t)))_x = 0 \tag{2.20}$$

where $q(x,t)$ is the quantity conserved and $F(q)$ is the flux of q. Conservation laws reflect physical principles and can be used to provide realistic physics when waves break and discontinuous solutions result [Smo94]. For example, appropriate choices of conservation laws can be used as part of a model in stratified flows to understand the macroscopic consequences of the interfacial wave breaking [MT15] with or without entrainment between layers. They can also be useful to verify the accuracy of certain numerical methods and devise conservation law based ones [LeV02].

It is well known that the systems discussed here have exactly 6 linearly independent conservation laws [Bar06]: 2 conservations of mass, 2 conservations of circulation, conservation of total momentum and conservation of total energy. In what follows, we note that the variables h_j and u_j can be written as a function of the conserved quantities and hence the expressions below are consistent with Equation (2.20).

2.4.1 Consevation of mass

The conservation of mass in each layer is stated by equations (2.9), (2.10) obtained previously. Note that, since the flow is incompressible and ρ_j is constant, the conservation of mass can also be seen as *conservation of volume*.

2.4.2 Conservation of circulation

Expanding the derivatives in the momentum equations (2.11), (2.12) and using the conservation of mass above leads to conservation laws for the layer velocities:

$$u_{1,t} + \left(\frac{u_1^2}{2} + \tilde{\rho}_{11}h_1 + \tilde{\rho}_{21}h_2\right)_x = 0, \tag{2.21a}$$

$$u_{2,t} + \left(\frac{u_2^2}{2} + \tilde{\rho}_{22}h_1 + \tilde{\rho}_{22}h_2\right)_x = 0. \tag{2.21b}$$

with the new '*reduced*' densities given by $\tilde{\rho}_{i,j} = (\rho_i - \rho_0)/\rho_j$, for $j = 1, 2$.

Physically, these are better interpreted as conservation of circulation by taking their linear combinations. Define $w_1 = \rho_1 u_1 - \rho_2 u_2$. Then,

$$w_{1,t} + \left(\frac{1}{2}\left(\rho_1 u_1^2 - \rho_2 u_2^2\right) + (\rho_1 - \rho_2)h_1\right)_x = 0 \tag{2.22}$$

which states the conservation of circulation around Σ_1. Defining $w_2 = \rho_2 u_2 - \rho_0 u_0$, (recall $u_0 = 0$), then,

$$w_{2,t} + \left(\frac{u_2^2}{2} + (\rho_2 - \rho_0)(h_1 + h_2) \right)_x = 0 \tag{2.23}$$

which states the conservation of circulation around Σ_2.

2.4.3 Volume flux and conservation of total momentum

Defining $M = \rho_1 u_1 h_1 + \rho_2 u_2 h_2$ and adding the momentum equations gives

$$M_t + \left(\rho_1 u_1^2 h_1 + \rho_2 u_2^2 h_2 + (\rho_1 - \rho_0) \frac{h_1^2}{2} + (\rho_2 - \rho_0) \frac{h_2^2}{2} + (\rho_2 - \rho_0) h_1 h_2 \right)_x = 0 \tag{2.24}$$

A related quantity to momentum is the total volume flux (or discharge) defined by $Q = u_1 h_1 + u_2 h_2$. This quantity satisfies

$$Q_t + \left(u_1^2 h_1 + u_2^2 h_2 + \tilde{\rho}_{11} \frac{h_1^2}{2} + \tilde{\rho}_{22} \frac{h_2^2}{2} \right)_x + (\tilde{\rho}_{21} h_1 h_{2,x} + \tilde{\rho}_{22} h_2 h_{1,x}) = 0 \tag{2.25}$$

which is not a conservation law since $\tilde{\rho}_{21} \neq \tilde{\rho}_{22}$ in general. However, in the Boussinesq case, from equations (2.13), (2.14) we have

$$Q_t + \left(u_1^2 h_1 + u_2^2 h_2 + (\rho_1 - \rho_0) \frac{h_1^2}{2} + (\rho_2 - \rho_0) \frac{h_2^2}{2} + (\rho_2 - \rho_0) h_1 h_2 \right)_x = 0 \tag{2.26}$$

Thus, the Boussinesq approximation conserves discharge (which is indistinguishable from its "momentum").

These conservations laws should be contrasted with the rigid lid case for 2 (or more) layers. In that case, the discharge can be shown not to depend on x and in the Boussinesq approximation, to be a constant. Further, in the non-Bousinesq case, the evolution equation for Q is useful in calculating the nonlocal equation for the pressure [BM11] and the momentum is not generally conserved [CCF$^+$12].

2.4.4 Conservation of total energy

The total energy of the system can be defined as $E = K + P$, where K is the *kinetic energy*

$$K = \frac{\rho_1}{2} h_1 u_1^2 + \frac{\rho_2}{2} h_2 u_2^2$$

and P is the *potential energy*

$$\begin{aligned} P &= \int_0^{h_1} \rho_1 z dz + \int_{h_1}^{h_1+h_2} \rho_2 z dz + \int_{h_1+h_2}^{H_{\text{ref}}} \rho_0 z dz \\ &= \frac{(\rho_1 - \rho_0)}{2} h_1^2 + \frac{(\rho_2 - \rho_0)}{2} (h_1 + h_2)^2 + \frac{\rho_0}{2} g H_{\text{ref}}^2. \end{aligned}$$

The conservation law for E is therefore given by

$$E_t + \left(\frac{\rho_1 h_1 u_1^3 + \rho_2 h_2 u_2^3}{2} + (\rho_1 - \rho_2) h_1^2 u_1 + (\rho_2 - \rho_0)(h_1 u_1 + h_2 u_2)(h_1 + h_2) \right)_x = 0. \tag{2.27}$$

3 Dynamics and stability

The two-and-a-half-layer non-Boussinesq model discussed in this paper is a quasi-linear 4×4 system of PDEs which, by equations (2.9) to (2.12), can be written as

$$\mathbf{U}_t + A(\mathbf{U})\mathbf{U}_x = 0, \tag{3.1}$$

where

$$\mathbf{U} = (h_1, h_2, u_1, u_2)^T \tag{3.2}$$

and

$$A(\mathbf{U}) = \begin{pmatrix} u_1 & 0 & h_1 & 0 \\ 0 & u_2 & 0 & h_2 \\ \tilde{\rho}_{11} & \tilde{\rho}_{21} & u_1 & 0 \\ \tilde{\rho}_{22} & \tilde{\rho}_{22} & 0 & u_2 \end{pmatrix}, \tag{3.3}$$

with $\tilde{\rho}_{i,j}$ being the 'reduced' densities introduced in Section 2.4.2.

Physical solutions for (3.1) must satisfy $h_j \geq 0$, with no *a priori* restrictions on u_j. We note that $h_j = 0$ are invariant subspaces of codimension 1 in the four-dimensional phase space. Moreover, we note that a solution that initially satisfies $h_j \geq 0$ will never cross $h_j = 0$ and leave this region. In addition, a solution that is tangent to one (or both) of these hyperplanes at a point will remain tangent all throughout its evolution. This is numerically illustrated in Figure 2 for a solution initially satisfying $h_1(x_1, 0) = 0$ and $h_2(x_2, 0) = 0$.

3.1 Linear waves and fundamental modes

Consider the general situation showed in Figure 1 and described by equations (2.1a) to (2.5). Disturbing the uniform quiescent state of constant $h_j = H_j$ and zero u_j, v_j as in a standard Kelvin-Helmholtz linear stability analysis, one obtains travelling wave modes proportional to $e^{i(kx-\omega t)}$, with ω given by the following dispersion

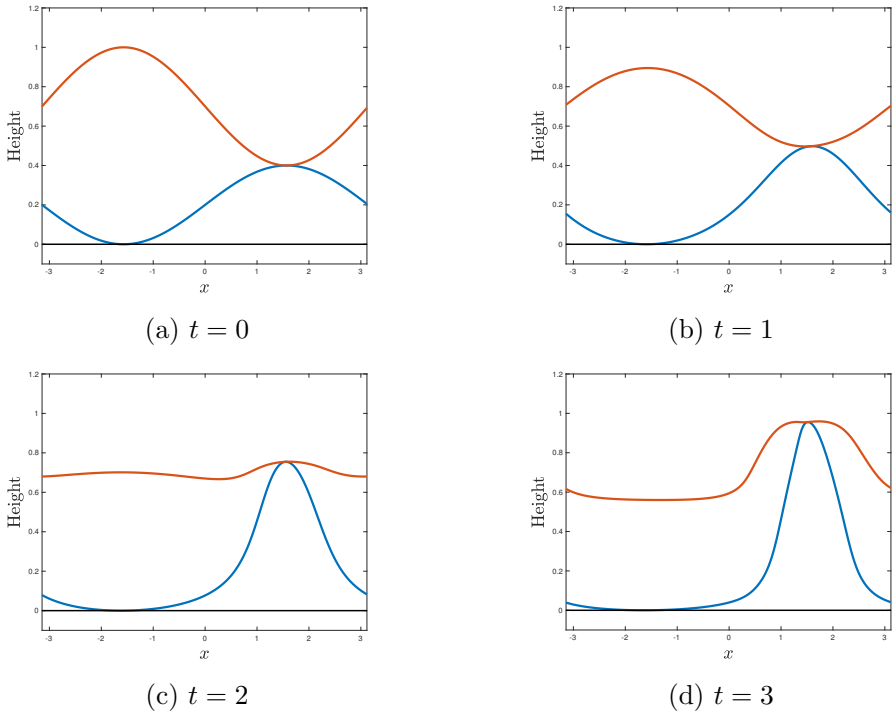

(a) $t = 0$ (b) $t = 1$

(c) $t = 2$ (d) $t = 3$

Figure 2: Numerical example of tangency to the hypersurfaces defined by $h_1 = 0$ and $h_2 = 0$. The profile in blue corresponds to h_1, while $h_1 + h_2$ is plotted in red. This solution has a initial condition satisfying $h_1(x_1, 0) = 0$ and $h_2(x_2, 0) = 0$, for $x_1 = -\pi/2$ and $x_2 = \pi/2$.

relation:

$$\begin{aligned}
&\Big(\rho_1 \coth(|k|H_1)(\rho_0 \sinh(|k|H_2) + \rho_2 \cosh(|k|H_2)) \\
&+ \rho_2(\rho_2 \sinh(|k|H_2) + \rho_0 \cosh(|k|H_2))\Big)\omega^4 \\
&+ g|k|\Big((\rho_2 - \rho_1)(\rho_0 \sinh(|k|H_2) + \rho_2 \cosh(|k|H_2)) \\
&\qquad - (\rho_2 - \rho_0)(\rho_1 \sinh(|k|H_2) \coth(|k|H_1) + \rho_2 \cosh(|k|H_2))\Big)\omega^2 \\
&+ g^2|k|^2(\rho_2 - \rho_0)(\rho_1 - \rho_2) \sinh(|k|H_2) = 0.
\end{aligned}$$

By rescaling the variables and taking the long wave limit , where $|k|H_j \ll 1$, one gets the equation for the wave-speeds $\lambda = \omega/|k|$:

$$\lambda^4 - (\tilde{\rho}_{11}R_1 + \tilde{\rho}_{22}R_2)\,\lambda^2 + \tilde{\rho}_{22}\epsilon R_1 R_2 = 0, \tag{3.4}$$

where $R_j = H_j/(H_1 + H_2)$ and $\epsilon = (\rho_1 - \rho_2)/\rho_1$.

Equivalently, one could linearize the system (3.1) around $\mathbf{U}_0 = (R_1, R_2, 0, 0)$. Substituting $\mathbf{U} = \mathbf{U}_0 + \tilde{\mathbf{U}}$ and dropping the nonlinear terms gives

$$\tilde{\mathbf{U}}_t + A(\mathbf{U}_0)\tilde{\mathbf{U}}_x = 0, \tag{3.5}$$

where

$$A(\mathbf{U}_0) = \begin{pmatrix} 0 & 0 & R_1 & 0 \\ 0 & 0 & 0 & R_2 \\ \tilde{\rho}_{11} & \tilde{\rho}_{21} & 0 & 0 \\ \tilde{\rho}_{22} & \tilde{\rho}_{22} & 0 & 0 \end{pmatrix}, \tag{3.6}$$

and the characteristic polynomial for (3.6) is given exactly by (3.4). The solutions for (3.4) are

$$\lambda_+^2 = \frac{1}{2}\left((\tilde{\rho}_{11}R_1 + \tilde{\rho}_{22}R_2) + \sqrt{(\tilde{\rho}_{11}R_1 - \tilde{\rho}_{22}R_2)^2 + 4\tilde{\rho}_{21}\tilde{\rho}_{22}R_1R_2}\right) > \tilde{\rho}_{11}R_1,$$
$$\lambda_-^2 = \frac{1}{2}\left((\tilde{\rho}_{11}R_1 + \tilde{\rho}_{22}R_2) - \sqrt{(\tilde{\rho}_{11}R_1 - \tilde{\rho}_{22}R_2)^2 + 4\tilde{\rho}_{21}\tilde{\rho}_{22}R_1R_2}\right) < \tilde{\rho}_{11}R_1.$$

This result corresponds to two modes in each direction. The two faster ones, whose interfaces are travelling in phase (see below), are called the *first baroclinic* (or *barotropic*) mode, and the two slower ones, whose interfaces are travelling out of phase (see below), are called the *second baroclinic* (or simply *baroclinic*) mode, respectively depending on the geophysical context [CRB11].

To illustrate this, we can solve the linear system (3.5) for λ_+ to get

$$h_1 = R_1 + \cos(x),$$
$$h_2 = R_1 + R_2 + \frac{1}{2R_1\tilde{\rho}_{21}}\left(\lambda_+^2 - \tilde{\rho}_{11}R_1\right)\cos(x).$$

Figure 3 (left) shows how this solution evolves in time. We note that as $\lambda_+^2 > \tilde{\rho}_{11}R_1$, this solution travels in phase. This is the case of a barotropic wave. On the other hand, by solving (3.5) for λ_- we get

$$h_1 = R_1 + \cos(x),$$
$$h_2 = R_1 + R_2 + \frac{1}{2R_1\tilde{\rho}_{21}}\left(\lambda_-^2 - \tilde{\rho}_{11}R_1\right)\cos(x).$$

This solution is shown in Figure 3 (right) and is an example of a baroclinic wave. Note that $\lambda_-^2 < \tilde{\rho}_{11}R_1$ and therefore the interfaces are out of phase.

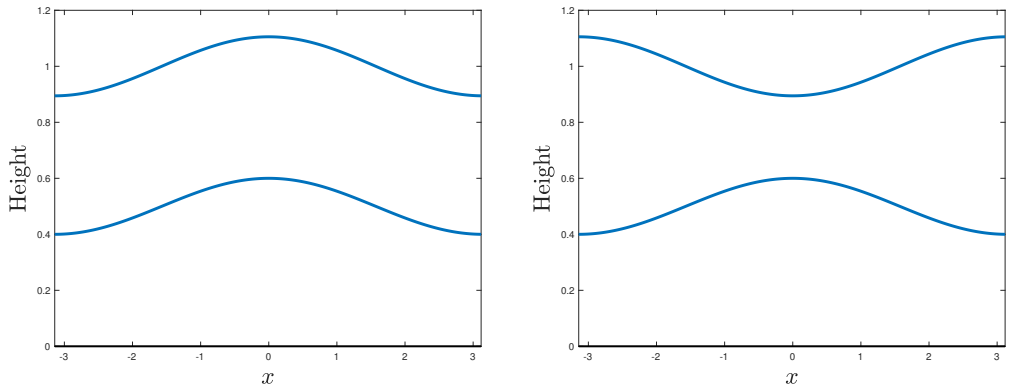

Figure 3: Numerical examples of a barotropic wave (left) and a baroclinic wave (right).

3.2 Nonlinear stability

The system (3.1) is *hyperbolic* [Joh78], [Whi74] if all its eigenvalues are real and its eigenvectors span $\mathbb{R}^4$. The eigenvalues, denoted by λ, are given by the roots of the characteristic polynomial

$$\begin{aligned} P(\lambda) &= \lambda^4 - 2(u_1+u_2)\lambda^3 + ((u_1+u_2)^2 + 2u_1u_2 - (\tilde{\rho}_{11}h_1 + \tilde{\rho}_{22}h_2))\lambda^2 \\ &- 2(u_1u_2(u_1+u_2) - (\tilde{\rho}_{11}h_1u_2 + \tilde{\rho}_{22}h_2u_1))\lambda \\ &+ (u_1u_2)^2 - (\tilde{\rho}_{11}h_1u_2^2 + \tilde{\rho}_{22}h_2u_1^2) + \epsilon(\tilde{\rho}_{22}h_1h_2). \end{aligned} \tag{3.7}$$

Note that in general, the polynomial above cannot be written as a bi-quadratic polynomial, which implies that the characteristic velocities are different in each direction (left and right) due to the shear $|u_2 - u_1|$.

An important question related to stability is whether an initially hyperbolic flow remains hyperbolic throughout its evolution. This is called *nonlinear stability* and is a form of long-time *well-posedness* for a Cauchy problem [Had02].

For the system (3.1), (3.2), (3.3), contrary to the two-layer rigid lid case, and consistent with the remarks of [CMM$^+$09b], a solution evolving from initially hyperbolic data might cross into the elliptic region of the phase space. This is shown in Figure 4 for $\rho_0 = 0$, $\rho_1 = 1$ and $\rho_2 = 0.9$.

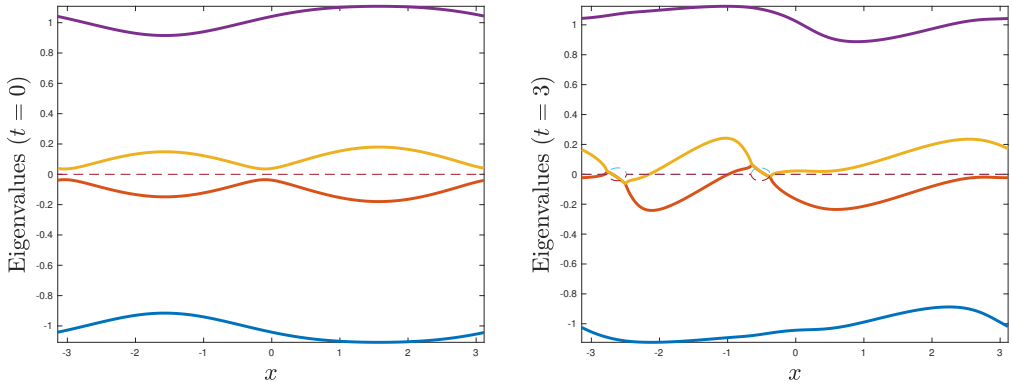

Figure 4: Numerical example of nonlinear instability in the two-and-a-half layer shallow water model. The real part and imaginary parts of the eigenvalues are shown in solid and dashed lines, respectively. On the left are shown the eigenvalues at initial stage for a hyperbolic initial condition. On the right one sees that transition occurs as the baroclinic speeds become complex conjugates, indicating a loss of hyperbolicity and ill-posedness.

3.3 The free surface case

The free surface case corresponds to zero density of the unbounded upper layer. The characteristic polynomial (3.7) becomes

$$\begin{aligned} P(\lambda) &= \lambda^4 - 2(u_1+u_2)\lambda^3 + ((u_1+u_2)^2 + 2u_1u_2 - (h_1+h_2))\lambda^2 \\ &- 2(u_1u_2(u_1+u_2) - (h_1u_2 + h_2u_1))\lambda \\ &+ (u_1u_2)^2 - (h_1u_2^2 + h_2u_1^2) + \epsilon h_1h_2. \end{aligned} \tag{3.8}$$

In order to understand the stability in the free surface case, we can locally change the variables in this polynomial so that $u_1 + u_2 = 0$. In fact, redefine u_j as

$$\tilde{u}_j = u_j - \left(\frac{u_1+u_2}{2}\right)$$

for $j = 1, 2$. Then, if we write $u = \tilde{u}_1$, we have $\tilde{u}_2 = -\tilde{u}_1 = -u$. In these new variables we have

$$P(\lambda) = \lambda^4 - (2u^2 + (h_1+h_2))\lambda^2 - 2u(h_1-h_2)\lambda + (u^4 - (h_1+h_2)u^2 + \epsilon h_1h_2). \tag{3.9}$$

This corresponds to a pointwise reference frame transformation in the original PDEs, whose main consequence was to drop the cubic term in the characteristic polynomial.

Next, for every $\gamma \in \mathbb{R} \setminus \{0\}$, the rescalings

$$\tilde{h}_j = \gamma h_j, \quad \tilde{u} = \gamma^{1/2} u, \quad \tilde{\lambda} = \gamma^{1/2} \lambda$$

do not change the roots. Now, by taking $\gamma = (h_1 + h_2)^{-1}$, we have the identity $\tilde{h}_1 + \tilde{h}_2 = 1$. Introducing the variables $w = \gamma^{1/2}\tilde{u}_1 - \gamma^{1/2}\tilde{u}_2 = 2u$ and $h = \tilde{h}_1 - \tilde{h}_2$. Then, the polynomial (3.9) depends *only* on the two variables h, w, instead of four. This surprising result shows that, in the free surface case, we can state the following theorem:

Theorem 3.1. *The stability of the free surface non-Boussinesq equations system (3.1)-(3.3) with $\rho_0 = 0$ depends only on the two dynamic variables $h = \dfrac{1}{(h_1+h_2)}(h_1 - h_2)$ (rescaled layer displacement) and $w = \dfrac{1}{(h_1+h_2)^{1/2}}(u_1 - u_2)$ (rescaled interfacial shear). The characteristic polynomial is*

$$P(\lambda) = \lambda^4 - \left(\frac{w^2}{2} + 1\right)\lambda^2 - (wh)\lambda + \left(\left(\frac{w}{2}\right)^4 - \left(\frac{w}{2}\right)^2 + \frac{\epsilon}{4}(1 - h^2)\right). \quad (3.10)$$

While the stability of the system depends on two quantities, the dynamics is still four-dimensional.

Theorem 3.1 is very helpful as it gives a precise picture of the hyperbolic region, as shown numerically in Figure 5 for different values of ϵ. Although these plots represent only a cross section of the phase space, Theorem 3.1 guarantees that such projections do not change along the other two directions and therefore they show precisely how a initial condition evolves in time. This fact allows, for instance, one to see the dynamics in the phase space for the nonlinear unstable example in Figure 4. This is presented in Figure 6, where it is possible to see that the solution enters the elliptic region indeed.

We note that the arguments used to prove Theorem 3.1 do not apply to the case $\rho_0 \neq 0$. In fact, as the upper layer is dynamically passive, its governing dynamical equation is $u_0 = 0$, which is not invariant under translations as equations (2.11) and (2.12).

3.3.1 Governing equations in the new variables

The ideas used to prove Theorem 3.1 suggests a novel way of writing the system (2.9)-(2.12), such that its phase space is precisely the one provided by the theorem. Introduce

$$H = h_1 + h_2 \quad \text{and} \quad G = \frac{u_1 + u_2}{2}.$$

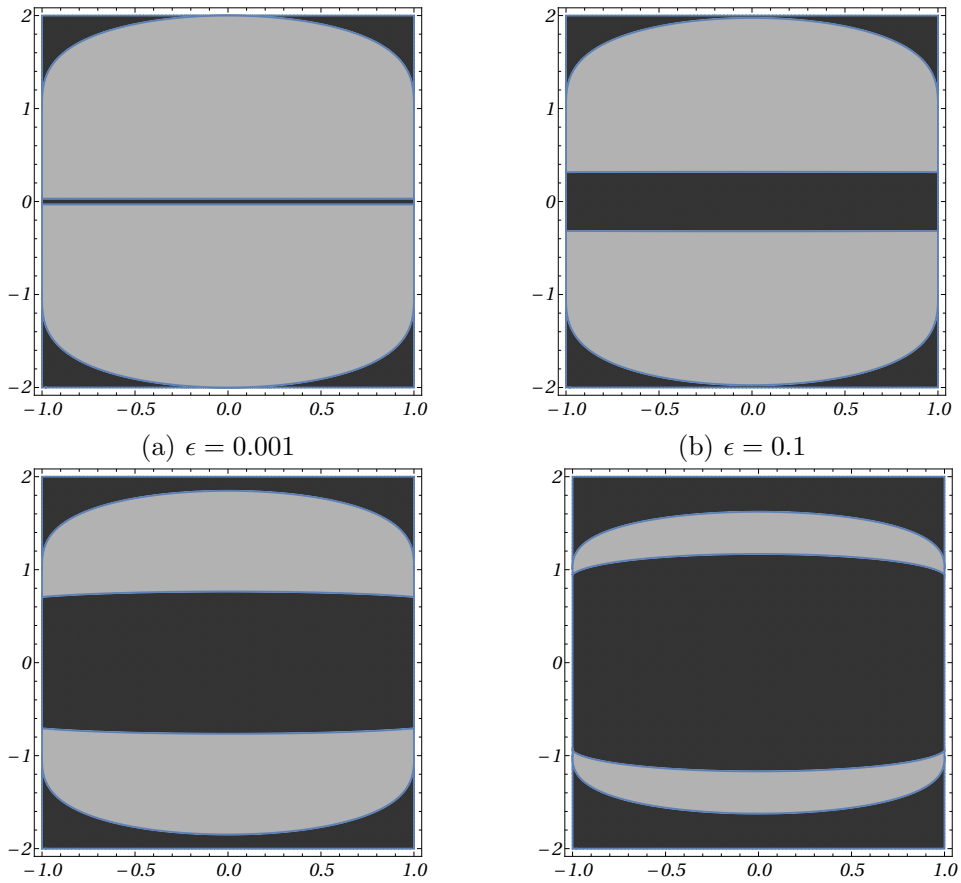

(a) $\epsilon = 0.001$ (b) $\epsilon = 0.1$

(c) $\epsilon = 0.5$ (d) $\epsilon = 0.9$

Figure 5: Examples of shear plane (h, w) for different values of ϵ, where the hyperbolic region is in grey and the elliptic region is in black. The physical region is given by $-1 < h < 1$ and $w \in \mathbb{R}$. Note that the solution is hyperbolic for $|w|$ small (weak shear) and become elliptic as the shear increases, indicating the transition to a regime where small scale effects are important and that is not captured by the model. Physically, this indicates the appearance of large-scale Kelvin-Helmholtz instabilities in the interface. The height of the hyperbolic region scales like $\sqrt{\epsilon}$ and when $\epsilon \ll 1$ converges to the rectangle $(h, w) = [-1, 1] \times [-\sqrt{\epsilon}, \sqrt{\epsilon}]$ corresponding to the hyperbolic region in (2.16)-(2.17).

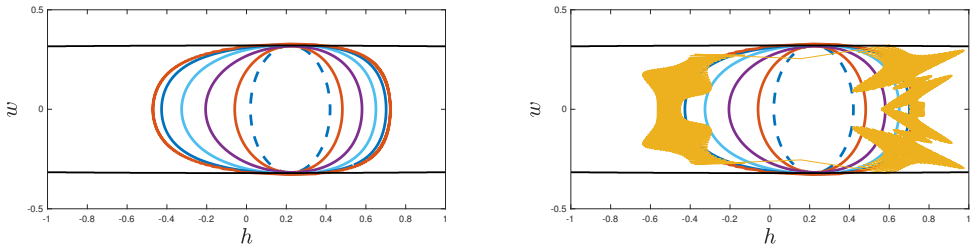

Figure 6: Numerical example of nonlinear instability in the free surface case presented in Figure 4, where $\epsilon = 0.1$. The image on the left shows the solution from an initial stage (blue dashed curve) where it is still inside the hyperbolic domain, up to the point where it crosses the parabolic boundary (red curve crossing the black line). On the right it is possible to see that the solution becomes unstable immediately after it moves into the elliptic region (yellow curve).

Under this change of variables, the equations (2.9) to (2.12) become, for $\rho_0 = 0$,

$$H_t + \left(\frac{H}{2}\left(2G + hw\sqrt{H}\right)\right)_x = 0, \tag{3.11a}$$

$$(hH)_t + \left(\frac{H}{2}\left(2Gh + w\sqrt{H}\right)\right)_x = 0, \tag{3.11b}$$

$$G_t + \left(\frac{4G^2 + w^2H}{8} + 2H + \epsilon\frac{H(1-h)}{4}\right)_x = 0, \tag{3.11c}$$

$$(w\sqrt{H})_t + \left(Gw\sqrt{H} + \epsilon\frac{H(1-h)}{2}\right)_x = 0. \tag{3.11d}$$

As before, these equations can be written as a 4×4 system of PDEs of the form (3.1), where $\mathbf{U} = (H, h, G, w)^T$. This system has characteristic polynomial given by Equation (3.10).

3.4 Simple waves

In a two-and-a-half-layer shallow water flow, the decoupling of characteristic modes is not possible as in the three-layer shallow water flow [dMVM17]. However, the study of pure baroclinic and barotropic waves is possible through special solutions called *simple waves*. These are very important solutions of the form

$$\mathbf{U}(x,t) = \mathbf{V}(\theta(x,t)). \tag{3.12}$$

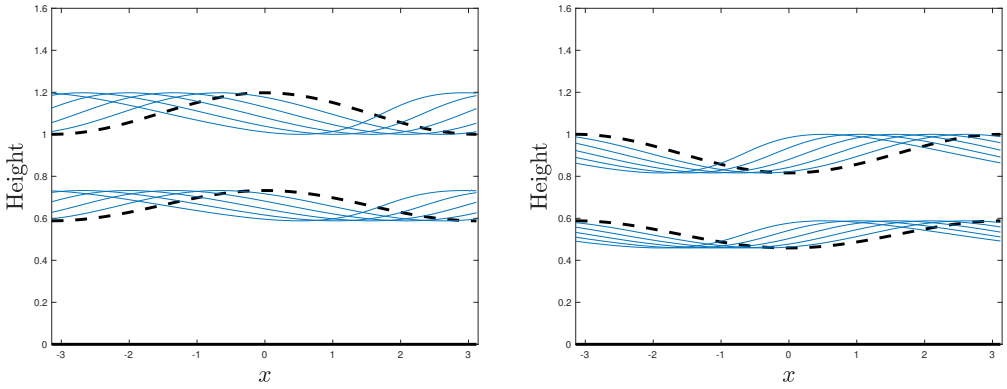

Figure 7: Two numerical examples of pure barotropic waves in the free surface case, computed along a particular simple wave curve, for $\epsilon = 0.1$. The initial wave is in black dashed line. Note the nonlinear steepening of each wave.

Replacing equation (3.12) into (3.1) yields

$$\mathbf{V}_\theta \, \theta_t + A(\mathbf{V})\mathbf{V}_\theta \, \theta_x = 0, \tag{3.13}$$

which has a solution if and only if $A(\mathbf{V})\mathbf{V}_\theta$ is proportional to $\mathbf{V}_\theta$, leading to the eigenvalue problem

$$[A(\mathbf{V}(\theta)) - \lambda(\theta) I] \, \mathbf{V}_\theta(\theta) = 0, \tag{3.14}$$

and where $\theta(x,t)$ must obey the evolution PDE

$$\theta_t + \lambda(\theta)\theta_x = 0, \tag{3.15}$$

which is hyperbolic if $\lambda(\theta)$ is real, for all θ. The eigenvectors $\mathbf{V}_\theta$ from equation (3.14) yield, for each eigenvalue family, a vector field in the phase space whose integral curves are the simple waves, meaning that $\mathbf{V}_\theta$ is tangent to these curves. For regions in phase space where our system is strictly hyperbolic, this implies the existence of 4 curves through each point. Each of these curves is a simple wave and is invariant under the evolution of the PDE: solutions starting on these curves remain on them, only the parametrisation $\theta(x,t)$ changes with time. Thus the 4 eigenvectors at each point yield a local basis of the phase space providing a decomposition based on in terms of the wave speeds $\lambda(\theta)$, or, physically speaking, in terms of the two baroclinic waves and the two barotropic waves. Examples of numerically computed evolution of simple waves in the physical system are shown in Figures 7 and 8 .

Simple waves are of crucial importance in the study of nonlinear first order hyperbolic PDEs. In two-dimensional systems, they define invariant regions

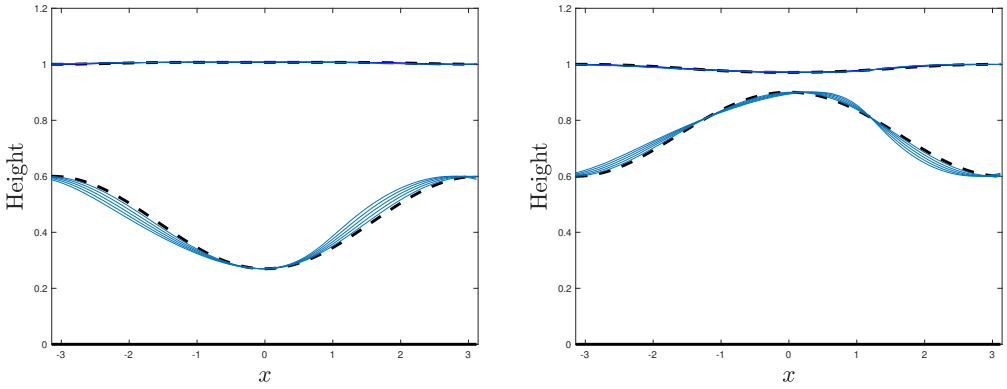

Figure 8: Two numerical examples of pure baroclinic waves in the free surface case, computed along a particular simple wave curve, for $\epsilon = 0.1$. The initial wave is in black dashed line. Note the nonlinear steepening of each wave.

[CMM+09a], [BM11] due to the property that simple waves do not allow a general solution to cross it tangentially [CT10]. That is the case discussed in the beginning of Section 3: the hyperplanes $h_j = 0$ are not only invariant subspaces, but they are also generated by simple waves, so that any solution that is tangent to one (or both) of these hyperplanes is actually tangent to a three-dimensional surface of simple waves, which prevents the solution to go into the elliptic region.

Furthermore, for mixed-type first order PDE systems, if an initial condition can be bounded by simple waves that do not themselves reach the boundary of the hyperbolic region, then the solution will remain hyperbolic until breaking. Therefore, using simple waves one can build the largest such region, which can be seen as a sharp bound to on hyperbolic initial data that prevents the solution straying into the elliptic region and therefore rendering the problem ill-posed [BM11].

In systems larger than two-dimensions, simple waves still provide a construction of "pure" wave solutions, but are less useful for bounding solutions, except in particular cases, for example when there is an invariant subspace of dimension two as in a three-layer shallow water Boussinesq problem [dMVM17].

Ideally, we would like to find manifolds generated by families of two (or even three) simple waves. These manifolds would contain families of both simple waves that exist for each mode of motion and would allow one to construct initial data that has waves propagating in both directions in a single mode of the system.

However, such manifolds do not exist for general systems of PDEs. The reason is due to the non-existence of an integrating factor for general differential forms in dimensions greater than two and, which implies that Riemann invariants, which

would allow us to construct such manifolds, do not exist generically, as discussed in [dMVM17].

4 Conclusions

We have derived and studied the long wave dynamics of a two-layer flow with third unbounded and dynamically passive layer above, in both Boussinesq and non-Boussinesq cases. Some limit cases were discussed, particularly the situation when the density of the upper unbounded layer is zero. In this case, physically motivated changes and rescaling in the dependent variables show that the stability depends only on two of these quantities: the shear and the difference in the layer thickness. We use that feature to visualize the phase plane and to show, numerically, that a nonlinear unstable solution indeed leaves the hyperbolic region. By visualising the phase (shear) plane, we noticed the existence of another hyperbolic region for large shears. Preliminary numerical investigations showed that the solutions starting in that region are extremely unstable and move towards the elliptic region in a very fast pace, but this is a matter that deserves further investigation. We use the same change of variables to rewrite the equations in a more appealing way and study the simple waves in this new system. All these results were proven for the free surface case and, although that is the only relevant case in most applications (*e.g.* ocean), it is of mathematical interest to investigate the case in which the density in the upper unbounded layer is weak, but nonzero.

Acknowledgements

The work of F.d.M.V. was supported by CNPq - Conselho Nacional de Desenvolvimento Científico e Tecnológico (Brasil), under the grant 249770/2013-0, to whom both authors are grateful. F.d.M.V. also acknowledges the 'QJMAM Fund for Applied Mathematics' for partially funding the presentation of this work at the 12^{th} European Fluid Mechanics Conference, held in Vienna, 2018; and Ricardo Barros for his help with the software Mathematica®.

References

[Arm86] Laurence Armi. The hydraulics of two flowing layers with different densities. *J. Fluid Mech.*, 163:27–58, 1986.

[Bai95] Peter G. Baines. *Topographic Effects in Stratified Flows*. Cambridge University Press, Cambridge, 1st edition, 1995.

[Bar06] Ricardo Barros. Conservation laws for one-dimentional shallow water models for one and two-layer flows. *Math. Mod. and Meth. in Appl. Sci.*, 16:119–137, 2006.

[BC08] Ricardo Barros and Wooyoung Choi. *On the hyperbolicity of two-layer flows*, pages 95–103. World Scientific, 2008.

[Ben66] David John Benney. Long non-linear waves in fluid flows. *Journal of Mathematics and Physics*, 45(1-4):52–63, 1966.

[BM11] Anakewit Boonkasame and Paul A. Milewski. The stability of large-amplitude shallow interfacial non-Boussinesq flows. *Stud. in Appl. Math.*, 128:40–58, 2011.

[CC99] W. Choi and R. Camassa. Fully nonlinear internal waves in a two fluid system. *J. Fluid Mech.*, 396:1–36, 1999.

[CCF+12] R. Camassa, S. Chen, G. Falqui, G. Ortenzi, and M. Pedroni. An inertia 'paradox' for incompressible stratified Euler fluids. *J. Fluid Mech.*, 695:330–340, 2012.

[CDFNGVn11] M. J. Castro-Días, E. D. Fernández-Nieto, J. M. González-Vida, and C. Parés-Madro nal. Numerical treatment of the loss of hyperbolicity of the two-layer shallow-water system. *J. Sci. Comput.*, 48:16–40, 2011.

[CMM+09a] Lyuba Chumakova, Fernando A. Menzaque, Paul A. Milewski, Rodolfo R. Rosales, and Esteban G. Tabak. Shear instability for stratified hydrostatic flows. *Comm. on Pure and Applied Math*, 62:183–197, 2009.

[CMM+09b] Lyuba Chumakova, Fernando A. Menzaque, Paul A. Milewski, Rodolfo R. Rosales, Esteban G. Tabak, and Cristina V. Turner. Stability properties and nonlinear mappings of two and three layer stratified flows. *Stud. in Appl. Math.*, 122:123–137, 2009.

[CMP01] Manuel Castro, Jorge Macías, and Carlos Parés. A Q-scheme for a class of systems of coupled conservation laws with source term. Application to a two-layer 1-D shallow water system. *Mathematical Modelling and Numerical Analysis*, 35:107–127, 2001.

[CRB11] Benoit Cushman-Roisin and Jean-Marie Beckers. *Introduction to Geophysical Fluid Dynamics - Physical and Numerical Aspects*. Academic Press, Waltham, 2nd edition, 2011.

[CT10] Lyuba Chumakova and Esteban G. Tabak. Simple waves do not avoid eigenvalue crossings. *Comm. on Pure and Applied Math*, 63:119–132, 2010.

[dMV18] Francisco de Melo Viríssimo. *Dynamical System Methods for Waves in Fluids: Stability, Breaking and Mixing*. PhD thesis, Department of Mathematical Sciences, University of Bath, United Kingdom, in preparation, 2018.

[dMVM17] Francisco de Melo Viríssimo and Paul A. Milewski. Three-layer flows in the shallow water limit. *Submitted to Stud. in Appl. Math.*, 2017.

[GK14] Sergey Gavrilyuk and Masha Kazakova. Hydraulic jumps in two-layer flows with a free surface. *J .Appl. Mech. Tech. Phy.*, 55:209–219, 2014.

[GPT97] Roger Grimshaw, Efim Pelinovsky, and Tatjana Talipova. The modified korteweg-de vries equation in the theory of large-amplitude internal waves. *Nonlinear Processes in Geophysics*, 4(4):237–250, 1997.

[Had02] Jacques Salomon Hadamard. Sur les problèmes aux dérivées partielles et leur signification physique. *Princeton University Bulletin*, pages 49–52, 1902.

[HM05] Karl R. Helfrich and W. Kendall Melville. Long nonlinear internal waves. *Annu. Rev. Fluid Mech.*, 38:395–425, 2005.

[JC14] Tae-Chang Jo and Young-Kwang Choi. Dynamics of strongly nonlinear internal long waves in a three-layer fluid system. *Ocean Sci. J.*, 49:357–366, 2014.

[Joh78] Fritz John. *Partial Differential Equations*. Springer-Verlag, New York, 3rd edition, 1978.

[Law90] Gregory A. Lawrence. On the hydraulics of Boussinesq and non-Boussinesq two-layer flows. *J. Fluid Mech.*, 215:457–480, 1990.

[LeV02] Randall J. LeVeque. *Finite Volume Methods for Hyperbolic Problems*. Cambridge University Press, Cambridge, 1st edition, 2002.

[Maj03] Andrew Majda. *Introduction to PDEs and Waves for the Atmosphere and Ocean*. Society for Industrial and Applied Mathematics, 1st edition, 2003.

[Miy88] Motoyasu Miyata. Long internal waves of large amplitude. In *Nonlinear water waves*, pages 399–406. Springer, 1988.

[MM08] Alexei A. Mailybaev and Dan Marchesin. Hyperbolicity singularities in Rarefaction Waves. *J. Dynam. Differ. Eq.*, 20:1–29, 2008.

[Mon15] Ronan Monjarret. Local well-posedness of the two-layer shallow water model with free-surface. *SIAM J. Appl. Math.*, 75:2311–2332, 2015.

[MT15] Paul A. Milewski and Esteban G. Tabak. Conservation law modelling of entrainment in layered hydrostatic flows. *J. Fluid Mech.*, 772:272–294, 2015.

[MTT+04] Paul A. Milewski, Esteban G. Tabak, Cristina V. Turner, Rodolfo R. Rosales, and Fernando A. Menzaque. Nonlinear stability of two-layer flows. *Comm. Math. Sci.*, 2:427–442, 2004.

[Ovs79] L. V. Ovsyannikov. Two-layer "shallow" water model. *Journal of Applied Mechanics and Technical Physics*, 20:127–135, 1979.

[Ped82] Joseph Pedlosky. *Geophysical Fluid Dynamics*. Springer-Verlag, New York and Berlin, 1st edition, 1982.

[RSG10] J. H. Ritcher, F. Sassi, and R. R. Garcia. Toward a physically based gravity wave source parametrization in a general circulation model. *Journal of the Atmospheric Sciences*, 67:136–156, 2010.

[Smo94] Joel Smoller. *Shock Waves and Reaction-Diffusion Equations*. Springer-Verlag, New York, 1st edition, 1994.

[SO98] T. P. Stanton and L. Ostrovsky. Observations of highly nonlinear internal solitons over the continental shelf. *Geophys. Res. Lett.*, 25:2695–2698, 1998.

[SS53] J. B. Schijf and J. C. Schonfeld. Theoretical considerations on the motion of salt and fresh water. *Proceedings Minnesota International Hydraulic Convention*, 1953.

[Whi74] Gerald B. Whitham. *Linear and Nonlinear Waves*. Wiley-Interscience, 1st edition, 1974.

3.2. Vertical Velocities

The equations for the vertical mean velocities read, for each layer, as

$$\rho_1 \left((h_1 \overline{v_1})_t + (h_1 \overline{u_1 v_1})_x \right) = 0,$$
$$\rho_2 \left((h_2 \overline{v_2})_t + (h_2 \overline{u_2 v_2})_x \right) = 0.$$

It is precisely the shallow water hypothesis, discussed in detail in Chapters 1 and 2, that allow us to decouple the system of 6 equations into two systems of PDEs: one is the set of the 4 equations for u_j, h_j given by Equations (2.9) to (2.12) and the other is the set of 2 equations above which gives v_j, for $j = 1, 2$. The former is independent of the latter but the converse is not true. However, once we found u_j and h_j, we can then solve the equations above for v_j.

In order to do that, we note that the shallow water approximation (see Equation (28) in [dMVM17]) also results in

$$\overline{u_j v_j} = (\overline{u_j})(\overline{v_j}),$$

which makes the equations above dependent of the average of the functions u_j, h_j and v_j only. We can then drop the bars and rewrite

$$(h_1 v_1)_t + (h_1 u_1 v_1)_x = 0,$$
$$(h_2 v_2)_t + (h_2 u_2 v_2)_x = 0.$$

These equations can be simplified if we use the conservation of mass equations (2.9) and (2.10), so that

$$v_{1,t} + u_1 v_{1,x} = 0,$$
$$v_{2,t} + u_2 v_{2,x} = 0.$$

This implies that the vertical velocity in each layer is given by the *advection equation*. Once we know u_j, these equations can be easily solved via their characteristics [Dur99], [CJ13]. We could also write

$$\mathbf{V}_t + c(\mathbf{u}_h)\mathbf{V}_x = 0,$$

where

$$\mathbf{V} = (v_1, v_2)^T, \quad \mathbf{u}_h = (u_1, u_2)^T$$

and

$$c(\mathbf{u}_h) = \begin{pmatrix} u_1 & 0 \\ 0 & u_2 \end{pmatrix}.$$

For the three-layer shallow water equations in Chapter 2, a similar calculation gives

$$v_{1,t} + u_1 v_{1,x} = 0,$$
$$v_{2,t} + u_2 v_{2,x} = 0,$$
$$v_{2,t} + u_2 v_{2,x} = 0,$$

which shows that the vertical velocities are advected with speed given by the horizontal velocities, and are independent of the unknown pressure in the rigid lid [dMVM17].

3.3. Conclusions

We have discussed the two-and-a-half-layer shallow water problem in the more general non-Boussinesq case. Although the Boussinesq case is sufficient for geophysical applications, we remark that there is not a significant difference between these: both are modelled by local equations (the pressure is not an additional unknown). In addition, both cases are described by semilinear PDEs which may be hyperbolic or elliptic depending on the flow. This is in contrast to the two-layer rigid lid case [BM11], where the Boussinesq approximation has strong mathematical consequences. We also remark on the conservation laws for both cases and their physical interpretation.

After these considerations, we investigate a limiting situation, the so-called free surface case, which attained by making $\rho_0 = 0$. This simplification is physically reasonable for the ocean-atmosphere case and has a profound mathematical implication: it makes the system be Galilean invariant and allow us to deduce that its stability depends only on the layer displacement h and the interfacial shear w, a result that has several consequences. First, it allow us to visualise the hyperbolic region, which is originally a four dimensional set, as a projection onto a plane. Second, one can rewrite the system in terms of these two 'stability' variables h and w plus two other variables, the mean velocity G and the total layer thickness H, resulting in a system with characteristic polynomial depending only on h and w.

This new system of equations is then used to find pure baroclinic and barotropic solutions as simple waves of the system. The use of simple waves as a dynamical system tool to study stability is also discussed and directions for future investigations are indicated.

A question of interest is what happen to a smooth hyperbolic solution after breaking. This question is approached in the next chapter.

Chapter 4

Conservation Law Modelling of Entrainment in Stratified Two-layer Shallow Water Flows

In this chapter, we turn to the study of the solutions after a wave breaks. This is done through a new methodology, proposed in the works of [MJT08] and [MT15]. After reviewing the main ideas of this methodology, we apply it to study the dam-break and lock exchange problems in the two-layer shallow water configuration, in the more general (*i.e.* non-Boussinesq) case. The study is validated through numerical simulations, with extensions also proposed at the end.

The work presented in this chapter is joint with Paul A. Milewski, and is currently the draft of a forthcoming submission [dMVM18a].

4.1. Outline of the Article

As a nonlinear phenomena, shallow water waves in fluids are subject to breaking, an evident fact for anyone who has been to a coastal beach, for example. Shallow water waves, whose evolution is modelled by PDEs, lose smoothness after a wave breaks, as this constitutes a singularity in the wave slope and the horizontal velocity field. Consequently, after breaking, classical solutions to the PDEs do not make sense, which poses an additional difficulty in the modelling of breaking waves [Smo94].

A way of overcoming this is to reinterprete the equations in terms of their integral, or 'weak', formulation [LeV02]. An integral formulation allows non-differentiable (and even discontinuous) solutions, which are the case of a shock that propagates after a wave breaks. However, contrary to the Cauchy problem for PDEs, there are many possible integral formulations leading to different weak solutions, and allowing various possible scenarios for a wave after a shock is formed. Therefore, when modelling shocks, it is crucial to find a way of 'choose' among these for the most physical solution for the problem in question [Fri17].

In Section 1, we review this methodology and its results for a two-layer shallow water system with a rigid lid in the Boussinesq approximation and introduce the two-layer general (non-Boussinesq) model, which is one-dimensional in space. In Section 2, the conservation laws for the system are discussed, all of which can be found through a PDE given in Corollary 2.1. In Section 3, two scenarios are proposed for investigation: in the first, we opt for conserving mass and a quantity that represents circulation; in the second, conservation of mass is proposed to be replaced by conservation of energy. Numerical simulations are performed using a semidiscrete central-upwind scheme derived in [KNP01].

Finally, we conclude with Section 4, where we also indicate further directions for the present work.

Appendix B: Statement of Authorship

This declaration concerns the article entitled:									
Conservation Law Modelling of Entrainment in Stratified Two-layer Shallow Water Flows									
Publication status (tick one)									
draft manuscript	X	**Submitted**		**In review**		**Accepted**		**Published**	
Publication details (reference)	Manuscript draft in preparation Authors: Francisco de Melo Viríssimo, Paul Antoine Milewski								
Candidate's contribution to the paper (detailed, and also given as a percentage).	The bulk of the calculations have been performed by the author of the thesis (100%). All authors contributed equally to the presentation of the content (50%). The numerical computations have been performed by the author of the thesis (100%).								
Statement from Candidate	This paper reports on original research I conducted during the period of my Higher Degree by Research candidature.								
Signed					**Date**	7.11.2018			

CONSERVATION LAW MODELLING OF ENTRAINMENT IN STRATIFIED TWO-LAYER SHALLOW WATER FLOWS

F. DE MELO VIRÍSSIMO[1] AND P. A. MILEWSKI[2]

Abstract. In this paper, we focus on the study of a new methodology for modelling entrainment in two-layer hydrostatic flows. This is done by using non-standard conserved quantities instead of the usual layerwise conservation of mass. We consider here the two-layer shallow water model in the more general non-Boussinesq case. After stating the problem, we show that any conservation law for this problem can be found as a solution of a nonlinear PDE, and we use this result to write some conserved quantities for the system. The physical relevance of each of these conservation laws is discussed. Two cases are then studied numerically: the first is a non-entrainment scenario, where we consider the conservation of mass and the conservation of a new 'weighted' circulation. In the second scenario we replace the conservation of mass by conservation of energy, which allows entrainment and exchange between the layers. Extensions and further developments are discussed at the end.

1 Introduction

Stratified flows (*i.e.*, flows whose density varies in the vertical) are ubiquitous in nature and their dynamics is responsible for a large part of observed atmospheric and oceanic phenomena [Whi74], [CRB11]. One important aspect in stratified flows is the existence of internal wave motion due to the restoring force of buoyancy [Lon56], [SO98]. Waves will propagate energy without appreciable net fluid transport, and therefore are important in the energy balance of climate studies. Mathematical studies of these are particularly important, since wave motion tends not to be resolved by most numerical climate models due to their fast scales, and thus need to be understood and parameterized [RSG10]. Yet smaller scale events

[1]Department of Mathematical Sciences, University of Bath, UK. e-mail: F.de.Melo.Virissimo@bath.ac.uk.

[2]Corresponding Author. Department of Mathematical Sciences, University of Bath, UK. e-mail: F.de.Melo.Virissimo@bath.ac.uk.

such as wave breaking can be missed altogether. These events mix the underlying fluids and affect the medium in which the waves are propagating [WTM12].

Two natural mathematical questions pose themselves for the case of internal waves in stratified fluids. First, whether the evolution is "well-posed" or "stable". In particular, in models that allow for some shear, there is the question whether the shallow water models are governed by hyperbolic (i.e. well-posed) or elliptic (i.e. ill-posed as an initial value problem) equations, and whether the evolution of the solution can cause a transition from one type to the other. (Ill-posedness in these models can be shown to arise from a form of the the Kelvin-Helmholtz instabilities, hence sometimes the hyperbolic behaviour is called "stable" and the ill-posedness "unstable".) Second, if the evolution is hyperbolic, the solutions are expected to break. The question then arises as to how to extend the solution in a physically relevant way past the breaking time, that is to understand the propagation of discontinuities (shocks).

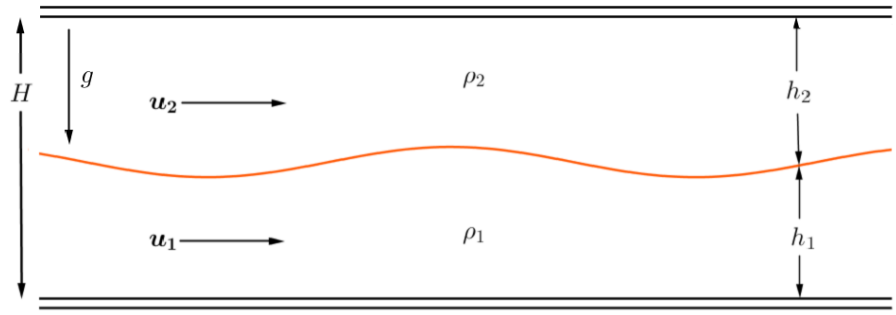

Figure 1: Schematic representation of the two-layer problem.

One of the simplest models for layered stratified flows is the two-layer shallow water model, described schematically in Figure 1. In the so-called Boussinesq case (when the density difference contributes only in the buoyancy effects), the two-layer shallow water equations are

$$h_t + \left(\frac{w}{2}(1-h^2)\right)_x = 0, \tag{1.1}$$

$$w_t + \left(\frac{h}{2}(1-w^2)\right)_x = 0, \tag{1.2}$$

where $h = h_2 - h_1$ (difference of layer thickness) and $w = u_2 - u_1$ for the (shear stress between the layer) and the system was rescaled so that $H = (h_1 + h_2)/2 = 1$ and $(\rho_1 + \rho_2)/2 = 1$. This model was proven to be nonlinear stable (or well-posed in the Hadamard sense): solutions that are initially hyperbolic evolve as such until they break [MTT+04], as shown in Figure 2.

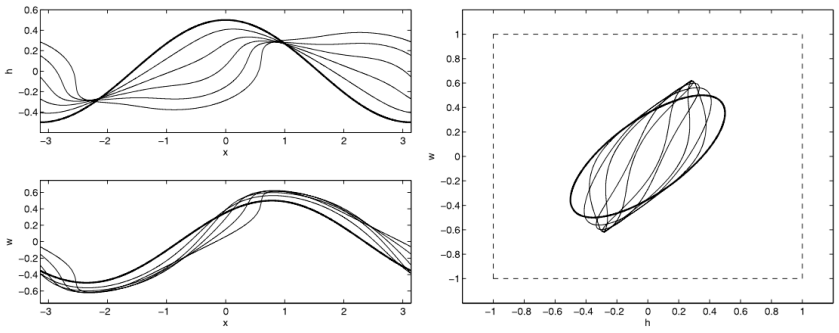

Figure 2: Typical solution of (1.1)-(1.2) up to breaking time; on the left, h and w are shown in physical space at various times. On the right, the evolution is shown in the phase space together with the boundary of the hyperbolic region. Reproduced with permission from Boonkasame *et al.* [BM11].

The task is then to follow a solution after the breaking time. As a solution breaks, it loses smoothness and no longer satisfies the differential equations above. Although one can continue it as a solution of the integral, or 'weak', formulation, there are usually several choices as the integral formulation does not admit a unique solution in general [LeV02], [Smo94]. Hence, the question of how to continue the solution after a wave breaks. This is an important question and its resolution must include some additional information usually in the form of physical constraints. There is an accepted solution to this in shallow water hydraulics (hydraulic jumps), but this is not the case for internal waves [MJT08], [RKBM11], [Fri17].

A possible answer to this problem was given in [MT15], based on the choice of conservation laws that allow for entrainment. In their case, the layerwise conservation of mass was replaced by conservation of energy, and the conservation of total momentum was replaced by conservation of circulation. Figure 3 shows, as an example, the comparison of an entrainment solution and a solution that does not allow it, in the case of a two-layer shallow water flow with a free surface under the Boussinesq approximation [MT15].

Any conservation law $q(h, w)$ of (1.1)-(1.2) can be found as solutions of the PDE [MT15]

$$(1 - w^2)q_{ww} - (h^2 - 1)q_{hh} = 0. \tag{1.3}$$

A consequence of (1.3) is that the two-layer Boussinesq system has an infinite number of conservation laws and although many of these might not have physical meaning, the choosing of possible closures among this infinite number available for the system is highly non-trivial.

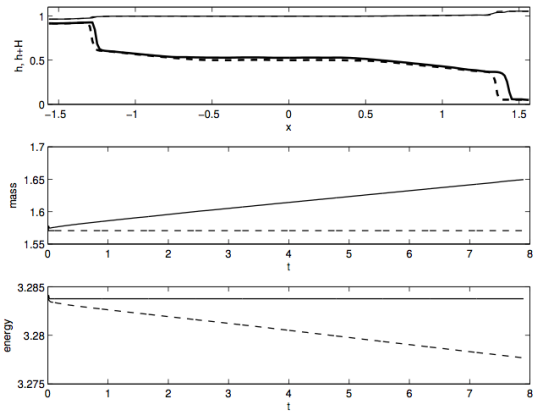

Figure 3: Lock-exchange in the two-interface flow. Comparison of entraining and non-entraining cases. In all panels the dashed line is the non-entraining case and the solid line is the entraining case. The upper panel shows the final interfacial shapes. The middle and lower panels show the resulting total volume of the lower layer and total energy of the system, respectively. Reproduced with permission from Milewski *et al.* in [MT15].

1.1 Outline of the paper

The aim of this paper is to follow the aforementioned approach to study the discontinuous shock solutions of the two-layer shallow water non-Boussinesq model. The governing equations for this problem are [BM11]

$$h_t + \left(\frac{w}{2}(1-h^2)\right)_x = 0, \tag{1.4}$$

$$w_t + \left(\frac{h}{2}(1-w^2)\right)_x + \frac{2r}{(1-rh)}\left(\frac{(1-h^2)w^2}{4} + \frac{h^2}{8}\right)_x = 0, \tag{1.5}$$

with h and w as in the Boussinesq case and $r = (\rho_1 - \rho_2)/2 \geq 0$ being the average difference of densities, often referred as an Atwood number [Bai95]. Note that, in the limit $r \longrightarrow 0$, the Boussinesq equations (1.1)-(1.2) are recovered. For this reason, we shall refer to this as the *Boussinesq limit*. In general, the non-Boussinesq model results in nonlocal equations. The equations above are local and are valid only when no flux condition are imposed at the boundaries.

Contrary to Equations (1.1)-(1.2), the non-Boussinesq system (1.4)-(1.5) is not always nonlinearly stable: this means that wave-like solutions can leave the hyperbolic region before a shock occurs, as shown in Figure 4 [BM11].

Although this loss of hyperbolicity might happen for a general solution, it is possible to construct invariant regions inside the hyperbolic domain in which the

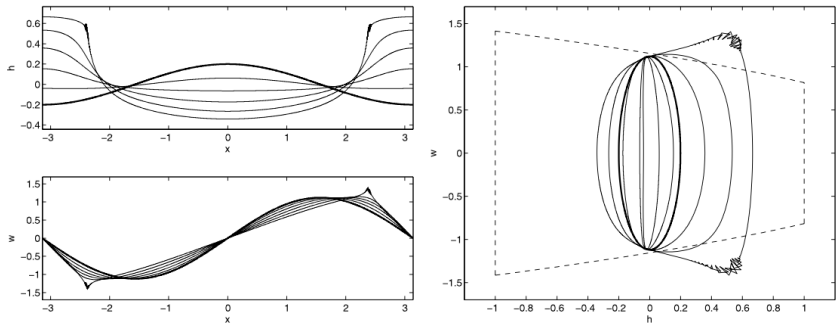

Figure 4: Sloshing solution of (1.4)-(1.5) for $r = 0.5$ with initial data near boundaries of the hyperbolic region; the numerical solution is of course unreliable outside the hyperbolic region. Reproduced with permission from Boonkasame *et al.* [BM11].

system is nonlinearly stable [BM11]. This is done through the use of simple waves, as these possesses the property that a general solution cannot cross a simple wave transversally [CT10]. Hence, a solution trapped in a region bounded by simple waves will never leave this region and will propagate until it breaks. In this paper, we are interested in investigating the behaviour these solutions once they break and lose smoothness.

The paper is divided as follows. In Section 2, the conservation laws for the non-Boussinesq system are discussed. In particular, we derive an equivalent of Equation (1.3) for the system (1.4)-(1.5). We then use this new PDE to find conservation laws and discuss the many possible conservation laws to choose. We then use this apparatus in Section 3, in order to conduce a numerical study of the weak solutions of the system (1.4)-(1.5). For the numerical studies of shock solutions, we implement a Godunov-type finite volume scheme [LeV02] proposed by Kurganov *et al.* in [KNP01].

2 Conservation laws for the non-Boussinesq system

The two-layer non-Boussinesq model discussed in this work is a quasi-linear 2×2 system of PDEs which, by Equations (1.4) and (1.5), can be written as

$$\mathbf{U}_t + A(\mathbf{U})\mathbf{U}_x = 0, \tag{2.1}$$

where $\mathbf{U} = (h, w)^T$ and

$$A(\mathbf{U}) = \begin{pmatrix} -hw & \dfrac{1-h^2}{2} \\ \dfrac{1-(1+rh)w^2}{2(1-rh)} & \dfrac{(r-h)w}{1-rh} \end{pmatrix}. \tag{2.2}$$

As observed in [MT15], one can find an analogous of Equation (1.3) for the non-Boussinesq system through the following proposition.

Proposition 2.1 ([MT15]). *A general 2×2 system of equations of the form*

$$u_t + au_x + bv_x = 0, \tag{2.3}$$

$$u_t + cu_x + dv_x = 0 \tag{2.4}$$

has a conservation law $q(u, v)$ satisfying

$$(q(u, v))_t + (F(u, v))_x = 0 \tag{2.5}$$

if, and only if $F(u, v)$ is of class C^2 and $q(u, v)$ is a solution of

$$(aq_u + cq_v)_v - (bq_u + dq_v)_u = 0, \tag{2.6}$$

Proof. Expanding the conservation law (2.5) gives

$$q_u u_t + q_v v_t = -(F_u u_x + F_v v_x).$$

Replacing Equations (2.3), (2.4) into that gives

$$(aq_u + cq_v)u_x + (bq_u + dq_v)v_x = F_u u_x + F_v v_x.$$

Hence, if F is of class C^2, then $F_{uv} = F_{vu}$. Therefore,

$$(aq_u + cq_v)_v = (bq_u + dq_v)_u,$$

and (2.6) follows. The converse can be proven in a similar fashion. □

A similar result holds for a $n \times n$ system of PDEs. This result is presented and discussed in Appendix A, where it is shown that for $n \geq 3$ the resulting system is in general overdetermined, as it gives two or more equations for the only unknown $q(u, v)$.

Corollary 2.1. *A function $q(h, w)$ of class C^2 is a conservation law for the system (1.4) and (1.5) if, and only if, it solves the equation*

$$\left(\frac{1-h^2}{2}\right) q_{hh} + \left(\frac{(1+rh)w^2 - 1}{2(1-rh)}\right) q_{ww} + \left(\frac{rw(1-h^2)}{1-rh}\right) q_{hw} + \left(\frac{r^2 w(1-h^2)}{(1-rh)^2}\right) q_w = 0. \tag{2.7}$$

It follows from this corollary that the system has an infinite number of conservation laws. It is important to notice that this is not the case with the two-layer free surface model discussed in [MT15], as it was proven that it admits only 6 linearly independent conservation laws [Bar06].

2.1 Possible choices of conservation laws

Note that Equation (1.4) is written in a conservative form, where the quantity $q(h, w) = h$ states the *conservation of volume*. Since the density on each layer is constant, the conservation of volume is equivalent to the *conservation of mass*.

On the other hand, the system *does not conserve the circulation* w as shown by Equation (1.5). However, this equation can be rewritten in a conservative form as the quantity $q(h, w) = w(1 - rh)$ is conserved. This new quantity can be seen as a *weighted circulation*. One then gets

$$(w(1 - rh))_t + \left(\frac{(1 - w^2)h}{2} + r \left(\frac{1 + w^2}{4} \right) \right)_x = 0. \tag{2.8}$$

It follows from the PDE (2.7) that, for example, $q(h, w) = w(1 - rh)^2$, $(1 - rh)hw$ and $(1 - r^2h^2)w$ are also conserved. Note that the non-Boussinesq rigid lid model in general does not conserve total horizontal momentum [CCF+12], [dMVM17].

The *total energy* is given by

$$E(h, w) = -\frac{1}{4}(1 - h^2)(1 - w^2) - \frac{rhw^2}{4}(1 - h^2) + \frac{h}{2}. \tag{2.9}$$

The respective conservation law is given by

$$E_t + \left(\frac{(1 - h^2)(1 + h - hw^2)w}{4} + \frac{rw^3}{8}(1 - h^2) \right)_x = 0. \tag{2.10}$$

3 Numerical simulations

In this section, we present the results of numerical studies performed for shock solutions of the two-layer model. First, we discuss the case of a dam-break initial solution for the system given by Equations (1.4) and (2.8), where both volume h and the weighted circulation $w(1 - rh)$ are conserved. Following this, we suggest an alternative scenario, where the conservation of volume is replaced by the conservation of energy, given by Equation (2.10), which allows entrainment and the mixing between layers.

3.1 Details of the method

In order to solve Equations (1.4) and (2.8), as well as Equations (2.8) and (2.10), we use a semidiscrete central-upwind scheme for one-dimensional conservation laws, proposed by Kurganov *et al.* in [KNP01].

Notation. Here we consider only uniform grids (t^n, x_j) with grid-size $(\Delta t, \Delta x)$, where

$$t^n = n\Delta t, \quad x_j = j\Delta x, \quad x_{j\pm\frac{1}{2}} = (j \pm 1/2)\Delta x. \tag{3.1}$$

We also denote the solution evaluated at the nodes as $u_j^n = u(x_j, t^n)$.

The starting point for this scheme is the equivalent integral formulation of the conservation law

$$u_j + \nabla_x \cdot f(u) = 0, \tag{3.2}$$

which is given by

$$\begin{aligned}\overline{u}(x, t+\Delta t) = \overline{u}(x,t) &- \frac{1}{\Delta x}\left(\int_t^{t+\Delta t} f(u(x+\Delta x/2, \tau))d\tau\right) \\ &+ \frac{1}{\Delta x}\left(\int_t^{t+\Delta t} f(u(x-\Delta x/2, \tau))d\tau\right),\end{aligned} \tag{3.3}$$

where

$$\overline{u}(x,t) = \frac{1}{\Delta x}\int_{I(x)} u(\eta, t)d\eta \text{ and } I(x) = \{\eta : |\eta - x| < \Delta x/2\}. \tag{3.4}$$

Polynomial reconstruction. At time level $t = t^n$, we consider the problem above with the piecewise polynomial initial condition

$$\tilde{u}(x, t^n) = p_j^n(x), \text{ where } x_{j-\frac{1}{2}} < x < x_{j+\frac{1}{2}}, \tag{3.5}$$

for all j, obtained from the cell averages $\overline{u}_j^n = \overline{u}(x_j, t^n)$, computed at previous time step. Here, $\tilde{u}$ is the initial condition of the system. Note that this polynomial reconstruction should be conservative, non-oscillatory and accurate (up to a certain order). As second-order schemes require only a piecewise linear reconstruction, we will be implementing these for simplicity.

The method. We start with a piecewise polynomial reconstruction (of any order), with possible discontinuities at the interface points $\{x_{j+\frac{1}{2}}\}$. The method can be written as

$$\frac{d}{dt}\overline{u}_j(t) = -\frac{H_{j+\frac{1}{2}}(t) - H_{j-\frac{1}{2}}(t)}{\Delta x}, \tag{3.6}$$

where the numerical fluxes $H_{j+\frac{1}{2}}$ are given by

$$H_{j+\frac{1}{2}}(t) = \frac{a^+_{j+\frac{1}{2}} f(u^-_{j+\frac{1}{2}}) - a^-_{j+\frac{1}{2}} f(u^+_{j+\frac{1}{2}})}{a^+_{j+\frac{1}{2}} - a^-_{j+\frac{1}{2}}} + \frac{a^+_{j+\frac{1}{2}} a^-_{j+\frac{1}{2}}}{a^+_{j+\frac{1}{2}} - a^-_{j+\frac{1}{2}}}\left(u^+_{j+\frac{1}{2}} - u^-_{j+\frac{1}{2}}\right). \tag{3.7}$$

Here, $a^+_{j+\frac{1}{2}}$ and $a^-_{j+\frac{1}{2}}$ denotes the right- and left-sided local speeds respectively, which can be estimated by

$$a^+_{j+\frac{1}{2}} = \max_{\omega \in \mathcal{C}\left(u^-_{j+\frac{1}{2}}, u^+_{j+\frac{1}{2}}\right)} \left\{\lambda_N \left(Jf(\omega)\right)\right\}, \tag{3.8}$$

$$a^-_{j+\frac{1}{2}} = \min_{\omega \in \mathcal{C}\left(u^-_{j+\frac{1}{2}}, u^+_{j+\frac{1}{2}}\right)} \left\{\lambda_1 \left(Jf(\omega)\right)\right\}, \tag{3.9}$$

where $\lambda_1 < ... < \lambda_N$ are the N eigenvalues of the Jacobian Jf and $\mathcal{C}\left(u^-_{j+\frac{1}{2}}, u^+_{j+\frac{1}{2}}\right)$ is the curve in the phase space that connects $u^+_{j+\frac{1}{2}} = p_{j+1}(x_{j+\frac{1}{2}})$ and $u^-_{j+\frac{1}{2}} = p_j(x_{j+\frac{1}{2}})$.

Remark 3.1. The semi-discrete scheme above is a system of time-dependent ODEs, which can be solved by any stable ODE solver.

Remark 3.2. As noticed in [KNP01], this method has the characteristic of a Godunov-type central scheme, which is based on exact evolution and averaging over Riemann fans, and as such it does not employ Riemann solvers and characteristic decomposition. Such distinctive feature makes this method a universal, simple and efficient tool for a variety of problems. In addition, it has a very low dissipation and consequently can achieve a very high resolution.

3.2 Conservation of volume and weighted circulation: a non-entrainment but dissipative scenario

In this scenario, we are solving the system

$$h_t + \frac{1}{2}\left(w(1-h^2)\right)_x = 0,$$
$$(w(1-rh))_t + \left(\frac{(1-w^2)h}{2} + r\left(\frac{1+w^2}{4}\right)\right)_x = 0,$$

where h stands for volume and $w(1-rh)$ gives the weighted circulation as stated previously. In all our simulations, a grid of $N = 400$ grid points and a time step $\Delta t = 0.4$ are used. At the lateral boundaries, conditions modelling a vertical wall were imposed. All solutions are shown at times $t^n = n\Delta t$, with $n = 0, ..., 6$.

Figures 5 to 8 show the evolution of a dam-break shock initial solution [EP11] for the system above, for a Boussinesq parameter $r = 0.1$ and $r = 0.5$ respectively. In all of these, the initial condition is given by $h = 1$ if $x < 0$, $h = -1$ if $x > 0$ and $w = 0$.

In Figures 5 and 7 we can see the evolution of the interface h_1 and the lower layer horizontal velocity u_1, as well as the other relevant quantities h and w.

Note that while the mass is conserved, energy is being dissipated during the shock wave propagation. The solution by construction prevents entrainment, and dissipates energy ensuring that the shock is entropic [Smo94]. This better seen in Figures 6 and 8 where both total energy and total mass are plotted, together with the weighted circulation, over time.

Comparatively, we also simulated weaker (step-like) dam-break shock such that $h = -0.2$ if $x < 0$, $h = -0.8$ if $x > 0$ (or equivalently $h_1 = 0.4$ if $x < 0$, $h_1 = 0$ if $x > 0$), with the same initial shear $w = 0$. As shown in Figures 9 and 10, a similar behaviour occurs.

A modified 'smooth' version of the dam-break problem is also considered in this study. Figures 11 and 12 show the evolution of a smooth wave-like initial condition for the system, in the case $r = 0.5$. We note that while the solution starts smooth, a shock arises and is propagated in finite time. After the shock formation, the energy decreases linearly as shown in Figure 12.

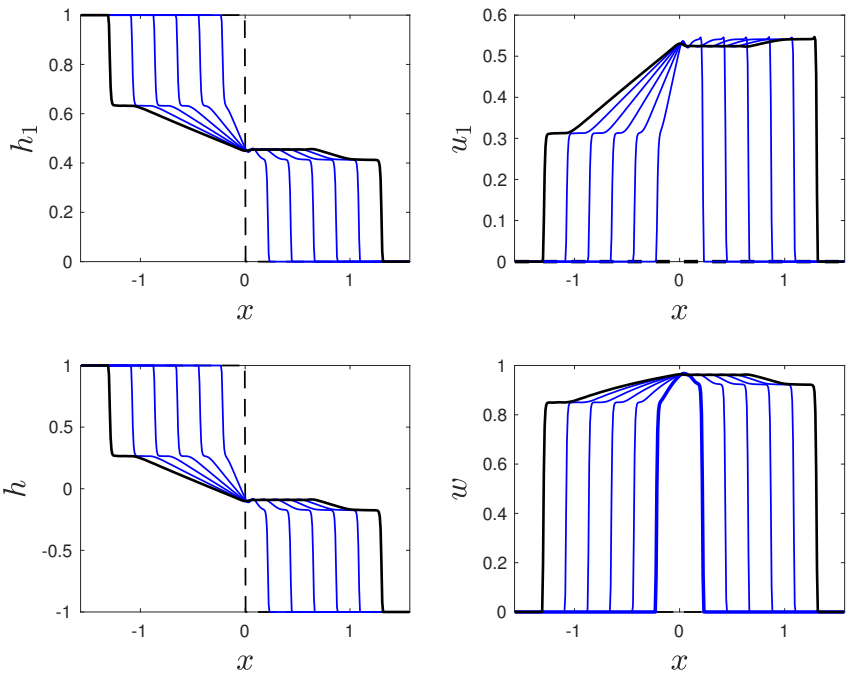

Figure 5: Dam-break problem in a two-layer non-Boussinesq flow, with $r = 0.1$. This figure shows a non-entrainment scenario, where the mass is conserved.

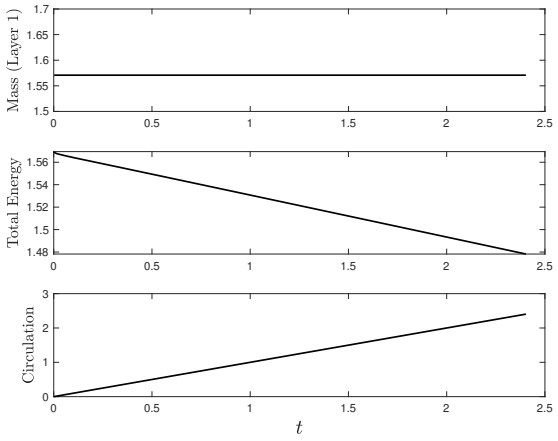

Figure 6: Mass, total energy and weighted circulation for the solution in Figure 5.

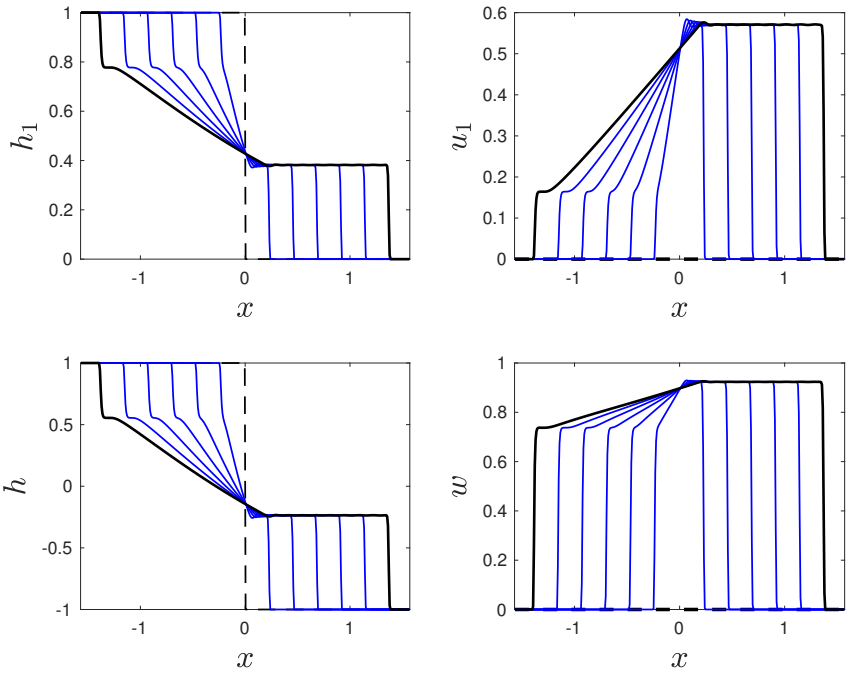

Figure 7: Dam-break problem in a two-layer non-Boussinesq flow, with $r = 0.5$. This figure shows a non-entrainment scenario, where the mass is conserved.

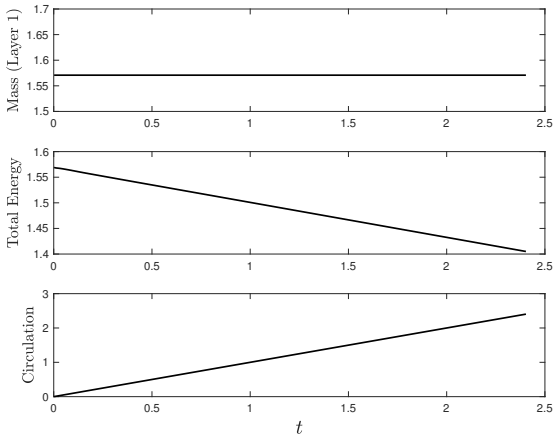

Figure 8: Mass, total energy and weighted circulation for the solution in Figure 7.

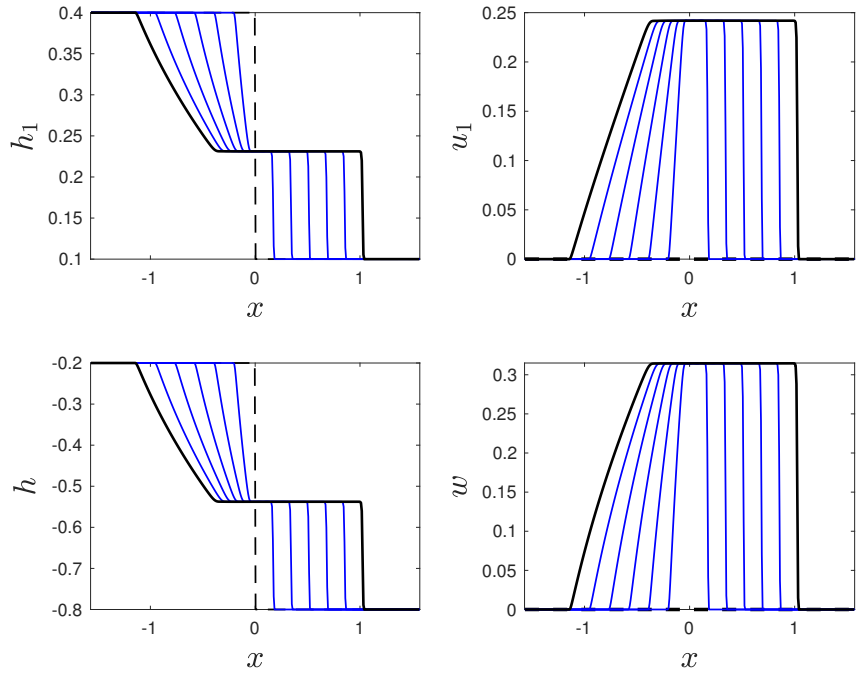

Figure 9: 'Smooth' Dam-break problem in a two-layer non-Boussinesq flow, with $r = 0.5$. This is a non-entrainment scenario, with mass being conserved.

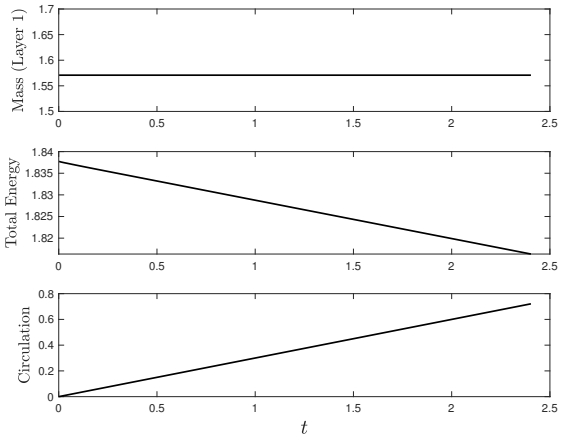

Figure 10: Mass, total energy and weighted circulation for the solution in Figure 9.

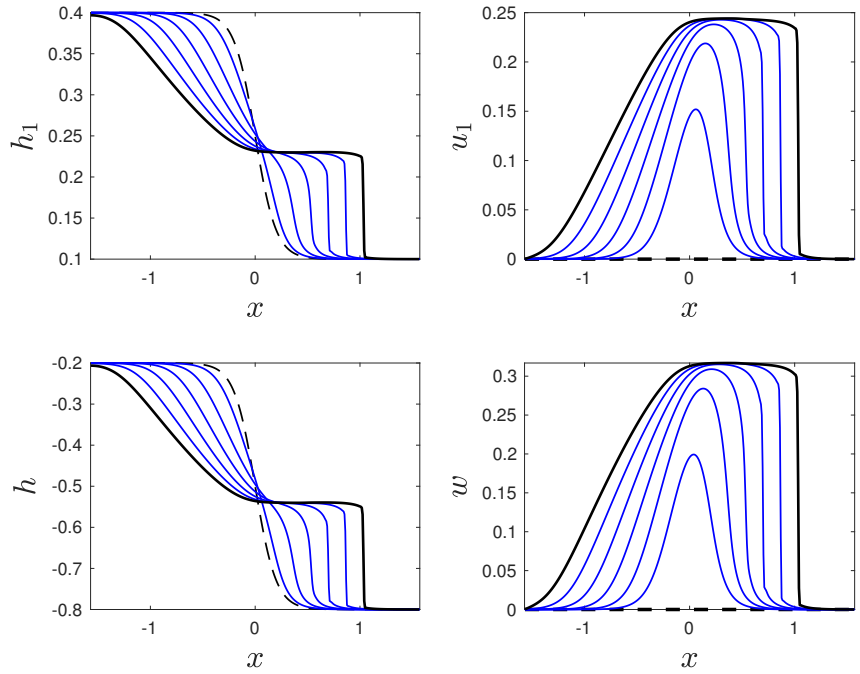

Figure 11: Evolution of a smooth wavelike in a two-layer non-Boussinesq flow, with $r = 0.5$, followed before and after breaking in non-entrainment scenario.

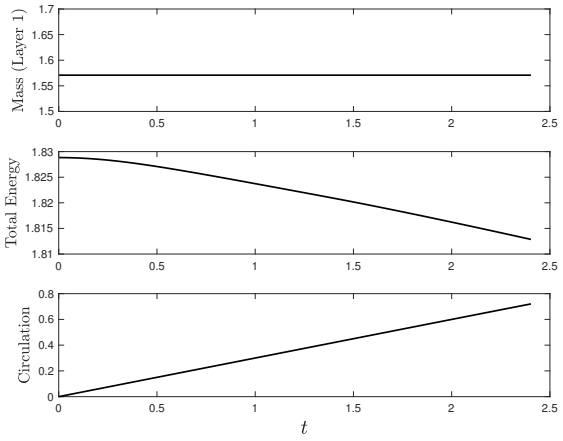

Figure 12: Mass, total energy and weighted circulation for the solution in Figure 11.

3.3 Conservation of energy and weighted circulation: an entrainment scenario

Alternatively, we could consider the case where energy is conserved instead of mass. This is represented by the equations

$$(w(1-rh))_t + \left(\frac{(1-w^2)h}{2} + r\left(\frac{1+w^2}{4}\right)\right)_x = 0,$$
$$(E(h,w))_t + \left(\frac{(1-h^2)(1+h-hw^2)w}{4} + \frac{rw^3}{8}(1-h^2)\right)_x = 0,$$

where

$$E(h,w) = -\frac{1}{4}(1-h^2)(1-w^2) - \frac{rhw^2}{4}(1-h^2) + \frac{h}{2}.$$

With conservation of mass not imposed *a priori*, the system allows entrainment: instead of dissipating energy, fluid from one layer entrains into another layer. In order to solve this system, it is necessary to compute the variables h and w from $w(1-rh)$ and E, which can be done numerically by implementing a Newton solver. This part is work in progress and will appear in the final version of this paper.

4 Conclusions

This paper presented a study of non-smooth solution of a two-layer shallow water model in the non-Boussinesq case. A novel strategy to follow such solutions is

introduced and applied to the this solution system for a range of different initial conditions, for several values of the density differences r. This was done for the physical case where no entrainment occurs, so that the volume (and consequently the mass) of each layer were preserved. It was noted that, although the mass was being conserved, the energy was dissipated during the evolution and therefore it is not conserved after a shock. We then proposed and discussed an alternative possibility, where the conservation of mass was replaced by conservation of energy, which is another case of physical relevance. This latter extended to a non-Boussinesq scenario the study of Milewski *et al.* in [MT15].

Acknowledgements

F.d.M.V. is very grateful to Professor Wen Shen for the opportunity to work in this project while his student at the University of Oxford. This work of F.d.M.V. was supported by CNPq - Conselho Nacional de Desenvolvimento Científico e Tecnológico (Brasil), under the grant number 249770/2013-0, to whom both authors are grateful.

Appendix A - Conservation laws for a $n \times n$ system

One of our aims in future is to extend this study to the realm of three-layer shallow water flows, which requires the knowledge of physically relevant quantities conserved by the model. For this purpose, we present below a extension of Proposition 2.1 for the case of an n-dimensional quasilinear system of PDEs.

Theorem 4.1 (Conservation laws for a $n \times n$ system)**.** *A general $n \times n$ system of equations of the form*

$$u_{i,t} + \sum_{j=1}^{n} a_{ij} u_{j,x} = 0$$

with $a_{ij} = f(u_1, ..., u_n, x, t)$ permits conservation laws for q satisfying

$$(q(u_1, ..., u_n))_t + (Q(u_1, ..., u_n))_x = 0$$

if and only if

$$F_{u_i,u_j} = F_{u_j,u_i}$$

for all $i, j \in \{1, 2, ..., n\}$, where

$$F_{u_k} = \sum_{j=1}^{n} a_{jk} q_{h_j}.$$

In particular, for a general 4×4 system of the form

$$\begin{aligned}
h_{1,t} + a_1 h_{1,x} + b_1 h_{2,x} + c_1 u_{1,x} + d_1 u_{2,x} = 0,\\
h_{2,t} + a_2 h_{1,x} + b_2 h_{2,x} + c_2 u_{1,x} + d_2 u_{2,x} = 0,\\
u_{1,t} + a_3 h_{1,x} + b_3 h_{2,x} + c_3 u_{1,x} + d_3 u_{2,x} = 0,\\
u_{2,t} + a_4 h_{1,x} + b_4 h_{2,x} + c_4 u_{1,x} + d_4 u_{2,x} = 0,
\end{aligned}$$

which is the case of a three-layer shallow water flow [dMVM17] we have that

$$\begin{aligned}
F_{h_1} = a_1 q_{h_1} + a_2 q_{h_2} + a_3 q_{u_1} + a_4 q_{u_2},\\
F_{h_2} = b_1 q_{h_1} + b_2 q_{h_2} + b_3 q_{u_1} + b_4 q_{u_2},\\
F_{u_1} = c_1 q_{h_1} + c_2 q_{h_2} + c_3 q_{u_1} + c_4 q_{u_2},\\
F_{u_2} = d_1 q_{h_1} + d_2 q_{h_2} + d_3 q_{u_1} + d_4 q_{u_2},
\end{aligned}$$

and the conditions are

$$\begin{aligned}
F_{h_1,h_2} = F_{h_2,h_1},\\
F_{h_1,u_1} = F_{u_1,h_1},\\
F_{h_1,u_2} = F_{u_2,h_1},\\
F_{h_2,u_1} = F_{u_1,h_2},\\
F_{h_2,u_2} = F_{u_2,h_2},\\
F_{u_1,u_2} = F_{u_2,u_1}.
\end{aligned}$$

In general, for a $n \times n$ system, this theorem gives $C_{n,2}$ equations to be solved, where

$$C_{n,2} = \frac{n!}{(n-2)!2!}.$$

This corresponds to 1 equation to a two-layer model, and 6 equations for a three-layer model as shown above. Therefore, for $n \geq 3$, the resulting system is overdetermined.

References

[Bai95] Peter G. Baines. *Topographic Effects in Stratified Flows.* Cambridge University Press, Cambridge, 1st edition, 1995.

[Bar06] Ricardo Barros. Conservation laws for one-dimentional shallow water models for one and two-layer flows. *Math. Mod. and Meth. in Appl. Sci.*, 16:119–137, 2006.

[BM11] Anakewit Boonkasame and Paul A. Milewski. The stability of large-amplitude shallow interfacial non-Boussinesq flows. *Stud. in Appl. Math.*, 128:40–58, 2011.

[CCF+12] R. Camassa, S. Chen, G. Falqui, G. Ortenzi, and M. Pedroni. An inertia 'paradox' for incompressible stratified Euler fluids. *J. Fluid Mech.*, 695:330–340, 2012.

[CRB11] Benoit Cushman-Roisin and Jean-Marie Beckers. *Introduction to Geophysical Fluid Dynamics - Physical and Numerical Aspects*. Academic Press, Waltham, 2nd edition, 2011.

[CT10] Lyuba Chumakova and Esteban G. Tabak. Simple waves do not avoid eigenvalue crossings. *Comm. on Pure and Applied Math*, 63:119–132, 2010.

[dMVM17] Francisco de Melo Viríssimo and Paul A. Milewski. Three-layer flows in the shallow water limit. *Submitted to Stud. in Appl. Math.*, 2017.

[EP11] J. G. Esler and J. D. Pearce. Dispersive dam-break and lock-exchange flows in a two-layer fluid. *J. Fluid Mech.*, 667:555–585, 2011.

[Fri17] Robert Friel. *Optimization Closures for Mixing Shocks in Stratified Hydrostatic Flows*. PhD thesis, New York University, 2017.

[KNP01] Alexander Kurganov, Sebastian Noelle, and Guergana Petrova. Semidiscrete central-upwind schemes for hyperbolic conservation laws and Hamilton-Jacobi equations. *SIAM J. Sci. Comput.*, 23:707–740, 2001.

[LeV02] Randall J. LeVeque. *Finite Volume Methods for Hyperbolic Problems*. Cambridge University Press, Cambridge, 1st edition, 2002.

[Lon56] R. Long. Long waves in a two-fluid system. *J. Meteorol.*, 13:70–74, 1956.

[MJT08] Paul. A. Milewski, T. Jacobsen, and Esteban G. Tabak. Mixing closures for conservation laws in stratified flows. *Stud. in Appl. Math.*, 121:89–116, 2008.

[MT15] Paul A. Milewski and Esteban G. Tabak. Conservation law modelling of entrainment in layered hydrostatic flows. *J. Fluid Mech.*, 772:272–294, 2015.

[MTT+04] Paul A. Milewski, Esteban G. Tabak, Cristina V. Turner, Rodolfo R. Rosales, and Fernando A. Menzaque. Nonlinear stability of two-layer flows. *Comm. Math. Sci.*, 2:427–442, 2004.

[RKBM11] R. Rotunno, J. B. Klemp, G. H. Bryan, and D. J. Muraki. Models of non-Boussinesq lock exchange flow. *J. Fluid Mech.*, 675:1–26, 2011.

[RSG10] J. H. Ritcher, F. Sassi, and R. R. Garcia. Toward a physically based gravity wave source parametrization in a general circulation model. *Journal of the Atmospheric Sciences*, 67:136–156, 2010.

[Smo94] Joel Smoller. *Shock Waves and Reaction-Diffusion Equations*. Springer-Verlag, New York, 1st edition, 1994.

[SO98] T. P. Stanton and L. Ostrovsky. Observations of highly nonlinear internal solitons over the continental shelf. *Geophys. Res. Lett.*, 25:2695–2698, 1998.

[Whi74] Gerald B. Whitham. *Linear and Nonlinear Waves*. Wiley-Interscience, 1st edition, 1974.

[WTM12] C. B. Whalen, L. D. Talley, and J. A. MacKinnon. Spatial and temporal variability of global ocean mixing inferred from Argo profiles. *Geophys. Res. Lett.*, 39, 2012.

4.2. Conclusions

The modelling of shock solutions for the two-layer shallow water non-Boussinesq equations was considered. This novel approach was discussed in Section 1 and used in the later sections to study the mixing and entrainment phenomena that originate from shock waves. We focused on two main scenarios: one with mass conservation and energy dissipation; and another where energy was conserved, allowing mass to be exchanged between the layers. The former was numerically studied for several initial shock conditions, and for different choices of r, which extends the work from [MT15] to the more general non-Boussinesq case. Simulations for the latter case will be part of the submitted manuscript.

A question that remains unanswered and that worth attention is the of mixing in three-layer flows. This is challenge we aim to investigate in future works.

Chapter 5

Conclusions

In this thesis, we considered the dynamics and stability aspects of multilayered shallow water flows, in the cases of various two- and three-layer configurations. Both models were formulated and their governing equations were derived in the more general non-Boussinesq case.

In Chapter 2, we focused on the evolutionary properties of the three-layer shallow water model, in the simpler Boussinesq case. We showed that these equations are local in contrast to the non-Boussinesq case, which are non-local and consequently do not conserve momentum, even in the absence of external forces (the so-called "Benjamin-Camassa paradox"). The existence of mode one and mode two waves was remarked and it was shown that the latter constitutes a two-dimensional invariant subspace in the full phase space (which has dimension 4). This result motivated a new change of variables, in which this mode 2 symmetry became clear. From there, one could use simple waves to find individual mode 1 waves, even though these do not lie in an invariant space. We attempted to construct such invariant regions through simple waves and, although they were shown not to exist, we found that reduced two-dimensional models approaches these mode 1 waves quite well. The same was shown to be true for mode 2 waves and these models were compared to the full system through numerical simulations, with an excellent agreement.

In Chapter 3, we explored the dynamics and stability of a two-and-a-half-layer model, focusing on the case where the upper layer density is negligible, also known as the free surface case. It was shown that in this configuration, the stability of the resulting 4×4 system depends only on two 'baroclinic' variables, in the same way as the two-layer rigid lid model does. We use this fact to restrict our attention only to a two-dimensional projection of the phase space, being this enough to monitor the stability of the system. This result also motivated a change of variables in which the resulting system is written in terms of the two 'baroclinic' variables and the two 'barotropic' variables, and which the characteristic polynomial (and therefore the hyperbolicity) depends only on the baroclinic variables. We then discussed the use of simple waves as a tool to find sharp bounds for solutions, as well as invariant subspaces where the nonlinear stability could be better studied.

Finally, in Chapter 4 we considered the study of waves after breaking, also called shock solutions. A conservation laws based methodology was discussed, which allows one to study the overall effect of mixing and entrainment without looking into the small scales of the phenomenon. We applied this methodology to study shock waves in a two-layer shallow water flow between two rigid walls, in the non-Boussinesq case. Two scenarios were considered and numerical simulations were performed and discussed.

5.1. Further work

The work presented in this thesis leads to a number of questions of immediate interest on the subject of multilayered stratified flows.

It remains as a main task to prove whether there are sharp bounds or not for the three-layer shallow water Boussinesq equations discussed in Chapter 2. In such an investigation, the reduced 'modal' models proposed there can useful. Being two-

dimensional models, one could find sharp bounds for these in the plane and then project them back, giving approximate locations for such invariant hyperbolic regions, in case they exist. Another immediate task would be to study the dynamics of the non-Boussinesq case and compare it to the results presented in the paper for the Boussinesq case.

For two-layer flows with a free surface, it would be interesting to see how the transition to the elliptic regime occurs. Figure 4 in Chapter 3 suggests that only the baroclinic (internal) modes become complex, and this might be possible to prove by looking at the characteristic polynomial given in Theorem 3.1. Also, one could use the change of variables given by this theorem, in combination with simple waves, to investigate the existence of approximate baroclinic subspaces, that would be given by $H \approx$ constant.

Another immediate direction for research is to explore the conservation laws methodology for shock solutions in the context of a three-layer flow in both Boussinesq and non-Boussinesq cases. This could be then compared to other models, as well as to experiments, in order to validate the approach.

Bibliography

[Ach90] David J. Acheson. *Elementary Fluid Dynamics*. Oxford University Press, Oxford, 1990.

[Bai95] Peter G. Baines. *Topographic Effects in Stratified Flows*. Cambridge University Press, Cambridge, 1st edition, 1995.

[Bar06] Ricardo Barros. Conservation laws for one-dimentional shallow water models for one and two-layer flows. *Math. Mod. and Meth. in Appl. Sci.*, 16:119–137, 2006.

[Ben66] David John Benney. Long non-linear waves in fluid flows. *Journal of Mathematics and Physics*, 45(1-4):52–63, 1966.

[BK00] John Billingham and Andrew Charles King. *Wave Motion*. Cambridge University Press, Cambridge, 1st edition, 2000.

[BM11] Anakewit Boonkasame and Paul A. Milewski. The stability of large-amplitude shallow interfacial non-Boussinesq flows. *Stud. in Appl. Math.*, 128:40–58, 2011.

[CC99] W. Choi and R. Camassa. Fully nonlinear internal waves in a two fluid system. *J. Fluid Mech.*, 396:1–36, 1999.

[CCF+12] R. Camassa, S. Chen, G. Falqui, G. Ortenzi, and M. Pedroni. An inertia 'paradox' for incompressible stratified Euler fluids. *J. Fluid Mech.*, 695:330–340, 2012.

[CJ13] José Alberto Cuminato and Messias Meneguete Junior. *Discretização de Equações Diferenciais Parciais - Técnicas de Diferenças Finitas*. Sociedade Brasileira de Matemática, Rio de Janeiro, 1st edition, 2013.

[CMM+09] Lyuba Chumakova, Fernando A. Menzaque, Paul A. Milewski, Rodolfo R. Rosales, Esteban G. Tabak, and Cristina V. Turner. Stability properties and nonlinear mappings of two and three layer stratified flows. *Stud. in Appl. Math.*, 122:123–137, 2009.

[Con11] Adrian Constantin. *Nonlinear Water Waves with Applications to Wave-Current Interactions and Tsunamis*. Society for Industrial and Applied Mathematics, 1st edition, 2011.

[Cra04] Alex D. D. Craik. The origins of Water Wave Theory. *Annu. Rev. Fluid Mech.*, 36:1–28, 2004.

[CRB11] Benoit Cushman-Roisin and Jean-Marie Beckers. *Introduction to Geophysical Fluid Dynamics - Physical and Numerical Aspects*. Academic Press, Waltham, 2nd edition, 2011.

[CT10] Lyuba Chumakova and Esteban G. Tabak. Simple waves do not avoid eigenvalue crossings. *Comm. on Pure and Applied Math*, 63:119–132, 2010.

[CZ10] Lawrence C. Cheung and Tamer A. Zaki. Linear and nonlinear instability waves in spatially developing two-phase mixing layers. *Physics of Fluids*, 22:052103, 2010.

[CZ11] Lawrence C. Cheung and Tamer A. Zaki. A nonlinear PSE method for two-fluid shear flows with complex interfacial topology. *Journal of Computational Physics*, 230:6756–6777, 2011.

[dMVM17] Francisco de Melo Viríssimo and Paul A. Milewski. Three-layer flows in the shallow water limit. *Submitted to Stud. in Appl. Math.*, 2017.

[dMVM18a] Francisco de Melo Viríssimo and Paul A. Milewski. Conservation law modelling of entrainment in stratified two-layer shallow water flows. *In prepapation*, 2018.

[dMVM18b] Francisco de Melo Viríssimo and Paul A. Milewski. Nonlinear stability of two-layer shallow water flows with a free surface. *To be submitted to Euro. J. Mech. B/Fluids*, 2018.

[Dur99] Dale R. Durran. *Numerical Methods for Wave Equation in Geophysical Fluid Mechanics*. Springer-Verlag, New York, 1st edition, 1999.

[FLS89] R. Feymann, R. Leighton, and M. Sands. *The Feynman Lectures on Physics*. Millennium Books, 1989.

[Fri17] Robert Friel. *Optimization Closures for Mixing Shocks in Stratified Hydrostatic Flows*. PhD thesis, New York University, 2017.

[GPT97] Roger Grimshaw, Efim Pelinovsky, and Tatjana Talipova. The modified korteweg-de vries equation in the theory of large-amplitude internal waves. *Nonlinear Processes in Geophysics*, 4(4):237–250, 1997.

[Gro76] M. Grant Gross. *Oceanography*. Merrill Physical Science. C. E. Merrill Publishing Company, 1976.

[HM05] Karl R. Helfrich and W. Kendall Melville. Long nonlinear internal waves. *Annu. Rev. Fluid Mech.*, 38:395–425, 2005.

[KNP01] Alexander Kurganov, Sebastian Noelle, and Guergana Petrova. Semidiscrete central-upwind schemes for hyperbolic conservation laws and Hamilton-Jacobi equations. *SIAM J. Sci. Comput.*, 23:707–740, 2001.

[Lan13] David Lannes. *The Water Waves Problem*. American Mathematical Society, 1st edition, 2013.

[LeV02] Randall J. LeVeque. *Finite Volume Methods for Hyperbolic Problems*. Cambridge University Press, Cambridge, 1st edition, 2002.

[Lon56] R. Long. Long waves in a two-fluid system. *J. Meteorol.*, 13:70–74, 1956.

[LWV15] K. G. Lamb and A. Warn-Varnas. Two-dimensional numerical simulations of shoaling internal solitary waves at the ASIAEX site in the South China Sea. *Nonlin. Processes Geophys.*, 22:289–312, 2015.

[Maj03] Andrew Majda. *Introduction to PDEs and Waves for the Atmosphere and Ocean*. Society for Industrial and Applied Mathematics, 1st edition, 2003.

[Miy88] Motoyasu Miyata. Long internal waves of large amplitude. In *Nonlinear water waves*, pages 399–406. Springer, 1988.

[MJT08] Paul. A. Milewski, T. Jacobsen, and Esteban G. Tabak. Mixing closures for conservation laws in stratified flows. *Stud. in Appl. Math.*, 121:89–116, 2008.

[MT15] Paul A. Milewski and Esteban G. Tabak. Conservation law modelling of entrainment in layered hydrostatic flows. *J. Fluid Mech.*, 772:272–294, 2015.

[MTT+04] Paul A. Milewski, Esteban G. Tabak, Cristina V. Turner, Rodolfo R. Rosales, and Fernando A. Menzaque. Nonlinear stability of two-layer flows. *Comm. Math. Sci.*, 2:427–442, 2004.

[Mun50] Walter Munk. Origin and generation of waves. *Coastal Engineering Proceedings*, 1(1):1, 1950.

[Ovs79] L. V. Ovsyannikov. Two-layer "shallow" water model. *Journal of Applied Mechanics and Technical Physics*, 20:127–135, 1979.

[RKBM11] R. Rotunno, J. B. Klemp, G. H. Bryan, and D. J. Muraki. Models of non-Boussinesq lock exchange flow. *J. Fluid Mech.*, 675:1–26, 2011.

[RSG10] J. H. Ritcher, F. Sassi, and R. R. Garcia. Toward a physically based gravity wave source parametrization in a general circulation model. *Journal of the Atmospheric Sciences*, 67:136–156, 2010.

[Smo94] Joel Smoller. *Shock Waves and Reaction-Diffusion Equations*. Springer-Verlag, New York, 1st edition, 1994.

[SO98] T. P. Stanton and L. Ostrovsky. Observations of highly nonlinear internal solitons over the continental shelf. *Geophys. Res. Lett.*, 25:2695–2698, 1998.

[SS53] J. B. Schijf and J. C. Schonfeld. Theoretical considerations on the motion of salt and fresh water. *Proceedings Minnesota International Hydraulic Convention*, 1953.

[Sto48] J. J. Stoker. The formation of breakers and bores. *Comm. on Pure and Applied Math*, 1(1):1–87, 1948.

[Wal91] J. M. Walker. Farthest North, Dead Water and the Ekman Spiral. *Weather*, 46:158, 1991.

[Wika] Wikipedia. "Boussinesq Approximation" verbete on wikipedia. https://en.wikipedia.org/wiki/Boussinesq_approximation_(buoyancy). Accessed: 07-11-2018.

[Wikb] Wikipedia. "Dead Water" verbete on wikipedia. https://en.wikipedia.org/wiki/Dead_water. Accessed: 27-09-2018.

[WTM12] C. B. Whalen, L. D. Talley, and J. A. MacKinnon. Spatial and temporal variability of global ocean mixing inferred from Argo profiles. *Geophys. Res. Lett.*, 39, 2012.

[YFC+09] Yiing Jang Yang, Ying Chih Fang, Ming-Huei Chang, Steven R. Ramp, Chih-Chung Kao, and Tswen Yung Tang. Observations of second baroclinic mode internal solitary waves on the continental slope of the northern south china sea. *Journal of Geophysical Research: Oceans*, 114(C10), 2009.

[Zie] Tomasz G. Zieliński. Fundamentals of Fluid Dynamics: Waves in Fluids (lecture notes). http://bluebox.ippt.pan.pl/~tzielins/doc/ICMM_TGZielinski_FluidWaves.Slides.pdf. Accessed: 06-11-2018.